GAS SENSING PROPERTIES OF NANOSTRUCTURED TIN/ZINC OXIDE THIN FILMS

A

Thesis

Submitted in fulfillment of the requirement for the award of the degree

Of

DOCTOR OF PHILOSOPHY

Submitted by

RAJESH KUMAR

Registration No. 950906036

Supervisors

Dr. Rajesh Khanna, Professor
Department of ECE,
Thapar University,
Patiala, Punjab, India

Dr. G.L. Sharma, Professor
Department of ECE,
N.C. College of Engineering,
Israna, Panipat, Haryana, India

DEPARTMENT OF ELECTRONICS & COMMUNICATION ENGINEERING

PATIALA (PUNJAB)-147004, INDIA

JULY 2016

CERTIFICATE

I, **Rajesh Kumar** hereby certify that the work which is being presented in this thesis entitled **"Gas Sensing Properties of Nanostructured Tin/Zinc Oxide Thin Films"** in fulfillment of requirements for the award of degree of the Doctor of Philosophy in Electronics and Communication Engineering from Thapar University, Patiala, Punjab is an authentic record of my own work carried under the supervision of **Dr. Rajesh Khanna** and **Dr. G.L. Sharma.**

The matter presented in this thesis has not been submitted in any other University/Institute for the award of any degree or diploma.

Date **(Rajesh Kumar)**

Signature of Candidate

This is to certify that the above statement made by the candidate is correct to the best of our knowledge.

Date

Dr. Rajesh Khanna
Professor,
Department of ECE,
Thapar University, Patiala,
Punjab, India

Dr. G.L. Sharma
Professor,
Department of ECE,
N.C. College of Engineering,
Israna, Haryana, India

ABSTRACT

In the present world of industrialization, because of the production of harmful gases as a by-product of the factories and automobiles, sensors are essentially required in all aspects of life. In many industries, various harmful, toxic and explosive gases including H_2, CH_4, NO_X, NH_3, SO_X etc. have become increasingly important as raw materials. In case of accidental leakage these gases can be life threatening also and hence it has become very important to develop highly sensitive gas sensors. Gas sensors based on semiconducting metal oxides have gained a lot of interest in last few decades. However, some unresolved issues that require special attention include the realization of gas sensors with low operating temperature, higher response towards low concentration of target gas, fast response and recovery speeds, low power consumption, low cost etc.

Hydrogen is a colorless, odorless, explosive, and extremely flammable gas having low minimum ignition energy (0.017 mJ), high heat of combustion (142 kJ/g H_2) and wide flammable range (4−75%), as well as a high burning velocity and detonation sensitivity. Hydrogen is envisioned as the most attractive basic and sustainable energy source for the future generation due to its high efficiency and renewable properties. Hydrogen gas is important in the synthesis of ammonia and methanol, the hydration of hydrocarbons, the desulphurization of petroleum products and the production of rocket fuels, in metallurgical processes etc. However, leakage of H_2 may lead to some fatal accidents which can be prevented if detected timely. To monitor such leakages, the development of sensors with improved sensitivity and selectivity is essentially required. Recently, metal oxide semiconductor thin films have attracted considerable interest as gas sensing materials due to their higher specific surface area and smaller grain size than bulk materials, which can lead to higher response, lower operating temperatures and fast response processes. Moreover, nanocrystalline thin films are more compatible with current micro-fabrication processes and circuits. Therefore in this thesis thin films of Tin/Zinc oxide have been developed to investigate the gas sensing properties.

Nowadays, investigation is directed, rather than to new sensors, to improve the gas sensing properties of existing sensors. Ideal gas sensor should present: high sensitivity towards target gas, high selectivity, high stability, high reliability and low

sensitivity to humidity and temperature, robust, durable, short reaction and recovery time, easy calibration and have small dimensions. Unfortunately, creating a sensor that satisfies all these requirements adequately has not yet been realized and there is no universal decision for simultaneous optimization of all such sensors parameters. Therefore, one should always seek a compromise between these parameters of the developed gas sensor. Most of the above desired requirements are dependent not only on the used material, but also on the method used for its synthesis and specially on the additives present on the material surface and the method used for their addition. Consequently, in the present work Sol-Gel and PLD techniques have been exploited for the growth of nanocrystalline SnO_2/ZnO thin films for the development of suitable gas sensor.

Most of the tin/zinc oxide based gas sensors operate at quite high temperatures normally between 250 ºC to 450 ºC, which is inconvenient for using such sensors at high temperatures. Because high working temperature of the gas sensor is energy intensive, increases operating cost and requires high operational safety measures in an environment with explosive gases like hydrogen etc. Moreover, higher power consumption and short battery life time are also the other drawbacks of higher sensing temperature. Besides, high working temperature, high response for low concentration of target gas and good selectivity of the present sensors are also major concern. The modulation of electronic properties of sensing layer with suitable catalyst are expected to improve the sensing response characteristics to a great extent, which can be easily attained using thin film technology. Incorporation of optimum quantity of suitable catalyst with novel dispersal in sensing layer is expected to improve the sensing response, selectivity and operating temperature significantly.

In the present work, attempt has been made to realize efficient H_2 gas sensors based on semiconducting tin/zinc oxide thin films having suitable catalyst in optimum quantity and novel dispersal manner, showing high response at relatively low operating temperature for low concentration of gas. Undoped and doped SnO_2/ZnO thin films sample series have been deposited by sol-gel technique and spin coating process on quartz substrates. The sample series of silver doped SnO_2 nanocomposite thin films were successfully synthesized by chemical route. These deposited films were annealed at different temperatures (300 ºC, 350 ºC, 400 ºC, 450 ºC and 500 ºC). The structural analysis and surface morphology of as prepared silver doped SnO_2 thin films were characterized by complementary techniques such as X-ray diffraction and

scanning electron microscopy. The tetragonal structure of SnO_2 was confirmed by XRD and, for all the annealed samples, the appearance of the sharp peaks and similarities in all XRD profiles in terms of the peak positions and the half peak width indicate a well-developed crystallinty. The crystalline domain size estimated from Sherrer diffraction formula and the average crystalline size was found to be ≈18.62 nm. It is evident from the SEM images and particle size distribution that by increasing the annealing temperature particle size increases, which is consistent with the XRD information.

In the present work highly sensitive and selective gas sensor for hydrogen gas has been developed utilizing copper doped zinc oxide (Cu-ZnO) thin films. These films were fabricated using pulsed laser deposition (PLD) technique on quartz substrates with interdigitated platinum electrodes. The structural and surface characteristics of obtained films were investigated by X-ray diffraction technique and atomic force microscopy. The gas sensing properties of as grown films were tested by I-V measurements techniques using a gas sensing unit for different concentration of H_2 and CH_4 gases at substantially reduced operating temperatures of 50 ºC, 100 ºC and 150 ºC. It is observed that for 3% Cu-doping the optimum parameters are 1000 ppm of hydrogen gas at 150 ºC in the voltage range of 0-1volt. More importantly this sensor responds to 10 ppm of hydrogen gas even at low operating temperature i.e. 50 ºC. The novelty of this sensor is that the sensitivity for CH_4 and H_2 can be completely reversed if measurements are performed at 150 ºC as compared to 50 ºC or 100 ºC.

In addition to above we have also studied undoped ZnO, and 1 to 8% Li-doped ZnO thin film sample series for hydrogen sensing and these films were characterized by an X-ray diffraction and scanning electron microscopy. The gas sensing measurements were performed by a PC connected to a Keithley 2401 low voltage source, picoammeter through GPIB interface and lab view v8.5 software. It is observed that highly resistive 2% Li-doped ZnO thin films exhibit optimum performance at 150 °C to a flow of 50sccm (standard cubic centimeters per minute) of hydrogen, whereas high lithium doping (8%) show excellent sensing performance at 50°C for the same flow of hydrogen. The response time of the 2% Li- doped ZnO films is about 55 seconds and recovery time is about 220 seconds.

List of Author's Publications from This Thesis

1. Rajesh Kumar Malik, Rajesh Khanna, G.L. Sharma, S.P. Pavunny, R.S. Katiyar, "Lithium Doped Zinc Oxide Thin Film Hydrogen Gas Sensor at Reduced Operating Temperature," *Sensor Letters*, Vol. 12, No.12, pp. 1769-1775, December 2014, ISSN: 1546-198X.

2. Rajesh Kumar Malik, Rajesh Khanna, G.L. Sharma, S.P. Pavunny, R.S. Katiyar, "Hydrogen Sensing Properties of Copper Doped Zinc Oxide Thin Films," *IEEE Sensors Journal*, Vol.15, No.12, and pp.7021-7028, December 2015, ISSN: 1530-437X.

ACKNOWLEDGEMENTS

गुरुर्ब्रह्मा गुरुर्विष्णुः गुरुर्देवो महेश्वरः ।
गुरुः साक्षात्परब्रह्म तस्मै श्री गुरवेनमः ।।

(I prostrate to that Shree Guru (teacher), who is himself Brahma, Vishnu, and God Maheshwara, and who is verily the Supreme Absolute itself.)

On the completion of my thesis, I would like to remember my first Gurus, my parents who led the foundation by generating quest of the knowledge in my mind and to all other Gurus for making me competent enough to complete the research work. The completion of any academic work is inconceivable without the expert guidance of mentors. I acknowledge and extend my deepest gratitude to my respected guides **Dr. G.L. Sharma**, Retd Principal Scientific Officer, Physics Department, IIT Delhi, and **Dr. Rajesh Khanna,** Professor (ECE), Thapar University, Patiala, whose indispensable tutelage and wise counsel at every step of my work enabled me to complete the work without obstruction. I am deeply indebted to my esteemed supervisor, **Dr. G.L. Sharma**; a personage of striking insight has played a pivotal role in my life as a researcher. Working under a man of unimpeachable integrity and uncompromising principles was indeed a matter of pride for me. Despite his various personal and professional assignments, he spread his precious time and took great pains in discussing even in minute details of this work.

Out of deep sense of gratefulness, I would like to express my sincere gratitude to **Dr. O.P. Pandey**, Dean (RSP), **Dr. Sanjay Sharma**, Head ECE, **Dr. A.K. Chatterji**, and **Dr. Kulbir Singh** the members of doctorate committee for continuous appreciation and support. I am also obliged to **Dr. R.S. Katiyar** and **Dr. S.P. Pavunny,** University of Puerto Rico, USA for their valuable suggestions, guidance and experimental supports.

I would like to greatly acknowledge and thanks the entire Administration and Management of N.C. College of Engineering, Israna, Panipat for enabling and supporting me for this research work. Specifically, I pay my humble gratitude to **Dr. Satsangi,** Professor, IIT Kharagpur, who was the **Director, NCCE (Israna)** when I started this work. I am very grateful for the financial support provided by

AICTE, New Delhi in research promotion scheme (8023/RID/RPS/78/11/12) to N.C.C.E., Israna, (Panipat) Haryana, India.

I would like to extend my cordial thanks to the various research facilitators like AIRF- JNU (New Delhi Campus), SAI LAB-Thapar University-(Patiala), SAIF-Punjab University, Chandigarh, Esc. Department –Kurukshetra University, Physic Dept- IIT-Delhi, and CEERI- Pilani, Rajasthan for allowing me to carry out characterization of our developed sensors at their premises.

I am also thankful to the International Journals, **Sensor Letters** of American Scientific Publication and **IEEE Sensors** Journal who examined my research papers. Their suggestions and comments have really helped me in bringing this thesis to the present shape.

I must express my sincere thanks to my dear friends and relatives such as Dr. Sanjay Thakral, Dr. Krishan Dahiya, Dr. Sandeep Jaglan, Dr. Rupesh Malik, Mr. Rakesh Malik, Mr. Ajit Boora, Mr. Amit Deswal, Mr. Anil Lohan and Mr. Virender Boora who supported me throughout this odyssey. I am also thankful to all faculty colleagues for their constant support in various forms. However, my special thanks to my dear friend **Dr. Vijender Singh**, Associate professor, Baddi University for his unconditional help and invaluable guidance throughout this thesis is commendable.

To my mother **Birmati (Om Shanti)**, my father **Sh. R.P. Malik,** my wife **Kamal Malik**, and our son **Priyanshu Malik,** all I can say is it would take another thesis to express my deep love for all of you. Your patience, love and encouragement were a booster for me, especially in those days when I spent more time with my laptop than with you.

Last but not the least; I owe my reverence to the Almighty, by whose grace I have been able to complete my research work successfully.

Rajesh Kumar Malik

TABLE OF CONTENTS

List of Figures

List of Tables

List of Abbreviations

0D	Zero-Dimensional
1D	One-Dimensional
AFM	Atomic-Force-Microscope
Ag	Silver
Ar	Argon
Au	Gold
CH_4	Methane
Cu	Copper
CVD	Chemical Vapor Deposition
GPIB	General Purpose Interface Bus
H_2	Hydrogen
KrF	Krypton Fluoride
Li	Lithium
MOS	Metal Oxide Semiconductor
O_2	Oxygen
PLD	Pulsed Laser Deposition
Pt	Platinum
ppm	Part Per Million
rpm	Rate Per Minute
sccm	Standard Cubic Centimeters per Minute
SEM	Scanning Electron Microscope
SiO_2	Silicon Dioxide
SnO_2	Tin Oxide
XRD	X-ray Diffraction
ZnO	Zinc Oxide

Chapter 1 Introduction

1.1 The Interest in Gas Sensing

The last century has seen increased industrial growth worldwide and the side effect of this development is an exponential increase in pollution of earth, air and water, especially in densely populated areas such as metropolitan cities. As land pollution is locally restricted and great efforts have been made to improve the quality of rivers. But, air pollution is not so easily reduced. Wind, rain and other meteorological phenomena make it difficult to predict and impossible to control. The measures taken over the last years are therefore focusing on preventing or reducing the emission at its source, e.g. the use of air filters for industrial combustion. However, complete prevention of pollutant emission is not always viable. Accordingly air pollution threatens nature and human health alike. People, especially in urban areas, are exposed to a high quantity of harmful, toxic and explosive gases at work, in traffic and at home. A large number of major/minor accidents are taking place worldwide every year. In 1979 and 2011, leakage of H_2 gas resulted in an explosion at Fukushima in Japan and Three Mile Island in USA respectively causing major loss of property including life of a number of mankind. In 1984, we may recall the incidence of Bhopal gas tragedy in India, where thousands of people died and thousands are still suffering from the aftermath of the incident on their health. Recent leakage of chlorine from an industry in Mumbai is amongst the several accidental happening frequently around us. Such kind of accidents could have been prevented by installation of on-site devices, to alarm the presence of toxic and explosive gases before reaching dangerous high level. Therefore, their exact nature and quantity must be known with a high spatial resolution.

Currently, the qualitative and quantitative analysis of gaseous compounds is performed by analytical instruments such as chromatography; spectroscopy and spectrometry. However, these classical analytical instruments are highly accurate and reliable devices, able to detect even traces of pollutants in mixtures and with lifetimes in the range of several years. But their drawbacks are a high initial cost, high maintenance costs, size and weight, high power consumption (no battery operation possible), the need for qualified personnel and a comparably low time-resolution. One answer to this growing need is the development of smaller, cheaper and autonomous measurement units – Gas sensors.

1.2 What is Gas Sensor?

Our ears, eyes, nostril and skin are physical sensors as they become aware of physical responses of hearing, watching, odor and warmth correspondingly. What we smell with the nose are actually small portions of odorant molecules. In a similar way gas sensor is a device, which can selectively respond to certain properties of the environment and transfer this response into an electrical signal for further treatment using transducer systems. However, the human physique can identify the gases and fragrances using its inbuilt sensing technique, mostly called as the olfactory technique in which olfactory system inside the nostrils detect fragrance molecules and send them to the mind as electrical signals. However the human cells in nostril has the ability of detecting and recognizing between a few countless numbers of odours, but it surely unable to detect immensely less concentrated gases as good as odorless, inflammable and explosive gases (like hydrogen). Hence it becomes necessary to develop gas sensors that satisfy these specifications.

As a consequence, our society needs gas sensors for home, automobile and industrial applications, due to the fact of detection of harmful gases in environmental monitoring or harmful discharges. So, major reasons for the need of gas sensors are observing of environmental pollutants and controlling their emission. Moreover, the main difference between classical analytical instruments and gas sensors is cost and accuracy. In contrast to classical analytical instruments, gas sensors are small and cheap devices with lower lifetime and accuracy. The one's strengths are the others weaknesses. Attempts to close this gap from both sides are currently made by the industry and researchers alike: increasing the accuracy of gas sensors and miniaturizing classical instruments.

Nowadays, the market, based on the new regulations, demands a higher reliability in domestic and environmental gas sensors for sensing the combustible, toxic and explosive gases. For gas sensing and controlling, various sensor methods may also be utilized. Spectroscopic, optical and solid states are the three important types of gas sensing methods. Spectroscopic methods use fundamental gas properties, like vibrational spectrum or molecular mass for direct analysis and optical sensor structures are based on light stimulation and the absorption spectra detection and measurement. While solid state gas sensors are based on the change in sensing material's chemical and/or physical properties after gas exposure. The changes in

properties of gas sensing materials result in variations of its electrical parameters. A solid state gas sensing device is thus a sensor that experiences a change in its physical properties (e.g. resistance, mass, capacitance) upon its exposure to a targeted gas in a way that can be quantified and measured. Solid state gas sensors may be commonly differentiated on the basis of the principle of operation into metal-oxide, infrared, electro-chemical, and piezo-electric sensors.

Metal oxide gas sensors normally contain a semiconductor material deposited on a substrate connected to two metallic electrodes through heat energy. The semiconductor surface reacts with gas molecules and produces sensing of various gases. Infrared (IR) sensors sense various gases on the basis of their absorption spectra, when gas molecules are thermally agitate by IR radiations. Catalytic-bead sensors used to detect combustible gases work on the basis of catalytic surface kept up at high temperatures. Temperature change is observed, when fast ignition of combustible gas molecules reacts with the catalyst surface. Electrochemical sensors incorporate a detecting anode and a counter cathode drowned in an electrolyte. When gas molecules react with the detecting electrode a change in the current, measured between the electrodes, is observed. Sensors in view of the piezoelectric influence, like surface acoustic wave (SAW) and quartz crystal monitors (QCM) experience a change in surface resonating frequency on interaction with gases. Each kind of gas sensor, has its own arrangement of points of interest and impediments, is generally chosen relying upon the sort of utilization.

1.3 Historical Background of Gas Sensors

A canary, normally an extremely songful feathered creature, is more sensitive than people to lack of oxygen, CO or methane gas. In light of its very good response towards gasses, individuals utilized them to distinguish toxic gasses in mines. They would stop singing and inevitably pass on within the sight of these gasses, flagging the excavators to leave the mine rapidly. This was the main sort of gas sensor utilized in 1920s. Later, individuals Davey's lamp was used as a gas sensor. Depending on the amount of gas present in the environment the height of the flame was adjusted. The flame acclimated to particular height in natural air and elevated flame implies methane gas while short flame implies less oxygen.

The use of semiconductors materials sensitive to gases ways back to 1953 when Nobel Prize winning physicist Walter Brattain, (working at Bell Labs) and

Bardeen reported that the conductance of Germanium semiconductor changes because of the changes in the arrangement of encompassing gas [1]. These gases react with Germanium and change its conductance. Later Heiland, Bielanski in 1957 [2] and Seiyama in 1962 discovered gas-sensing consequences for metal oxides [3]. In 1968, Taguchi (Figaro) brought semiconductor sensors as an industrial product instead of metal oxides [4]. Since then, the technology of metal oxide based semiconductor gas sensors has been evolving due to the significant contributions from researchers across the globe. These days, many firms are proposing metal oxide semiconducting gas sensors, like Figaro, Applied Sensor, UST, FIS, MICS, CityTech, Microsens and Paragon as shown in Fig 1.1.

Fig. 1.1: Different commercially available single sensors using semiconductor technology, Figaro Engineering

1.4 Choice of Metal Oxide Semiconductors

Metal oxides are a class of materials covering the properties from insulators to semiconductors and metals and all parts of physics and material science in areas including magnetism and superconductivity. Metal oxides have a wide scope of physical, electrical and chemical properties that change according to the chemicals present in the surrounding environment. Numerous researchers and scientists have examined structural simplicity of metal oxide as electronic semiconductor materials having minimal cost. The gas detection using metal oxides is done when electrical conductivity of semiconductors changes with the content of the compound/gas climate encompassing them. The gas detection of these metal oxide semiconductor sensors is based on the changes in

- Mass of sensing element
- Resistance
- Work function

- Dielectric constant

The presence and percentage of the gas in surrounding environment is measured on the basis of change in any one of the above mentioned parameters. The vast majority of customary sensors utilizes massive or heavy films for detecting the gas. However, in recent time, nanostructured thin films are utilized, since it gives good control on gas detecting properties of a material and large surface to volume ratio. The gas sensors based on thin films material used are classified as follows:

- Metal oxides thin film gas sensors (SnO_2, ZnO, Ga_2O_3 etc.)
- Catalytic metal thin film gas sensors (Pd and Pt)
- Special class of organic material thin film gas sensor (Phthalozyanine, Poly-pyrol)

As a result of selectivity issue in catalytic sensor, nonappearance of similarity of natural materials films, short life span of natural material thin film sensors, thin metal oxide film sensors have become popular in business community. There are numerous metal oxides appropriate for sensing flammable, reducing, or oxidizing gases based on conductive measurements. Accompanying oxides demonstrate a gas sensing in their conductivity: SnO_2, ZnO, In_2O_3, WO_3, TiO_2, Cr_2O_3, Mn_2O_3, Co_3O_4, NiO, CuO, V_2O_3, Fe_2O_3, GeO_2, Nb_2O_5, Nd_2O_3, MoO_3, Ta_2O_5, La_2O_3, CeO_2 etc. Metal oxides chosen as gas sensors are found looking at their electronic structure. Based on widespread electronic structures of oxides these oxides were divided into the following categories:

1) Transition-metal oxides (Fe_2O_3, Cr_2O_3, NiO, etc.)
2) Non-transition-metal oxides, which include
    a) Pre-transition-metal oxides (Al_2O_3, MgO, etc.)
    b) Post-transition-metal oxides (ZnO, SnO_2, etc.)

It is realized that numerous transition-metal oxides are small band gap materials. Additionally, the band diagram shows that most of oxides, are having incompletely occupied d band i.e. for d^n ($0 < n < 10$) ought to be metallic. But it is not always true because of intervention of various types of electron–lattice and electron–electron interactions.

Transition-metal oxides perform in a different way as the energy gap difference between d^n state of cation as compared to d^{n+1} or d^{n-1} cation state is very small. Due to this small gap the most evident outcome shows that different compositions of stable oxides exist with various transition elements. Therefore it

shows that such stable oxides might be more appropriate for their application as gas sensors. Be that as it may, structure flimsiness and non-optimality of different properties vital for conductivity based gas sensors bound interest of their utilization. Rather than transition, pre-transition metal oxides are required to be entirely dormant, as their reduction and oxidation process is effortless. As far as materials, with wide band gap electronic structure are concerned, neither electrons nor holes can be easily separated. This property makes these oxides to behave as isolators. Due to their property of bad electrical conductivity wide band gap materials are not used as gas sensor [5].

Only transition-metal oxides with d^0 and d^{10} electronic configurations show their ability to be used in gas sensor devices. d^0 structure is available in binary transition-metal oxides like V_2O_5, TiO_2, and WO_3 etc. As we are probably aware, d^{10} structure are occupied with cations in the post-transition-metal oxides, for example in ZnO, $In_2O_3$and SnO_2. The post-transition oxides, and in addition most of the transition-metal oxides are responsible for "redox" reactions. The oxidation reaction occurs with samples which are mass reduced or where the surfaces are lack of oxygen. Free carriers are generated when post-transition oxides are reduced in the presence of oxygen, this significantly enhances the conductivity of metal oxide, required for sensor devices. Hence post-transition oxides are most widely studied compared to other metal oxides for gas sensor devices.

For post-transition-metal oxides, thin films are most popular materials for gas-sensing devices. Well known advantages of these materials are their higher response towards different gas species and low cost. Their surface conductivity modifications in response to adsorbed gases, labelled them a perfect candidate in the field of surface science. Yet, point defects ZnO surfaces are critical in gas detecting as they create huge variations in the surface conductivity. The predominant imperfections recognized in these films are oxygen deficiencies. Heating of these films to high temperatures creates these deficiencies [6]. These surface deformities don't create any new filled electronic states in the band gap, because of the stable oxidation state of the zinc. Such properties of ZnO mark it most appropriate material for gas sensing applications.

As most of the reports in the literature are focused on conductometric based thin film gas sensors therefore the present work is focused on nanostructured

ZnO/SnO_2 based thin film gas sensor devices. A brief discussion on SnO_2 and ZnO materials and their basic properties desired for gas sensing devices is presented in the following sections.

1.4.1 Tin Oxide (SnO_2) Basic Properties

Tin (Sn) is group 14 (4A) element of the periodic table between the metals and non-metals at their boundary. It is one of the happening element that is found as it can be used to form distinctive natural and inorganic composites. Stannous and stannic are divalent and tetravalent oxidation states of the tin respectively. Divalent and tetravalent tin also signified as Sn (II) and Sn (IV) based on stock oxidation-number frame work another experienced grouping framework. In composites, Tin can exist in the +2 or +4 oxidation state. In this work Tin (IV) oxide is considered; it is regularly known as stannic oxide, stannic anhydride and Tin oxide and written in equation form as SnO_2.

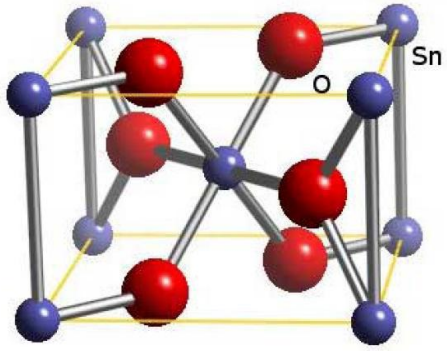

Fig.1.2: Tetragonal rutile structure of tin oxide [7]

Tin oxide is an n-type wideband gap (3.6eV) oxide semiconductor with high chemical and mechanical stabilities that have tetragonal rutile structure. It's unit cell contains six particles, two Tin, and four O_2. Each Sn molecule is at focal point of six O_2 particles found around at the edges of a general marginally disfigured octahedron. Three Tin atoms are roughly form the sides of an equilateral triangle encompassing each O_2 particle; important in a 6:3 coordination [7]. The lattice parameters a, b and c are 4.737 Å, 4.737 Å and 3.185 Å respectively with c/a ratio as 0.673. The radius of the ions O^{2-} and Sn^{4+} are 1.40 and 0.71 Å, respectively. Its electrical properties unfavorably depend on its stoichiometry with respect to oxygen, on the nature and amount of impurities or dopants present and on its size as well as shape of nanostructures. Practically speaking, SnO_2 contains oxygen vacancies and therefore it is non stoichiometric.

Table 1.1: Basic Properties of SnO_2 [7]

Parameter	Value
Molecular formula	SnO_2
Solubility in water	Insoluble
Boiling point	1800-1900 ^oC
Molar mass	150.71 g/mol
Appearance	White or light grey powder
Density	6.99 g/cm^3(24 ^oC)
Electron mobility (at 300 K)	250 cm^2/V.sec.
Melting point	1630 ^oC
Refractive index	2.006
Lattice constants	a_o = 4.737Å, c_o = 3.188Å
Odour	Odourless
Crystal structure	Rutile tetragonal
Energy gap	3.6 eV Direct
Decomposition into SnO and O_2	1500 ^oC
Heat of formation	6 eV
Electron effective mass	0.275 m_o
Electron effective mass	0.275 m_o
Mineral name	Cassiterite

1.4.2 Zinc Oxide (ZnO) Basic Properties

Zinc oxide (ZnO), is a member of II–VI semiconductor composites, is an extremely multipurpose and material of importance. ZnO is a wide direct band gap (3.37 eV) has a great binding energy of 60 meV [8]. It has a high optical transmittance and good electrical conductivity in the visible region. All listed properties help it in using as sensor in level show board, window layers in sun oriented cells and displays numerous other potential applications in territories, for example, laser diodes, gas sensors, optical gadgets [8] with immaculate probability. A wide band gap has various advantages like tolerating high temperature and power applications. It diminishes electronic commotion, allowing sustenance in substantial electric fields conceivable and increasing breakdown voltages.

- **Physical Properties**

Physically, ZnO resembles a snow like powder and is mentioned as Zinc white or zincite. To the extent dissolvability is worried, it's verging on insoluble in water and liquor however it promptly solvents in acids like HCl despite the fact that it's discolored in nearness of acids. The mineral type ZnO is of red or yellow shading rather than typical white because of nearness of polluting influences like manganese or different components.

Table 1.2: Physical Properties ZnO [8]-[10]

Property	**Value**
Appearance	Yellowish white powder
Exciton binding energy	60 meV
Molecular formula	ZnO
Density	5.606 g/cm^3
Odour	Odourless
Melting point	1975 ^{o}C
Band gap	3.4 eV Direct
Electron mobility (at 300 K)	200 cm2/V.sec.
Lattice constants	a_o = 3.2469 Å, c_o = 5.2069Å
Relative dielectric constant	8.66
Boiling point	2360 ^{o}C
Intrinsic carrier concentration	< 10^6 /cc
Molar mass	81.4084 g/mol
Electron effective mass	0.24
Refractive index	2.0041
Water Solubility	0.16 mg / 100 mL

- **Structural Properties**

ZnO one of most widely studied exist with a steady wurtzite structure having a = 0.325 nm and c = 0.521 nm with ABAB closest hexagonal close packing (HCP). The ZnO structure comprises of exchanging planes made out of O^{2-} and Zn^{2+} ions coordinated tetrahedrally and stacked along the c-axis on a substitute premise (Fig. 1.3). Zn^{2+} and O^{2-} ions make an ordinary dipole minute and moment polarization that brings about an enhancement of energy at surface [11]. The coordinated tetrahedral in

ZnO is responsible for the noncentral symmetric structure and thus brings about the properties of pyroelectricity and piezoelectricity in it.

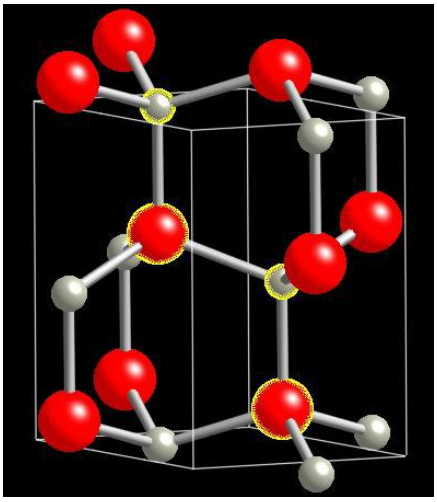

Fig.1.3: Zinc oxide hexagonal wurtzite structure [11]

- **Electrical Properties**

Zinc oxide (ZnO) has relative large excitation binding energy (60 meV) and a wide direct-bandgap of 3.37 eV. The pure ZnO thin films are naturally n-type semiconductor which has the electrical conductivity due to either oxygen vacancy or interstitial Zn that there are in ZnO lattice sites. Energy levels of the intrinsic defects are approximately 0.05 eV down the conduction band. Besides its large bandgap and wide excitation binding energy, Zinc Oxide can be used as chemical sensors, luminescence devices and solar cells etc.

- **Besides Gas Sensing Applications**

Besides gas sensors, ZnO is a multipurpose semiconductor that used for the making of LEDs, laser diodes, optical fibers, surface acoustic wave devices etc. [12]-[14]. Another significant region of application of ZnO is an energy component where it's utilized to construct different components like the cathodes and some of the time likewise as the fuel. ZnO could be used in solar cell as a photo catalyst [10], [15]. ZnO has turned out to be an aid for materials science as it has a mix of one of a kind properties like UV retention, against microbial properties, unfaltering warm and optical properties. Be in pottery, oils, treatments, cements or the elastic business ZnO has an exceptionally critical contribution [8], [10].

- The rubber industry is in charge of expending around half of the ZnO that is delivered all around. ZnO alongside stearic acid are an absolute necessity for actuating the procedure of vulcanization in rubber production.

- A mixture of ZnO with 0.5% Fe_2O_3 is used in engineering Calamine lotions identified as Calamine. Fine elements of ZnO are hostile to bacterial and freshening up qualities and henceforth these are utilized for bundling applications. Such belongings alongside its capacity of killing acids allows perfect use of it in germicide creams, mending creams and so forth they are likewise an imperative part of dental pastes and tooth prosthetics. ZnO is additionally utilized as a part of sunscreens and sunblocks to avoid sunburns due its property of retaining light. ZnO is additionally utilized as a part of the making cigarette channels as it aides in expelling unsafe substances like H_2S and HCN without influencing the flavor.
- ZnO can be generally added to nourishment items due to wellspring of Zn regarded as a fundamental supplement as ZnO aides in the execution of different physiological exercises for example development and appropriate working of the reproductive organs. Zinc Oxide is likewise mixed with grub as a Zn option for domesticated animals and it is utilized to produce Zinc Gluconate used in frosty aversion tablets.
- ZnO is a brilliant inhibitor of parasites, buildup and mold. ZnO paints keep up their adaptability and glue properties for a considerable length of time. The UV blocking capacities of ZnO likewise assume a critical part in enhancing the strength of the paint.

1.5 Others Types of Gas Sensors

Thin film gas sensors are available on conductometric or resistance changes, besides these researchers have also examined various types of gas sensors that might be classified based on their working principles as follows:

- **Acoustic Wave Gas Sensors**

Acoustic wave gas sensors work on the principle of sound. To radiate acoustic signals, this type of sensor utilize thin film piezoelectric material or piezo electric mass structure in which at least one transducers is layered on the top.

- **Capacitive Gas Sensors**

Such sensors detect the modification in dielectric constant of films depending on gas concentration. The working of capacitive sensor depend upon the spacing between two plates of a standard capacitor or inter-digitated electrode structures

- **Optical Gas Sensors**

A couple of materials experience a change is absorbance on presentation to the analyte. Optical sensor working depends on screening adjustment by retention of the target film on introduction to the source.

- **Calorimetric Gas Sensors**

The guideline of calorimetric gas sensors in light of modification in temperature at reactant surfaces consisting of dynamic metal surface film which reacts chemically with gas. (e.g. Palladium, Platinum, or Rhodium). Film blazes combustible gasses. Warmth is created because of ignition. The heat generated is balanced due to decrease by warming force due to electrical. In this way the power consumption determines the convergence of gas.

- **Electrochemical Gas Sensors(EGS)**

EGS are gas pointers which watch the centralization of an objective gas by oxidizing or diminishing the objective gas at a terminal and consequently by current measurement. The objective gas to be measured gets diffused through the dispersion hindrance into the cell. When objective gas touches the identifying cathode, the objective gas in the specimen encounters an electrochemical response (lessening and oxidation). The electrons produced from the lessening and oxidation allows a current to flow due to charging of the identifying anode.

1.6 Gas Sensing Mechanism of Metal Oxide Semiconductor

In order to understand the working mechanism of a metal oxide gas sensor, take gander in the path of sensor signal generated. Following parts are involved in a sensor element:

- Sensing layer (metal oxide semiconductor)
- Substrate (quartz or alumina)
- Electrodes (platinum or gold) for the measurement of the I-V characteristics.
- Heater, separated from the detecting layer and the electrodes by an insulating layer.

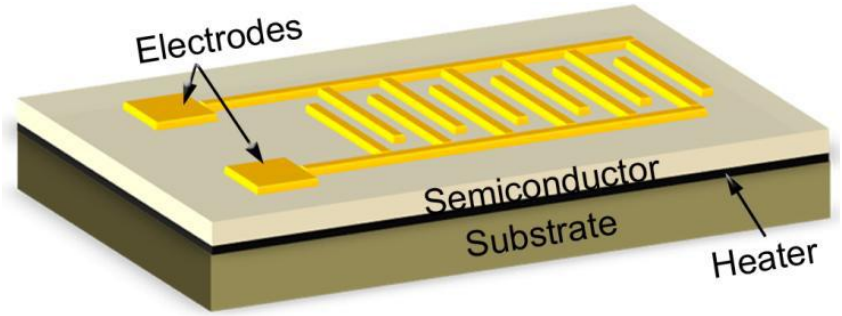

Fig.1.4: Schematic of a resistance based metal oxide gas sensor [16]

Despite the fact that it has been known for quite a while that desorption and adsorption of gas particles from and on the detecting surface of the component causes a change in its electrical conductance, the correct gas detecting instrument is yet to be completely caught on. In principle, gas detection with semiconducting metal oxide based gas sensors is simple. In air, for n-type material electrons are trapped from the bulk at their surface with increasing the resistance of the sensor in total due to the oxygen adsorbate nearly at temperatures within 150 and 450°C, but resistance will be decreased at p-type materials. Now existence of a target gas in the air, which reacts with preadsorbed oxygen. Also it may directly react with the oxide and determines a change in the sensor resistance, which is recorded as a sensor signal and the magnitude of which is correlated to amount of the specific gas. Here basic operational principle for a metal oxide gas sensor may be explained as follows:

- In air on the surface of a metal oxide semiconducting material, electrons are trapped from the conduction band by oxygen due to adsorption and causes an electronic charge transfer from the semiconductor creating ionized oxygen adsorbates like O_2^-, O^- and O^{2-} [7].

$$O_2\ (gas) \leftrightarrow O_2\ (adsorbed) \quad (1.1)$$

$$O_2\ (adsorbed) + e^- \leftrightarrow O_2^-\ (adsorbed) \quad (1.2)$$

$$O_2^-\ (adsorbed) + e^- \leftrightarrow 2O^-\ (lattice) \quad (1.3)$$

- These species of oxygen ions are stable at different temperatures viz. O_2^- below 100 ºC, O^- between 100 ºC and 300 ºC and O^{2-}above 300 ºC [16].
- In this way a negative charge is created at first glance that prompts to a space charge layer or depletion region close to surface and thus reducing conductance of the semiconductor.

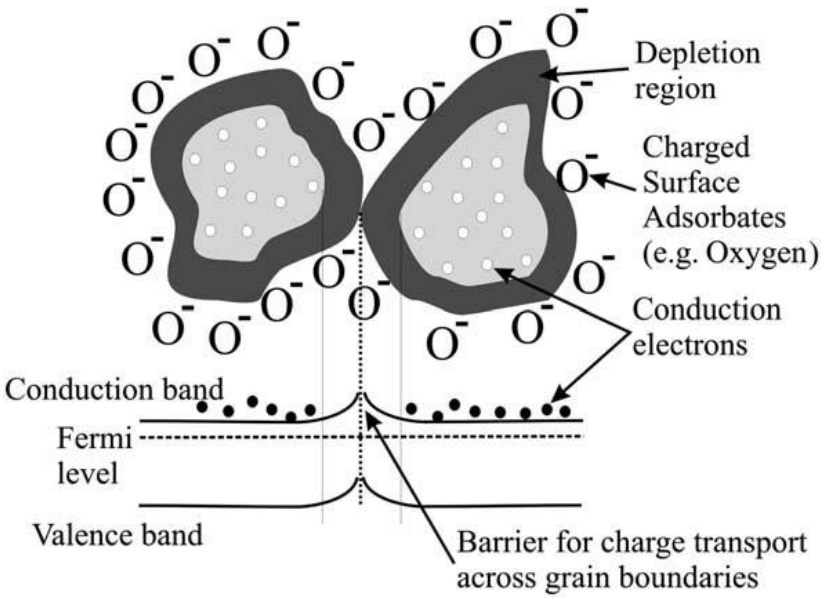

Fig. 1.5: Schematic diagram of charge carrier concentration in SnO_2 grains [7]

- At the point when this surface is presented to a gas that interact with pre-adsorbed oxygen ions and conductivity of the depletion region is balanced which is correspondingly measured as electrical signal. However, the correct key instruments that cause a gas reaction are still dubious, yet basically catching of electrons by the adsorbed atoms causes band twisting prompted by such charged particles are in charge of an adjustment in conductance. The negatively charge caught in such oxygen species caused an upward band bowing and consequently a decreased conductance contrasted with the level band circumstance [17].

In addition, the gas-recognition guideline of metal-oxide is likewise clarified on premise of varieties of the exhaustion layer at the grain limits within the sight of decreasing or oxidizing gasses that prompt to balances in stature of vitality boundaries for nothing, charge bearers to stream, along these lines prompting to an adjustment in the conductivity of the detecting material.

At the point when sensor is presented to inflammable gasses, surface oxygen species respond to frame burning items. Such response brings down the oxygen species scope, gives back the free electron charge bearers to greater part of the oxide material then increments electrical conductance. Such surface reactions are as follows:

$$R + O^- \rightarrow RO + e^- \quad (1.4)$$

$$H_2 + O^- \rightarrow H_2O + e^- \quad (1.5)$$

$$CH_3OH + O^- \rightarrow HCHO + H_2O + e^- \quad (1.6)$$

Amid the adsorption of oxygen species on the surface of recognizing component, capturing of electrons from conduction band and the related decline in the charge transporter concentration (e^-) prompts to the expansion in the resistance of n-type detecting component until it accomplishes harmony. In this way, the surface resistance increments and achieves balance amid the chemisorption procedure. Along these lines, the procedure that irritates the harmony state and prompts to an adjustment in the resistance of metal oxide semiconductor. Like manner the conductivity conduct of semiconductor metal oxide, the reaction differs. Table 1.3 plainly compresses the reaction of the detecting component near oxidizing and diminishing gasses and some of the n-type and p-type metal oxide semiconductor components are recorded in Table 1.4.

Table 1.3: Classification according to the response of sensing element

Classification	Oxidizing Gases	Reducing Gases
p-type	Resistance decrease	Resistance increase
n-type	Resistance increase	Resistance decrease

Table 1.4: Classification based on the conductivity type

Conductivity	Metal oxides
n – type	ZnO, MgO, CaO, TiO_2, WO_3, SnO_2, In_2O_3, Al_2O_3, Ga_2O_3,
p – type	Y_2O_3, La_2O_3, CeO_2, Mn_2O_3, NiO, PdO, Ag_2O, Bi_2O_3, Sb_2O_3

1.7 Gas Sensing Parameters of Metal Oxide Semiconductor

The main parameters that are frequently quoted to be the most appropriate characteristics a sensor should have 3 ‘S’ i.e. Sensitivity, Selectivity and Stability are:

Sensitivity: response to small concentrations or concentration changes of pollutants.

Selectivity: strong response to some pollutants, none to others.

Stability: signal reproducibility over time.

- **Sensitivity:**

Sensitivity means response of a gas sensor when there is per unit change in the gas concentration. Chemiresistivity is the basic principle of metal oxide gas sensors and it is normally described in terms of resistance/conductance. The adsorption of oxygen particles on detecting surface is either by chemisorption or physisorption depending on the temperature. Physisorption ordinarily happens at temperatures underneath 100 °C (e.g. room temperature), with powerless authoritative between the particles and the semiconductor held together by van der Waal strengths. Generally, metal-oxide gas sensors are worked at temperatures above 250 °C in order to keeping in mind the end goal to achieve sensible flag to clamor proportions. At these working temperatures, chemisorption is the commanding adsorption handle where in the oxygen atoms are related by method for dipole clinging to the semiconductor surface and frame concoction bonds after electronic charge exchange. The standard dynamic destinations for chemisorption incorporate typical locales, disengagements, grain limits adatoms, or polluting influence iotas and so on. Therefore the Conductivity/Sensitivity of metal oxide gas sensors is explained as follows:

Sensitivity $S = \frac{R_{gas} - R_{air}}{R_{gas}}$ for oxidizing gases like NO_2, NO, O_2, and:

Sensitivity $S = \frac{R_{air} - R_{gas}}{R_{air}}$ for reducing gases like CO, H_2 and CH_4 etc. where R_{air} is resistance of the gas sensor for air and R_{gas} is the resistance of the sensor under gas exposure. So, it is clear that when the gas is bring together in the ambient atmosphere, its reactivity will depend on the species adsorbed and the state of the surface is evidently gas dependent. Broadly, most of the investigated gases are sensed in the influence that these gases have on the oxygen stoichiometry of the surface. Typically, given a steady incomplete weight of oxygen in the encompassing medium, the conductivity change in the semiconductor is as per the convergence of the test gas species.

- **Selectivity:**

A sensor should react to only a specific particle in a blend of environment. The selectivity of a gas sensor towards a specific particle is the proportion of its reaction towards it and that of another prevailing intruding atom in the air.

Selectivity = (Sensitivity of a particular molecule / Sensitivity towards an interferent)

A gas sensor' selectivity should be greater than one.

- **Stability:**

Stability is the capability of a sensor to keep its performance upto the mark for a certain period of time. For the measurement of stability, sensed values are used i.e. the signal deviation for zero absorption.

- **Speed of response:**

Upon exposure of the target gas, it is the time required for a sensor to achieve 90% of its total response, for example, resistance upon introduction to the objective gas.

- **Recovery time:**

After the removal of target gas, it is the time required for a sensor to return back to 90% of its original baseline signal.

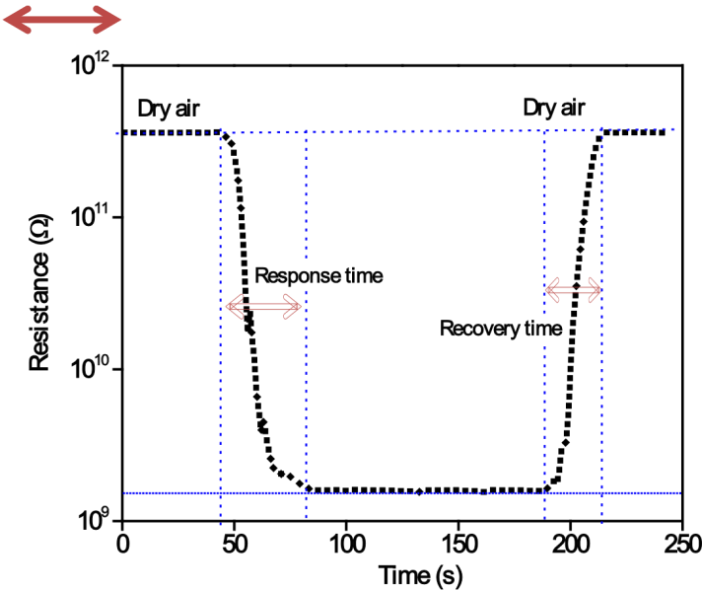

Fig.1.6: Schematic views of the response time and recovery time

- **Detection limit:**

At a particular temperature, it is the minimum concentration of the gas that can be sensed under specified conditions.

- **Accuracy:**

It is the degree of correctness of a measured value related to the true value.

As adsorption, reaction and desorption of gases are temperature activated processes; therefore most of the gas sensing properties depend on the temperature of

operation [16]. So, the operating temperature of the sensor is the important factor for its response towards specific gases.

Now, it is additionally vital to call attention to that the surface conductance and not mass conductance qualities are balanced and measured as electrical signs, thus it is profitable to have detecting surface as thin and permeable as could reasonably be expected. Therefore, the adsorption of gaseous species controls the surface and grain boundary resistance of the oxide. As gas adsorption is related to the surface of the material, therefore, polycrystalline and even nanocrystalline structures are preferred.

1.8 Importance of Nanotechnology in Gas Sensor Research

Nanotechnology can be defined as the engineering of functional systems at nanoscale. At this scale, properties exhibited by the materials are not similar to the properties at the macro scale. Nanocrystalline materials can be classified into different categories depending on the number of dimensions that are nanostructured (with dimensions lower than 100nm); a possible classification is zero-dimensional for clusters, mono-dimensional for nano-wires and two dimensional for films. These nanostructures, due to their peculiar characteristics and size effects, often show novel physical properties compared to those of the bulk. The potential of these innovative structures is being exploited for gas sensing applications. The significance of joining nanostructures into detecting components is different overlap; their staggeringly high surface to volume proportions give improved surface zones to association with gasses, their one of a kind electronic properties empower quick perceptible signal changes, their little sizes permits them to be incorporated into smaller than expected gadgets that can be worked at low powers [18].

With the advancement in technology, the need for precise and sensitive gas sensors continues to increase. Over the last few decades, researchers around the world have been able to meet this demand with the use of advanced technology. In this context, metal oxide semiconductor sensors have been gaining popularity and finding extensive use for their higher sensitivity and smaller size. Also, with the advent of nanotechnology, scientists have been able to achieve new horizons in the field of gas sensors. In the later past, the interest of researchers and specialists towards gas-delicate materials has increased huge energy because of the

introduction of nanotechnology. This idea is essentially because of the promising electronic, optical, and thermal properties of nanomaterials, their size and shape reliance and capacity to control the material structure by new trial systems. In 1991, Yamazoe et al. [19] showed that the decrease of crystalline size indicates to substantial increase in sensor performance. Since then the "small size effect" of metal oxides has been reported by many publications [20–23]. Thus, the increase in surface volume ratio has a great impact on increasing sensitivity. Nano sized grains of metal oxide semiconductors i.e. all the carriers are trapped in surface states transition interaction.

Some of the key advantages of nanotechnology in gas sensing research are:

- Very large surface-to-volume ratio, leads to the adsorption of gases on the sensor surface and thus increase the sensitivity of the sensor as the interaction between the targeted gas and the sensing part become more.
- Promising functionalization of nano-surface with a target-specific gases.
- Dimensions are comparable to the surface charge region.
- Operating temperature can be modulated to select the proper gas metal-oxide semiconductor interaction.
- Catalyst deposition is advantageous over the surface for inhibition of specific reactions.
- Charge confinement ability is concentrated in specific energy levels (Density of States of charge carriers).
- Sol-gel is relatively simple preparation method that allow large-scale production.
- Leads to enhancement of catalytic activity & surface adsorption.

In this manner, the key ranges of current metal oxide semiconductor gas sensor research incorporate the advancement of detecting platforms with enhanced sensing capacities, measure lessening of devices to enable low-power utilization and affordability. Gas sensors constructed at the nanoscale are extremely sensitive, selective, and responsive and thus, the impact of nanotechnology on gas sensors is huge. In these years, numerous kinds of nanostructures of several materials have been studied for gas sensing applications counting as nanoparticle films, nanowires, nanofibers, nanocrystalline thin films, nanorods, and nanopillars [21]- [27]etc.

It has been reported that thin film gas sensors exhibit higher sensitivities in comparison with other type of sensors. Recently, metal oxide semiconductor thin

films have appealed significant attention as gas sensing materials due to their higher specific surface area and reduced grain size than bulk materials, that can lead to lower operating temperatures, higher response, and fast response processes [28]-[29]. Moreover, nanocrystalline thin films are more compatible with current micro-fabrication processes and circuits. Such features make the application of nanocrystalline thin film gas sensors easier and flexible [30]-[31]. Therefore in this thesis work the nanocrystalline thin films of Tin/Zinc oxide have been developed to investigate the gas sensing properties.

1.9 Factors Influencing the Sensor Performance

Apart from three "S" i.e. high sensitivity towards target gas, high selectivity, and high stability commercial metal oxide semiconducting sensors also need to be cost-effective, high speed of response i.e. rapid detection of changes in surrounding environment and sensing response should increase linearly with increasing the concentration of target gas (linearity), reliable and operate at relatively low temperature with marginal power drain. Unluckily, creating a sensor that satisfies all these requirements effectively has not yet been realized and there is no universal judgment for concurrent optimization of all such sensors parameters. Therefore, one should always seek a negotiation between these parameters of the developed gas sensor.

Many academics have revealed that the revocable interaction of gas with the surface of material is the distinguishing of conductometric semiconducting metal oxide gas sensors. This response can be affected by many factors that include internal and external reasons, like microstructure of sensing layers, the natural belongings of base materials, surface area, surface additives, humidity, and temperature etc. There are countless metal oxide semiconductor based gas sensors existing commercially in the market with thick and thin film form of SnO_2 and ZnO as sensor elements.

Besides choice of sensing materials, form of sensing materials, metal electrodes etc., the gas sensing characteristics for an efficient thin film gas sensor could be controlled by the following physical parameters:

- Bulk and surface stoichiometry of the sensing film (no of oxygen vacancies on surface and bulk or charge carrier concentration)

- Electronic parameters of adsorbed species (adsorption/desorption energies, positions and distributions of local electronic levels in the forbidden gap etc.)
- Geometrical and structural parameters of the sensing thin film (roughness, thickness and porosity of the film etc., crystallographic structure and size of grains).
- Parameters related to dopants or catalysts (type, size, quantity of the catalyst and its way of dispersal etc.)

It is also well known that operating characteristics of metal oxide based semiconductor gas sensors are controlled by three independent factors such as transducer function, receptor function and utility (peculiarities of sensor construction). Receptor function affords the capability of the oxide surface to interrelate with the target gas, and transducer function offers the competency to convert the signal produced by chemical interface of the oxide surface into electrical signal. The last but not the least factor, utility, concerns the accessibility of inner oxide grains to the target gas [32].

As needs be, in the most recent years, scientists are moving in the direction of the advancements of metal oxide semiconductor based sensor components with higher affectability and enhanced selectivity. The advancement of basic parameters, for example, grain measure, grain arrange, porosity, surface, and so on are essential issues for enhancing gas-detecting qualities of resistive (conductometric) sort sensors. Sensor's reaction from the purpose of decreasing gas location relies on upon both the sensor material and the way of distinguishing gas.

a) Parameters of Sensor Elements

- Operating temperature
- Gas Sensitivity
- Selectivity of gas response
- Thermal stability
- Rate of Response

b) Parameters of Sensing Materials:

- Catalytic Activity
- Crystallographic Structure
- Surface Structure
- Morphology
- Chemical Composition

However, the alteration in any one of the above parameters may be complemented by an adversative change in other characteristics. For instance, sensitivity and stability are interrelated parameters as well. Though, lesser the

crystallite size, greater the sensor response is. However, the stability of gas sensors with finely distributed grains is normally decreased.

Therefore, during the time spent adjusting sensor execution by modifying the parameters of sensor component or gas sensors, one ought to know about the impact of one parameter over different parameters and thusly the reaction and selectivity [33]. However, there is no universal result for concurrent optimization of all such sensors parameters. Therefore, one should always hunt for a negotiation between high stability, high sensitivity and high selectivity of the developed sensors.

1.9.1 Role of Operating Temperature in Metal Oxide Thin Film Gas Sensors

Since every reaction taking place at the surface of the semiconductor, as well as the most probable species adsorbed and, hence temperature specially affects those properties related to the processes occurring at the surface of the sensor. Therefore, all the reaction sites are temperature dependent. For example, adsorption and desorption processes are temperature activated processes, as well as surface coverage by molecular and ionic species, chemical decomposition, and reactive sites. Along these lines, dynamic properties of the sensors, for example, reaction and recovery time and the static qualities of the sensor likewise rely upon the temperature of operation [16], and a temperature for which the sensitivity of a semiconductor gas sensor is most extreme called ideal temperature.

As talked about in the sensing mechanism that the species that tend to trap electrons from the semiconductor are the individuals who are effortlessly adsorbed. This infers, under regular working conditions (comprehended as a surrounding, for example, engineered air (79% N_2 + 21% O_2), in which some little amount of different gas is presented and certain wetness conditions), the surface of metal oxide semiconductor is fundamentally secured by oxygen and water species. Thus, the oxygen accessible and also the diverse species coming about because of water is vital for the comprehension of the working conduct. In this way, adsorbed oxygen species change at the surface of an oxide as per the general plan O_2 ads $\rightarrow$ $(O_2 \text{ ads})^-$ $\rightarrow$ $(\text{Oads})^-$ $\rightarrow$ $(\text{Olattice})^{2-}$, in which they are steadily getting to be wealthier in electrons. At room temperature every one of the structures are adsorbed, being the scope of the species at the surface confined by Weisz restrain [34]. Truth be told, at room temperature, the harmony of the $(O_2\text{ads})^-$ scope with vaporous O_2 is drawn closer

gradually. With increasing temperature $(O_2\ ads)^-$ proselytes to $2(Oads)^-$ by taking one electron from the mass, in this manner bringing about (at consistent oxygen scope) an expansion of surface accuse thickness of relating varieties of band twisting and surface conductivity. As per Yamazoe et al. [35] oxygen desorbs with a greatest temperature of desorption as physisorbed O_2 at 80 ^{0}C, as O^{2-}at 150 ^{0}C and O^-or O^{2-}at 520 ^{0}C, while at temperatures higher than 600 ^{0}C the thermal reduction happens and lattice oxygen is desorbed. Consequently, (O^-ads), which is a very sensitive species, is the prevailing specie in the case of metal oxide for temperatures between 423 and 933 K, whereas the O^{2-} species are extremely unstable and do not be considered for the sensitivity. Truth be told, this is the slightest stable type of oxygen in the gas stage, and gets to be balanced out just in the crystal lattice by the electric field made by its neighbouring activities. The net impact of surface states coming from adsorption of oxygen particles or from crystal structure imperfections is, the point at which a high grouping of surface states is available, a sticking of the Fermi level inside the band-gap. However, a gaseous species, which apparently has nothing to do with such a redox process, can also affect the electric resistance, as typically exemplified by the case of water vapor adsorption because of the dissociative adsorption of water. Water can be adsorbed in two states: molecular water, H_2O (physisorption), and hydroxyl groups, OH^- (chemisorption). Adsorption of H_2O vapor always yields a huge increase in electronic conductivity.

In this manner, there are diverse conceivable temperature-subordinate basic strides of sub-atomic acknowledgment with semiconductor gas sensors that must be improved for the particular discovery of a specific particle. These means firstly include the low-temperature surface responses. Illustrations are adsorption and synergist responses at dynamic locales (the last including characteristic point imperfections, for example, oxygen opportunities, as well as extraneous point surrenders, e.g., isolated metal particles) and comparative responses at grain limits or at three-stage limits (e.g., at metallic contacts or at surface metallic groups). These responses include adsorbed negatively charged sub-atomic ($O^{2-)}$ or nuclear (O^-) oxygen species. These means furthermore include the high temperature mass responses between point deserts in the metal oxide crystal and oxygen (O_2) in the gas stage. The key for the controlled operation of such sensors is the cautious modification of the operation temperature, since conduction changes upon

introduction to various gas segments as a rule indicate distinctive maxima as a component of temperature. The necessary reversibility of the sensor response under steady-state or constant-flow conditions requires that all of the involved reactions are thermodynamically or kinetically controlled. For low-temperature sensor operation, the surface concentration of adsorption or reaction complexes must be unequivocally given by the temperature and the partial pressures in the gas phase. For high-temperature operation this requires that the bulk defect equilibrium adjust the concentration of doubly charged oxygen vacancies in the oxygen sub lattice of metal oxide and the segregation distribution of dopants at the surface and interfaces. Many of these reactions lead to a change of the electron concentration and hence to a change of the partial electronic conductances at the surface, in the bulk, at contacts or at grain boundaries. So, it is clear that when a gas is introduced in the ambient atmosphere, its reactivity will depend on the species adsorbed and the state of the surface is evidently gas dependent. In general, most target gases are detected via the influence that they have on the oxygen stoichiometry of the surface.

It is evident that gas detection with metal oxide semiconductors cannot be totally clarified by only taking into account the charge transfer occurring at the surface of the semiconductor. Charge transfer only explains the situation in equilibrium and surface reactions have to be considered for a detailed understanding of the response to different gases. Indeed, it has been demonstrated that in porous sensors besides reactivity, diffusivity of gases or more precisely, difference in diffusivity between a target and oxygen gas, is an important factor determining the sensitivity of the sensor [36]. This makes the sensing properties of metal oxide semiconductor to be dependent on the molecular size of the sensed gases and of temperature, as all diffusion mechanisms are also highly temperature dependent.

1.9.1.1 Effect of Operating Temperature on Sensitivity and Selectivity

It is possible to improve the sensors selectivity by varying the sensor operation temperature [37]. The gas sensing mechanism of semiconductors makes their performance susceptible to temperature changes. Different pollutants have characteristic optimum oxidation and reduction temperatures and therefore give rise to characteristic resistance-temperature profiles. By varying the operation temperature of the sensor it is possible to increase or decrease its sensitivity and selectivity towards specific gases. This special attribute of semiconductor gas sensors was exploited to

maximize the sensor signal to each target gas, (i.e. increase the sensors sensitivity) and discern between two targeted gases (i.e. increase the selectivity) [38]. A higher working temperature will improve response time and the recovery time of the sensor [39], and is accordingly preferable. However, higher operating temperature of gas sensor is inconvenient because high working temperature of the gas sensor increases the operating cost and requires high operational safety measures in an environment with explosive gases like hydrogen. Higher power consumption and short battery life time are also other drawbacks of higher sensing temperature.

The targeted applications for the sensor system require a selective detection of one pollutant in a binary mixture. It is possible to detect hydrogen and methane qualitatively and quantitatively in a mixture of both gases. Single thin film sensor with the same sensitive material operated at different temperatures show a completely different reaction to hydrogen and methane. This behaviour allows establishing a calibration for the complete sensor system that discriminates between these two gases in mixtures.

The next step for increasing the sensor selectivity is naturally to move from constant to dynamically modulate temperatures [38]. The simplest way to observe a temperature dependent dynamic sensor response is literally to switch the sensor power supply at two optimal temperatures, with and without two gases in mixtures. The transient response of the sensor is characteristic of the gas to which the sensor was exposed. This behaviour indicates the potential for qualitative and quantitative analysis of gaseous mixtures [40]. More promising seems the application of a periodic heating voltage to the semiconductor gas sensor. Several advantages can arise from an oscillating heater voltage [41]. Firstly, because of the different reaction rates of various analyte gases at different temperatures, a cyclic temperature variation can give a unique signature for each gas. These “fingerprints” allow for detecting the presence of a specific gas in a mixture of gases and to some degree reveal quantitative information. Furthermore, if the response of one sensor is measured at n temperatures, the sensor becomes analogous to an array of n “sensors” [42]. Secondly, because low temperature operation can lead to the accumulation of incompletely oxidized contaminants, periodic shifts to higher temperatures may help to clean the sensor surface, increasing the desorption rate and reducing the sensor recovery time. Thirdly, thermal cycling leads to improvements in sensitivity.

1.9.1.2 Effect of Operating Temperature on Stability

The long haul stability is a key parameter for gas sensors, however it is dependably been disregarded by scientists, which has constrained the useful uses of the sensors, particularly when the sensors are working at hoisted temperatures. The grain size, necks and limits and in addition the surface deformities would be changed amid the long haul operation at high temperatures, which prompts to the variety of sensor reaction under a similar condition and declines the sensor stability [43]. Consequently, temperature is an important issue that greatly influences the sensor response of metal oxide semiconductor gas sensors. Generally, higher temperature would prompt to higher detecting execution because of the bringing down of initiation vitality for gas adsorption and desorption. However, high working temperature of the gas sensor is energy intensive, increases operating cost and requires high operational safety measures in an environment with explosive gases like hydrogen etc. Therefore, a noteworthy protest in the research of metal oxide semiconductor sensors is to reduce the working temperature with considering the lessened power utilization and removal of security issues. However, the temperature stability ought to be considered and somewhat higher temperature would be ideal to render the required stability.

Still, nanocrystalline thin films, that are two-dimensional nanostructures, have been explored for many years as gas detecting materials [27]. Additionally, alongside the advancement of synthesis procedures, gas sensors in view of metal oxide semiconductor thin films show great compatibility with integrated circuits for high integrated sensors. Therefore, as of late, a considerable measures have been researched for enhancing the detecting performance of thin film gas sensors, e.g., working temperature, porosity, particle size, doping impact, noble metal compositing and electrode engineering, and so on. Therefore in this thesis the sensitivity, selectivity and stability of nanocrystalline Tin/Zinc oxide thin films is investigated using catalytically active materials, such as Li, Pd, Cu or Ag in the host material as dopant.

1.9.2 Role of Additives in Metal Oxide Thin Film Gas Sensors

The presence of several interferents may affect the sensing response characteristics of semiconductor gas sensors and hence the selectivity (cross sensitivity) is an important issue in thin film metal oxide gas sensors. In order to

improve the selectivity of the sensor towards a particular target gas, incorporation of a suitable catalyst or additive in the sensing material is known to be the most effective solution. Integration of an appropriate type and optimum amount of catalyst with novel dispersal in sensing layer improves the sensing response and operating temperature significantly. Surface morphology and microstructure of the sensor surface defines the sensing properties which in turn depend on the growth kinetics of the thin film and processing parameters [44]. The presence of catalyst or additive improves the receptive function for the target gas molecules and the base sensing material can be independently optimized for enhanced transducer function. This leads to the enhancement of sensor response and enables it to sense even low concentrations of target gases. The improvement in response characteristics is attributed to several factors, including electronic and physico–chemical properties of the sensing matrix having catalyst/additives, surface potential and inter-crystallite barriers, sizes of crystallites etc. [45].

Catalytic additives produce sites for increased adsorption rates as well as dissociate the target gas molecules to produce a high concentration of active species which are easily adsorbed on the surface of sensing layer (SnO_2 or ZnO), thereby producing a large change in conductance of the sensor [46]. Therefore, the introduction of catalyst/additives can lead to a significant improvement in the gas sensor response by means of a selective promotion of the desired molecular reaction of the target gas species at the chosen sites on the metal oxide sensing layer [47]. Size, shape and distribution of the catalysts/additives are also considered to be important for enhanced gas sensing characteristics [48]. In spite of extensive literature on catalysts/additives in SnO_2 or ZnO for detection of harmful and toxic gases, very few efforts have been made towards the studies with the emphasis on the amount and distribution of catalysts to be incorporated in the sensing layer to achieve improved response [49]-[50].

From sensing point of view, newly reactive sites are added to the surface of the semiconductor. By definition, a catalyst interacts with educts while not changing itself. There are two ways in which a catalyst can influence a reaction. First, it can increase the concentration of reaction partners at the reaction site. Thereby the reaction probability is increased. And second, it can decrease the activation energy of the chemical reaction and thereby open new reaction paths. From a physical point of

view, dopants change the amount of free charge carriers in the conduction band by creating new donor (n-doped) or acceptor (p-doped) states. Metals of the oxidation number 3+ are used as acceptor type doping to decrease the conductivity (e.g. Al, B), whereas those with an oxidation number 5+ are used as donor doping to increase the conductivity (e.g. In, Sb) [5]. For metals with both oxidation states (3+, 5+) the effect on the conductivity depends on the doping concentration. Two theories for the influence of catalysts on sensing properties of semiconductors are discussed in literature [51] - [52]: the spill-over mechanism and the Fermi level control. Spill-over is attributed to the presence of metallic clusters at the surface of metal oxide grains. The catalyst forces a dissociation of reactants and thereby increases the concentration of reactive particles at the surface. Fermi level control is related to an electronic interaction in which oxygen adsorption on the catalyst removes electrons from the catalyst. The catalyst, in turn, removes electrons from the supporting semiconductor, thus controlling the energy of the Fermi level and influencing the band bending in the metal oxide grain.

There are reports on incorporating the catalyst into the sensing layer in various forms including composites, thin film over-layer, nanoclusters on surface, nanoparticles on surface or inside sensing layer, etc. [53]-[54]. Each type of incorporation of catalysts/additives has shown to be exhibiting different sensing response characteristics corresponding to a particular target gas [55]. Hence it is very important to identify the way of incorporating catalysts/additives into the sensing layer and its quantity should be optimized so as to obtain enhanced response characteristics towards a particular target gas. The research on gas sensors is related to many fields such as physics, chemistry, and electronics. Addressing these problems will be one of the great challenges and it is important to enhance interdisciplinary collaboration.

1.10 Applications of Metal Oxide Gas Sensors

Since the first commercial semiconductor gas sensors have been offered by the company Figaro in 1968, the sensor market has continued to grow steadily. Nowadays, millions of gas sensors are sold every year in many different applications, as demonstrated in Table 1.5.

Table 1.5: Actual and future areas of application for metal oxide gas sensors

Domestic Alarms	fire (CO), natural gas heating
Automobile	driver's cabin air quality, control of ventilation hatches, exhaust
Medical	disease detection through breath analysis
Military	chemical and biological warfare
Ventilation	air quality monitoring in tunnels or underground parking garages
Environment	environmental monitoring systems, personal exposure alarms
Industry	process-control, leakage alarm
Aerospace	Hydrogen leak detectors, sensors for oxygen, NOx, VOCs
Household Appliances	intelligent refrigerator or oven
Life-Style	bad breath detection, blood alcohol

Among them, domestic alarms, automobile air quality control and industrial process control are the most prominent areas of application. Other fields are currently experiencing strong research efforts by public and private societies. Gas sensors are also popular because of the applications of electronic noses. Electronic noses are a new concept of sensor application, which tries to mimic the human olfactory system by using an array of electronic gas sensors with partial specificity and appropriate pattern-recognition electronics, using artificial neural networks [56]. Electronic noses can be applied successfully to Environmental monitoring; - Medicine applications, as an electronic nose can examine odours from human body and thus can serve to identify diseases; - Food industry, which constitutes the largest market for electronic noses, whose applications include quality assessment in food production and inspection of food quality by odour [57]-[58].

Accordingly the next chapter of this thesis will cover the comprehensive literature survey on SnO_2 and ZnO based gas sensors for various gases and based on these studies objectives of this work will be defined.

Chapter 2 Literature Review and Objectives of the Thesis

2.1 Introduction

Nowadays, investigation is directed rather than to new sensors, to enhance the gas detecting characteristics of existing sensors. Ideal gas sensor must have: high sensitivity towards target gas, better selectivity, high stability, high reliability and minimal sensitive to humidity and low temperature, robust, durable, short reaction and recovery time, easy calibration and have small dimensions. However, till now no universal judgment regarding concurrent optimization of these sensors parameters. Therefore, we have to always seek a negotiation among these factors.

Although SnO_2/ZnO gas sensors are dominatingly solid-state gas distinguishing devices with numerous points of interest, for example, minimal effort, simple generation, reduced size, and hence have been broadly utilized as a part of numerous fields like public safety, and toxin checking. Be that as it may, there is some space to enhance the detecting capability of these gas sensors by controlling the structure and morphology of detecting materials.

It has been established that tin/zinc oxide gas sensors are used in different structural states i.e. single crystalline state, amorphous-like state, nanocrystalline state, and glass-state and polycrystalline state. The properties and characteristics of each state have their own merits and demerits which will affect their performance. Because of the single crystalline state one-dimensional structure has maximum stability and therefore could enhance the temporal stability of the device. Shockingly, the issue of division, measuring, and controlling the one-dimensional structures is not determined till now. To accomplish uniform sizing and orientation, new propelled advances should be actualized, and these future costly and not open for broad utilization. Accordingly, gas sensors in light of individual one-dimensional structures are not yet promptly accessible economically. Assist, the engineering expense of gas sensors in view of one-dimensional configurations would high than that of nanocrystalline. Therefore in near future, nanocrystalline and nanostructures would be dominant stage for solid-state gas devices. Consequently, for this thesis, focus is on the gas sensing properties of nanostructured SnO_2/ZnO oxides thin films because of their excellent gas sensing properties and widespread usage.

2.2 SnO_2 and ZnO Based Gas Sensors Literature Review

So far, nanostructured SnO_2/ZnO oxides are very complicated materials for study, since the electro-conductivity of such oxides rely on large number of parameters [59-68]. Consequently, to indicate ideal advancements for gas sensor producing the premise of these materials is extremely troublesome. In addition, there is absence of general articulation that setting up an association between structural parameters and sensor response parameters. In any case anyone can locate countless works in this field.

Egashira's group [69]-[72], led a subjective investigation of material porosity impact on sensor reaction while, Yamazoe and his associates have lot of investigation and finding in ceramic sensors [73]-[79], in which an immediate relationship between grain size and conductivity have been demonstrated for metal oxides sensors.

Morante's gathering [80]-[84], set up a relationship between structure and gas-detecting properties of metal oxides while, works of Korotcenkov's gathering underscored the requirement for a more extensive engineering for structural analysis of metal oxide semiconductor thin films for solid-state gas sensors [85]-[89].

In addition to the above groups, there is lot of works in this field; consequently, detailed literature review on SnO_2 and ZnO for the sensing of various toxic and harmful gases in the form of nanostructures and thin films is summarized in Table 2.1. A brief report on literature review will be discussed in the subsequent section. At the end of this chapter based on detailed survey and identified gaps, the research objectives of this work will be proposed and thesis organization has been explained in the next proceeding section.

Table 2.1: ZnO and SnO_2 for the sensing of various toxic and harmful gases in the form of thick films, thin films and nanostructures

Year	Material	Gas	Concen. (ppm)	Sensitivity Response (S)	Operating Temp. (°C)	Ref.
2016	Ag/Ag_2O-SnO_2	H_2	200	41	170	[90]
2016	ZnO	CO_2	5000	65	400	[91]
2015	ZnO/Pt	H_2	1000	15	300	[92]
2015	1% In: ZnO	H_2	500	45	300	[93]
2015	Fe-SnO_2	H_2S	10	14.5	225	[94]
2015	ZnO	C_2H_5OH	03	51	400	[95]
2014	Zn_2SnO_4/ ZnO	H_2	1000	47	277	[96]
2014	Pt-ZnO/SiC	H_2	400	20	600	[97]

2014	ZnO	CO	1000	52	400	[98]
2013	ZnO	H_2S	20	22	250	[99]
2013	ZnO	H_2S	20	19	325	[100]
2013	Sn-ZnO/TiO_2	H_2	1%	1.48	160	[101]
2013	3% Cu/ZnO	H_2	200	44	150	[102]
2013	Cu-ZnO	H_2S	20	0.38	250	[103]
2013	AlN-ZnO	NH_3	600	30	150	[104]
2012	ZnO	NH_3	1000	80.6	300	[105]
2012	ZnO	C_2H_5OH	200	22	550	[106]
2012	SnO_2	H_2	270	5	350	[107]
2012	ZnO	CO	250	46	400	[108]
2012	ZnO	C_2H_5OH	50	24	320	[109]
2012	SnO_2	H_2	1000	120	350	[110]
2012	ZnO	CO	100	11.2	300	[111]
2012	ZnO	H_2	500	11	280	[112]
2012	Pd: SnO_2	H_2	500	25.8	250	[113]
2012	Pt/ZnO	H_2	100	1	500	[114]
2012	SnO_2 + In_2O_3	H_2	4600	55	480	[115]
2012	Au:ZnO	H_2	300	33.5	200	[116]
2012	Pd:SnO_2	H_2	500	25.8	250	[117]
2012	ZnO	H_2	500	11	280	[118]
2012	SnO_2	H_2	10000	8	300	[119]
2012	ZnO	H_2	1000	8.5	500	[120]
2011	SnO_2	CO	4000	1.2	300	[121]
2011	$Mg_{0.1}$ $Zn_{0.9}O$	H_2	5000	50	300	[122]
2011	SnO_2-TiO_2	H_2	20	10.5	400	[123]
2011	Ni-SnO_2	C_2H_5OH	1400	85	300	[124]
2011	ZnO	H_2	1000	2.2	200	[125]
2011	SnO2	H_2	350	20	350	[126]
2011	ZnO	NO_2	0.463%	120	500	[127]
2011	Pd-SnO_2	H_2	1000	151.2	250	[128]
2011	CuO-Au-SnO_2	H_2S	10	18.7	230	[129]
2011	ZnO	H_2S	30	11	350	[130]
2010	Cu -SnO_2	LPG	500	1.3	300	[131]
2010	Pd-SnO_2	H_2	1000	26	280	[132]
2010	ZnO	H_2	1000	7.8	400	[133]
2009	SnO_2	NO_2	510 ppb	3.1	210	[134]
2009	SnO_2	H_2	100	2	300	[135]
2009	Au/Pt:SnO_2	H_2	10000	2	150	[136]
2009	SnO_2	H_2S	20	20	150	[137]
2008	SnO_2/Pd	C_2H_5OH	20	33	300	[138]
2008	ZnO:TiO_2	H_2S	1000	0.5	250	[139]
2008	CNT/SnO_2	H_2	1500	3	250	[140]
2008	SnO_2	H_2S	3	.07	300	[141]
2008	Cu-ZnO	LPG	625	52	190	[142]
2007	ZnO	H_2	1%	14	400	[143]
2007	ZnO/Si	H_2	3%	5.5	150	[144]

2007	ZnO	C_2H_5OH	1500	61	300	[145]
2007	Pd-Ag-ZnO	CH_4	1%	74	250	[146]
2007	ZnO	LPG	0.4%	43	400	[147]
2006	Cu-ZnO	CO	20	2.7	350	[148]
2006	Al: ZnO	C_2H_5OH	400	20	250	[149]
2006	SnO_2	CH_4	1000	65	360	[150]
2005	CuO/ZnO	H_2	4000	4.9	400	[151]
2005	SnO_2 sols	H_2S	5	104	150	[152]
2005	SnO_2 -Co_3O_4	H_2	1000	91	250	[153]
2005	Cu/Sn	H_2S	300	33	200	[154]
2005	Sn-ZnO	NO_2	1.5%	6	150	[155]

It may be observed from the above Table 2.1 that most of the sensors fabricated utilizing SnO_2/ZnO nanostructures or thick/thin films required normally higher operating temperatures (200 to 450°C) and exhibited low sensing response even at higher gas concentrations. Such high working temperature of the gas sensor is energy intensive, increases operating cost and requires high operational safety measures in an environment with explosive gases. Therefore, designing a sensor structure with higher sensing response at low operating temperature having capability of sensing low concentrations of target gas with good selectivity is the most challenging task. Since, gas detecting is primarily surface dominating phenomenon, thin films or nanostructures of SnO_2/ZnO are gaining extensive attention of research community due to enhanced surface to volume ratio in comparison to their bulk complement and are expected to give improved sensing response at low operating temperature. Moreover, nanocrystalline thin films are more compatible with current micro-fabrication processes and circuits [30]-[31]. Therefore in this thesis thin films of Tin/Zinc oxide have been developed to investigate the gas sensing properties.

Thin films of various metal oxides as sensing material are deposited using various deposition techniques like RF sputtering, spray pyrolysis, metal-organic chemical vapor deposition, sol-gel and pulsed laser deposition (PLD) technique etc. [156]-[159]. Each of these techniques has their own advantages and disadvantages like, sol-gel technique is advantageous due to the following reasons:

- Good control over composition
- Large area deposition, planner and non-planner substrates
- Ease of doping
- Non-vacuum processing.

However, pulsed laser deposition (PLD) technique is preferred because of the following reasons:

- Good quality metal oxide thin films with controlled stoichiometry
- Fast turn-around time for initial optimization (due to ease of target preparation)
- Introduction of external dopant and preparation of multilayered structure and heterojunction devices could be achieved easily using PLD.

Therefore, in the present work Sol-Gel and PLD techniques have been exploited for deposition of nanocrystalline SnO_2/ZnO thin films for development of suitable gas sensor. However, it is found to be very important at the first step to identify the target gases for which an efficient sensor need to be developed, so that the proper catalysts/additive could be identified for getting an enhanced response. This is followed by appropriate dispersal of the catalysts/additives in the sensing layer in optimized quantity.

2.3 Importance of Sensing Hydrogen

Lately, look into for perfect future fuel energy has been working on with astonishing pace. The energy must have nil emanations, be adequate in its natural form, and proficient. Hydrogen (H_2) as a fuel meets every one of the benchmarks impeccably. Not only H_2 promptly accessible in nature as well as when ignition happens the results given out are water and oxygen (O_2) making it an uncommonly ecological lovely fuel. The amount of energy created through H_2, is around three times the energy enclosed in the equivalent of gasoline and essentially seven times than the coal. Best resources of H_2 are electrolysis of water, present in nature as natural gas and decomposition of hydrogen containing composites. So, energy components are composed in light of H_2 and are thought to be “batteries without bounds”. In the most of space programs, H_2 is used to launch the space vehicles. The different space agencies have utilized liquefied H_2 since three decades for thrust in space vehicle and used in many more rockets for parking in their orbit. H_2 energy units control the shuttle's electrical frameworks, creating a perfect repercussion (unadulterated water), which the team drinks. Consequently, it is conceived that H_2 will shape the essential vitality foundation that determination future social orders. Moreover, H_2 is also used in metal smelting, semiconductor processing, glass making and petroleum extraction, due to its strong reducing properties. Though; suffocation

may be caused in the enclosed zone by its reducing nature for O_2 concentration. Due such oxygen deficiency could cause fast breathing, and even death [160]-[162].

Although, H_2 has lower explosive limit (LEL) i.e. 4% in atmosphere that suggests gathering of 4% concentration is risky means that a little start might light the blend. By means of H_2 is suggested to be utilized as the cutting edge's fuel, and by the fact that it become unsafe in juncture, therefore any leak must be remembered and it accordingly gets be important to check H_2 amount in the atmosphere. Consequently for the detection of H_2 such a low levels limit, high accuracy sensors must ne required that might sense a hole of small percentage i.e. 0.5% to 4 %. According to applications the level of acceptability changes. Therefore a hydrogen sensor must detect the leak in normal level of surrounding in atmosphere and also in the different environment depending upon the requirement according to situations. Furthermore, transport of H_2 is exceptionally troublesome, since it diffuses through generally materials. As needs be, H_2 transport and volume can be hazardous if not maneuvered carefully [163]. In this manner, security will be the top necessity for all parts in the H_2 energy, but detecting H_2 spills from volume and transportation gear has turned out to be exceptionally key.

As a matter of fact, Hydrogen (gas) is tasteless, colorless, inflammable, odorless, and explosive, so it cannot be sensed by the human beings. At present time, there are numerous sorts of industrially accessible H_2 gas devices like metallic, thermoelectric, electrochemical, semiconductor, optical and acoustic ones, though semiconductor metal oxide based gas sensors show high sensitivity, quick reaction, and high stability [164]-[165].

However, SnO_2/ZnO thin film based gas sensors are usually not very selective. Nowadays, the research on these materials is focused to increase their sensitivity, selectivity and stability, and one of the main issues to accomplish these issues is the presence of metals at low concentrations. To improve their performance catalytically active materials/impurities, such as Pd, Al, In, Fe, Mn, Sn, Li, Ag, Mg, and Cu etc., are often added in host material as dopant [55], [82], [122], [136],and [166]-[171]. Consequently, a trustworthy and economical metal oxide based thin film hydrogen gas sensor needs to be industrialized to save human lives as well as security component in the upcoming hydrogen based economy.

2.4 Motivation/Gaps in the Existing Work:

Research is a reasoned investigation. It may be seen from Table 2.1 that extensive efforts have been made towards utilization of ZnO and SnO_2 thin films for detection of various gases and literature is very vast due to the fact that both materials (ZnO and SnO_2) respond to a number of different oxidizing and reducing gases. As discussed, hydrogen gas is considered as one of the best renewable resources of clean energy, with high heat of combustion (142kJ/g), low minimum ignition energy (0.017 mJ) and wide flammable range (4-75%), as well as high burning velocity. Generally the sensitivity of SnO_2/ZnO based hydrogen gas sensors vary in accordance with the concentration (50 to 10000 ppm) of hydrogen at high operating temperature between (200 to 450 ºC). Following are the important parameters that motivate us for this work:

2.4.1 To Reduce the Operating Temperature of Gas Sensor

Still, the major problems associated with most of the SnO_2/ZnO thin film based hydrogen gas sensors are their high operating temperature normally between 200 to 450 ºC (as seen in Table2.1) and low sensitivity. Such, high working temperature of the gas sensor is energy intensive, increases operating cost and requires high operational safety measures in an environment with explosive gases like hydrogen etc. Moreover, higher power consumption and short battery life time are also the other drawbacks of higher sensing temperature. Thus, it is urgent to reduce the operating temperature of the SnO_2/ZnO thin film based hydrogen gas sensors. In order to overcome this drawback, considerable research and development are underway.

Therefore, our focus in this research work is to decrease the operating temperature of SnO_2/ZnO based hydrogen gas sensors by considering reduced power consumption and removal of safety problems.

2.4.2 To Increase the Sensitivity

To enhance the sensitivity of the sensor towards a specific target gas, incorporation of a suitable catalyst or additive in the sensing material is known to be the most effective solution. Integration of an appropriate type and optimum amount of catalyst with novel dispersal in sensing layer improves the sensing response and

operating temperature significantly. By definition, a catalyst interacts with educts while not changing itself i.e. it can increase the reaction probability through the spill-over mechanism and second, it can also decrease the activation energy of the chemical reactions with Fermi-level control. Thus the presence of catalyst or additive improves the receptive function for the target gas molecules and the base sensing material can be independently optimized for enhanced transducer function. This leads to the enhancement of sensor response and enables it to sense even low concentrations of target gases.

Nowadays, the research on SnO_2/ZnO thin film gas sensors is focused to increase their sensitivity. To improve their sensitivity catalytically active materials/impurities, such as Li, Ag, Sn, and Cu etc, are often added in host material as dopant.

However, it is very important

- **to identify the catalysts/additives and**
- **its way of incorporating into the sensing layer and**
- **Its quantity should be optimized so as to obtain enhanced response characteristics towards a particular target gas like hydrogen.**

2.4.3 To Improve the Selectivity

Selectivity for SnO_2/ZnO based gas sensors remains a great challenge. These sensors are usually not very selective but besides suitable dopants it is also possible to improve the sensors selectivity by varying the sensor operating temperature [52]. The gas sensing mechanism of semiconductors makes their performance susceptible to temperature changes [172]. Different pollutants have characteristic finest oxidation and reduction temperatures and therefore give upswing to characteristic resistance-temperature contours. By varying the operation temperature of the sensor it is possible to increase or decrease its sensitivity and selectivity towards specific gases [38]. This special attribute of metal oxide gas sensors was exploited to make the most of the sensor signal to each target gas, (i.e. increase sensors sensitivity) and discern between two targeted gases (i.e. increase the selectivity). The targeted applications for the sensor system require a selective detection of one pollutant in a binary mixture [40]. It is possible to detect hydrogen and methane qualitatively and quantitatively in a mixture of both gases.

Therefore, our focus in this work is to develop highly sensitive and selective hydrogen gas sensors that operate at low temperatures to save human lives as well as safety component in the future hydrogen based economy.

2.5 Objectives of the Thesis

Based upon the above review and identified gaps, the following research objectives have been proposed:-

1 Characterization of bulk and thin film samples by X-ray Diffraction (XRD), Scanning Electron Microscopy (SEM), and Atomic Force Microscopy (AFM).

2 Sensor fabrication and analysis of sensing properties of nanocrystalline tin/zinc oxide thin films for hydrogen and methane gases.

3 To increase sensitivity and selectivity of nanocrystalline tin/zinc oxide thin films gas sensor by using novel metals like Ag, Cu, and Li or by controlling the morphology of the films.

2.5.1 Compliance of the Objectives

To achieve the above objectives various sample series of undoped and doped SnO_2/ZnO thin films have been developed using two techniques:

- Sol-Gel techniques via chemical route and spin coating process on glass/quartz substrate, and
- Pulsed Laser Deposition techniques on quartz substrates with predeposited interdigitated platinum electrodes.

In order to achieve the objective 1, the as prepared thin film sample series of undoped and doped SnO_2/ZnO were characterized by complementary techniques such as X-ray diffraction (XRD), scanning electron microscopy (SEM), and atomic force microscopy (AFM).

For achieving the 2^{nd} and 3^{rd} objectives highly sensitive and selective gas sensor for hydrogen gas has been developed utilizing copper doped zinc oxide (Cu-ZnO) thin films. These films were deposited using pulsed laser deposition (PLD) technique on quartz substrates with predeposited interdigitated platinum electrodes. The as deposited films were characterized by X-ray diffraction (XRD) and atomic force microscopy (AFM). The gas sensing parameters of as grown thin films were

studied by I-V measurement technique, using a gas sensing setup fitted with programmable heating arrangement. The novelty of this sensor is that the sensitivity for methane and hydrogen gases can be completely reversed if measurements are performed at 150 ^{0}C as compared to 50 or 100 ^{0}C.

In addition to above for achieving the 2nd and 3rd objectives we have also studied the undoped ZnO, and 1to 8% Li-doped ZnO thin films for hydrogen sensing. These films were deposited by using pulsed laser deposition (PLD) technique on interdigitated quartz substrate at 300 °C, and as developed films were characterized by an X-ray diffraction (XRD) and scanning electron microscopy (SEM). It has been observed that Li plays a very important role in hydrogen gas sensing properties of ZnO thin films at reduced operating temperature i.e. between 50 ºC to 150 ºC.

In this way all the three objectives of this thesis have been achieved.

2.5.2 Organization of the Thesis

The thesis has been organized into six chapters. The contents of each chapter are briefly described as under:-

Chapter 1 provides brief description about the evolution and need of gas sensor, historical background of metal oxide semiconductor gas sensors, giving special attention to the state-of-the-art of the knowledge about gas-sensing mechanism and the properties related to it and at the end of the chapter highlighted the applications of metal oxide gas sensors. Chapter 2 covers the comprehensive literature survey of Tin oxide/Zinc oxide based gas sensors with gaps in the existing work. Based upon this review and identified gaps, the research objectives have been proposed and the organization of the thesis have been discussed. Chapter 3 considers the experimental techniques and procedures used to develop the various thin films sample series for achieving partially objectives 2nd and 3rd, while chapter 4 deals with the most important characterization techniques that have been used in this work and presents the results of the characterization of the SnO_2/ZnO based samples, beginning with the characterization of the undoped samples, and of the doped samples, followed by result discussion for achieving objective 1. Chapter 5 is devoted to gas sensing properties (sensitivity and selectivity) of Cu and Li doped ZnO thin films at substantially lower operating temperature for hydrogen and methane gases to achieve the 2nd and 3rd objectives of the proposed work. Afterwards, the original conclusions that can be extracted from the present work are presented in the chapter 6.

Chapter 1: Introduction

Origin and history of the gas sensor that includes the brief description about the motivation, evolution and definition of semiconductor metal oxide based gas sensor and the need for gas sensor that explain its importance to social life are discussed. After that the choice of metal oxide semiconductors for gas sensing and brief introduction to other types of gas sensors are presented and then move towards the basic sensing mechanism of metal oxide semiconductor gas sensor. Introduce the importance of nanotechnology in gas sensor research and the various factors influencing the sensor performance and at end of the chapter highlighted the applications of metal oxide semiconductor gas sensor.

Chapter 2: Literature Review and Objectives of the Thesis

This chapter covers the comprehensive literature survey of Tin oxide/Zinc oxide based gas sensors. A brief analysis on gas sensing properties of SnO_2/ZnO thin film gas sensors are presented in tabular form and then the importance of sensing hydrogen is discussed. Based on this literature review with identified gaps in the existing work like high operating temperature, low sensitivity and poor selectivity the objectives of this research work are listed in this chapter. Then at end of this chapter to achieve the objectives the organization of the thesis is summarized.

Chapter 3: Thin Film Samples Preparation and Experimental Work

This chapter describes the experimental techniques and procedures used to develop the various thin films sample series for achieving partially objectives 2^{nd} and 3^{rd}. Brief discussion about the methodologies adopted for the present work i.e. Sol-Gel and PLD techniques and their relative advantages and disadvantages in comparison with various other deposition techniques and then specify our experimental details i.e. the procedural details of the present work related to different thin films sample series.

Chapter 4: Thin Film Characterization Techniques and Result Discussions

This chapter gives a brief description of the most important characterization techniques that have been used in this work i.e. XRD, SEM and AFM and presents the results of the characterization of the as deposited samples, beginning with the characterization of the undoped samples, and of the doped samples, followed by result discussion for achieving partially objective 1.

Chapter 5: Gas Sensing Properties of as Deposited Thin Films

This chapter is devoted to gas sensing properties i.e. sensitivity and selectivity of Cu and Li doped ZnO thin films at substantially lower operating temperature for hydrogen and methane gases to achieve the 2^{nd} and 3^{rd} objectives of the proposed work.

Chapter 6: Conclusions

Finally this chapter covers the summary of conclusions drawn in all the three objective areas. In this thesis work it has been concluded that a highly sensitive and selective gas sensor for hydrogen gas can be developed by 3% copper doping in the ZnO host matrix. The novelty of this sensor is that the sensitivity for methane and hydrogen gases can be completely reversed if measurements are performed at 150 ^{0}C as compared to 50 or 100 ^{0}C. Furthermore, we have also studied undoped ZnO, 2% Li-doped ZnO and 8% Li-doped ZnO thin films for hydrogen sensing. It has been observed that Li plays a very important role in hydrogen gas sensing properties of ZnO thin films at reduced operating temperature i.e. between 50 ºC to 150 ºC.

In this way all the three objectives area of this thesis have been achieved. In the end the scope of future work has been presented. Finally, the references used along the writing of this memory are presented.

Chapter 3 Thin Film Samples Preparation and Experimental Work

3.1 Introduction

In last decade deposition systems for metal oxides have been enhanced for the methodology development and exhibitions of materials deposited, in addition to this new procedures have been progressed. Towards the starting there were few predetermined number of utilizations of coating procedures, whereas nowadays the modern applications include large range that reaches from sensors, protective layers, resistive films, and catalyzers. There are various thin film deposition techniques available for gas sensing application with their own advantages and disadvantages.

Thin films of metal oxides as sensing material are deposited using various deposition techniques including RF sputtering [98], [133], [158], thermal evaporation and epitaxial growth [41], [91], [154], [173]-[175] chemical vapour deposition [93], [94], [135], [176], sol-gel [80], [92], [116], [140], [146], [157], [169], spray-pyrolysis [44], [83] [89], [99]-[100], [103], [142], [147], [156], pulsed laser deposition [131], [144], [159], [177] etc. Each of the above techniques has their own advantages and disadvantages therefore depending upon the requirement appropriate technique may be utilized for the deposition of thin films.

Amongst them, sol-gel technique is the preferred choice for the deposition of thin films due to its advantages like, control over composition, large area deposition, planner, non-planner substrates, easy of doping and non-vacuum processing. On the other hand, pulsed laser deposition (PLD) technique is advantageous due to the following reasons: like, good quality metal oxide thin films with controlled stoichiometry, fast turn-around time for initial optimization (due to ease of target preparation), introduction of external dopant and preparation of multilayered structure and therefore heterojunction devices could be achieved easily using PLD.

Thus keeping in view of all such issues in order to achieve better quality thin films, Sol-Gel and PLD techniques have been used for the growth of SnO_2/ZnO thin films in this thesis to develop a suitable gas sensor. Brief descriptions of these two techniques are discussed in the following section.

3.2 Sol-Gel Method

Thin film can be developed by various deposition techniques like sol-gel, dip coating, spin coating, and electroplating by the use of fluid and solution phase. In this thesis we will discuss the sol-gel process because it is a most suitable and utilized

strategy for the development of metal oxide gas sensors. Moreover, it can also be utilized additionally for other purposes like powder readiness to develop thick-film generation. This technique is adaptable for making thin films. When all is said in done, the sol-gel prepare includes the evolution of a framework from fluid sol into a strong gel phase. By using the sol-gel process it is conceivable to create different materials in extensive assortment of structures: like ultra-fine or circular formed powders, thin film coatings, ceramic fibres, small scale permeable inorganic layers, solid pottery and glasses, or to a great degree permeable air gel materials. A simplest flow chart for the overview of the sol-gel process that has been used in this thesis is presented in Fig 3.1.

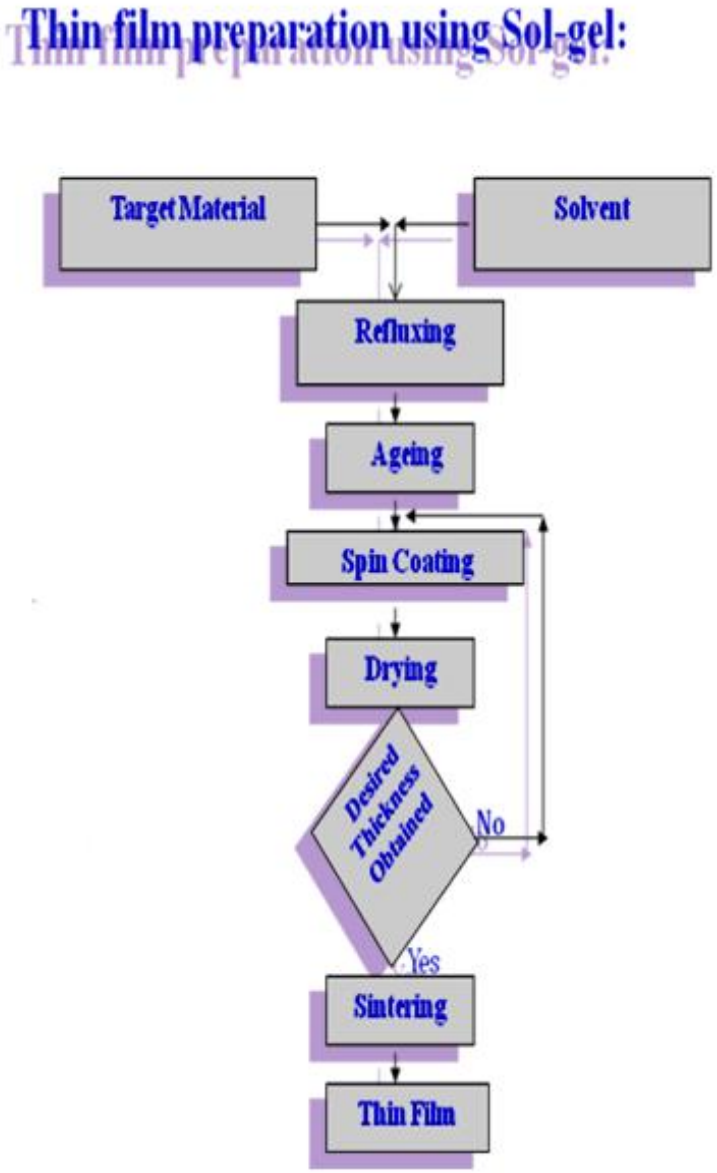

Fig. 3.1: Schematic representation of sol-gel process used for the deposition of thin films

The beginning materials used as a part for preparation of sol are commonly inorganic metal salts or natural metal compounds for instance metal alkoxides. In a standard sol-gel process, the forerunner is subjected to a movement of hydrolysis and polymeration responses to form a colloidal suspension, or sol. Advance distributing of the sol empowers one to make oxide materials in various structures. A sol is a diffusion of the solid elements in a fluid where simply the Brownian developments suspend the particles. A gel is the state where fluid and solid are diffused in each other that demonstrates a strong system having fluid parts. Sol-gel coating process more often comprises of four stages:

- a sol is formed by the dispersion of colloidal particles in the liquid,
- by spinning ,dipping or spraying the sol solution is deposited on the substrates,
- then the particles in sol are dispersed over the elimination of the stabilizing components and yield a gel in a state of a constant network,
- Lastly thermal actions remove the residual organic or inorganic constituents and give crystalline coating films.

The benefits of sol-gel process are its capability to grow high-purity metal oxide in light of way that organo-metallic precursor of the required metal oxides may be blended, broken up in an evaluated dissolvable and hydrolyzed into a sol, and after that a gel; the synthesis can be exceedingly sensible, the low temperature sintering capacity, normally 200–600˚C; and to wrap things up the simple, monetary and viable technique to deliver high-quality coatings. Moreover, it is conceivable to synthesize complex composition materials, to custom higher purity products through the use of high purity reagents. The sol-gel process permits obtaining high quality films up to micron thickness, difficult to achieve using the physical deposition techniques. Besides, it is possible to synthesize complex composition materials and to provide coatings over complex geometries [178].

3.3 Sample Series using Sol-Gel and Chemical Route Techniques

To attain the objectives of this research work the following sample series have been prepared by the sol-gel technique and chemical route method using spin coating processes:

- Sample Series-1 Undoped Tin Oxide thin films
- Sample Series-2 Sb-doped Tin Oxide thin films
- Sample Series-3 Undoped Zinc Oxide thin films
- Sample Series-4 Sn-doped Zinc Oxide thin films
- Sample Series-5 Ag-doped Tin Oxide thin films with PVA using $SnCl_4$
- Sample Series-6 Ag-doped Tin Oxide thin films with PVA using $SnCl_2$
- Sample Series-7 ZnO-SnO_2 based composite thin films with PVA

For undoped Tin Oxide thin films there are two different approaches generally employed in the Sol-Gel synthesis of SnO_2. The first consists in the hydrolysis of a tin alkoxides with low value of the H_2O/Sn ratio to avoid precipitation in the sol. This procedure has the advantage of minimizing the impurities in the final material, but the high cost of the precursors and the low time stability of the sol against the increase in the viscosity make this kind of approach not convenient. For this reason the sol gel preparation of SnO_2 is more commonly achieved through the hydrolysis of inexpensive precursors such as $SnCl_2$ or $SnCl_4$.

Substrate cleaning; Corning glass/quartz substrates were used in the present study to deposit the thin films of SnO_2 and ZnO sensing materials. Cleaning of the substrate is very critical for the deposition of good quality thin films, especially using sol-gel deposition technique. The substrate was cleaned thoroughly using a set of procedure prior to deposition of thin films. The presence of dirt or any oil particles on the surface of the glass substrates were removed by dipping them overnight in the freshly prepared chromic acid. Subsequently substrates were removed, rinsed with de-ionized (DI) water and dipped in a solution of hot detergent in water. The substrates were rinsed with hot de-ionized water and subjected to ultrasonic cleaning in water for 10 to 15 minutes. Finally, corning glass/quartz substrates were ultrasonically cleaned in tri-chloroethylene, acetone, followed by degreasing in iso-propyl alcohol. The substrates were dried by blowing with a jet of dry nitrogen gas prior to deposition process. After that substrates were ready for deposition of thin films.

Photographs of the equipment's in R&D Lab (ECED), NCCE, Israna (Panipat) Haryana, establish by us and funded by AICTE under Research Promotion Scheme, F. No. 8023/BOR/RPS-56/2006-07 and 8023/RID/RPS-78/11/12.

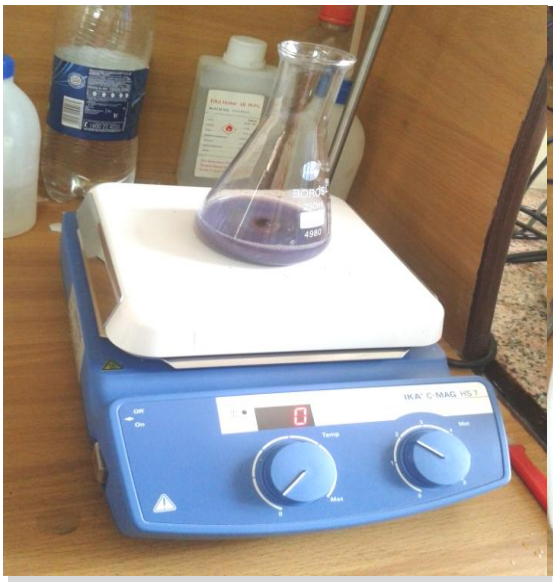

Magnetic Stirrer (a)

Digital Balance (b)

Hot Air Oven (c)

Ultra Sonic Cleaner (d)

Spin Coating Unit (e)

Fig.3.2: Photographs of the operational equipment's in R&D Lab, ECE Department, N.C.C.E. (Israna) Panipat, Haryana i.e. (a) Magnetic Stirrer, (b) Digital Balance, (c) Hot Air Oven, (d) Ultra Sonic Cleaner, and (e) Spin Coating Unit

3.3.1 Sample Series 1:- Undoped Tin Oxide Thin films

EXPERIMENTAL PROCEDURE

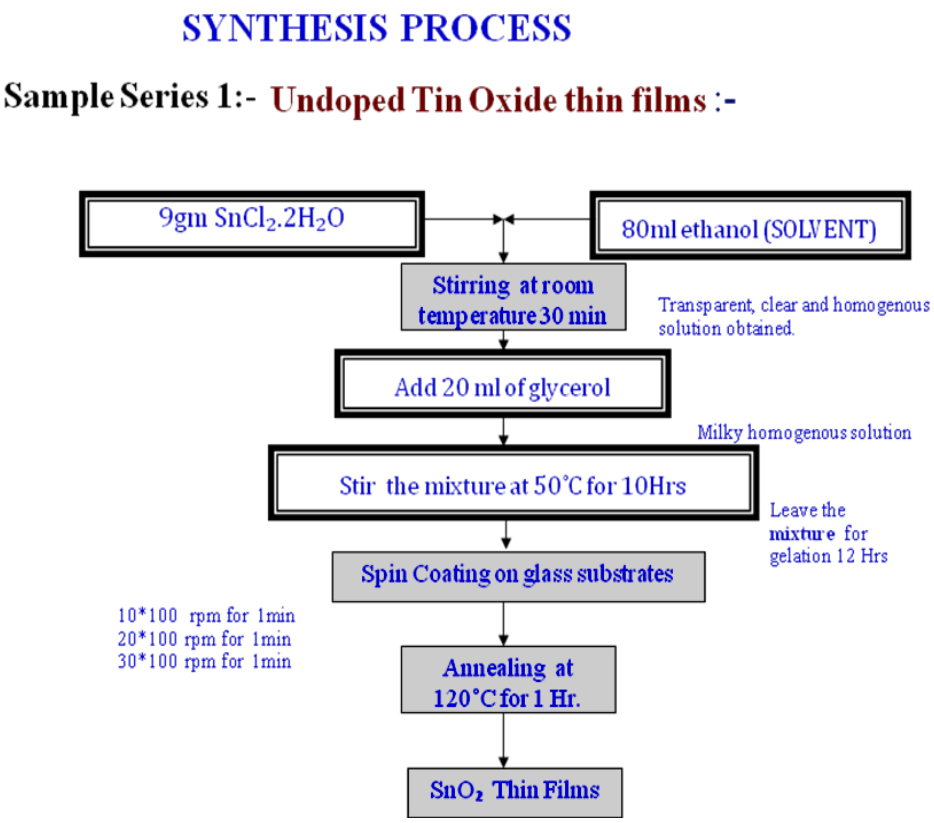

Fig.3.3: Synthesis Process of Sample Series 1: Undoped SnO_2 Thin Films

- 9 gm Tin Chloride ($SnCl_2.2\ H_2O$) was first dissolved in a mixture of 80ml ethanol (solvent). This mixture is prepared using magnetic stirrer for 30 minutes at room temperature.
- We get a clear, transparent and homogeneous solution; now add 20ml of glycerol as stabilizing agent following by continued stir at 50˚C for 10 hrs. We get a milky and homogeneous solution.
- Now left the solution for gelation 12hrs.
- Spin coating (using Milman unit) is performed on glass substrate at following rpm:
  - i) 10*100 rpm for 1min
  - ii) 20*100 rpm for 1min
  - iii) 30*100 rpm for 1min
- Annealing was performed at 120˚C for 1Hrs.
- Based upon the above procedure, we have developed the sample series of pure Tin Oxide thin films by changing the following parameters as follows:

- Stir the final mixture at 50˚C, 60˚C & 70˚C for 10 hrs. - 5 samples of each series
- By varying the 3rd stage Spinning speed at 30*100 rpm for 1min, 25*100 rpm for 1min, 25*100 rpm for 2min- 5 samples of each series
- By varying the annealing at, 150˚C , 200˚C - 5 samples of each series

3.3.2 Sample Series 2:- Sb-doped Tin Oxide Thin Films

- 11.38 gm Tin chloride ($SnCl_2.2H_2O$) was first dissolved in 100ml ethanol (solvent). This mixture is prepared using magnetic stirrer at room temperature for 2Hrs.
- We get a clear, transparent and homogeneous solution and now add 1.73 gm of $SbCl_3$ as doping and stir the mixture at 60˚C temperature for 2 Hrs, milky and homogenous solution obtained.
- Now leave the solution for gelation 24hrs.

Fig.3.4: Images of Various Sample Series

SYNTHESIS PROCESS

Sample Series 2:- Sb-doped Tin Oxide thin films

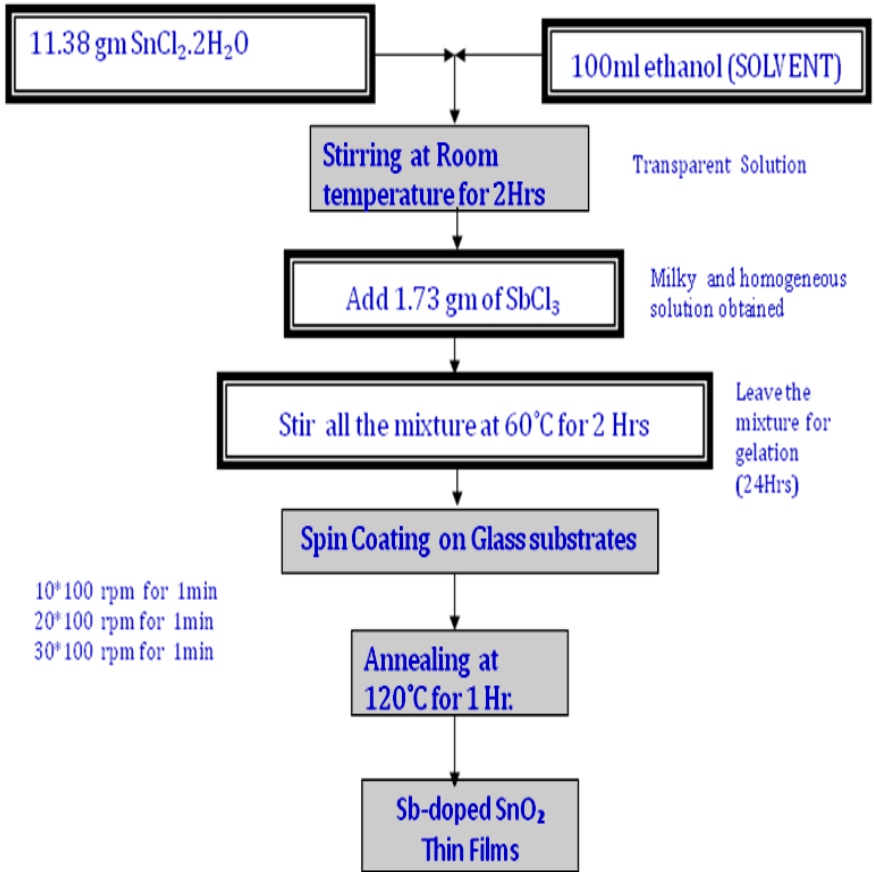

Fig.3.5: Synthesis Process of Sample Series 2: Sb-doped SnO_2 Thin Films

- Spin coating is performed on glass substrate at following rpm:
  - i) 10*100 rpm for 1min
  - ii) 20*100 rpm for 1min
  - iii) 30*100 rpm for 1min
- Annealing was performed at 120˚C for 1Hrs.
- Based upon the above procedure, we have developed the sample series of Sb-doped Tin Oxide thin films by changing the parameters as follows:
- On the same parameters as stated above develop the 5 samples for characterization.
- By varying the 3rd stage spinning speed at 30*100 rpm for 2min, 25*100 rpm for 1min, 25*100 rpm for 2min and develop the 5 samples of each series.
- By varying the annealing at, 150˚C, and 200˚C - 5 samples of each series.

3.3.3 Sample Series-3 Undoped Zinc Oxide Thin Films

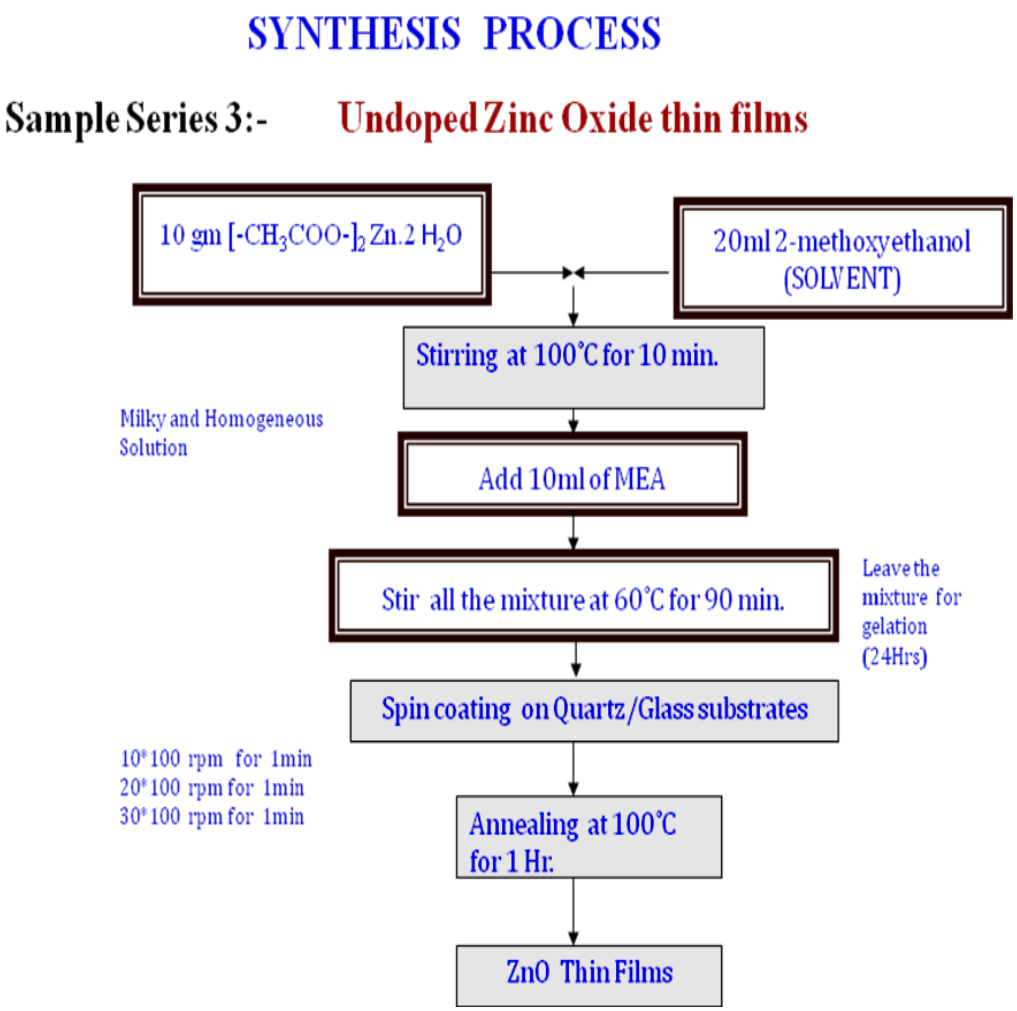

Fig.3.6: Synthesis Process of Sample Series 3: Undoped ZnO Thin Films

- 10 gm Zinc acetate dehydrates ([-CH_3COO-]$_2$ Zn.2 H_2O) was first dissolved in 20ml 2-methoxyethanol (solvent) and this mixture was prepared using magnetic stirrer for 10 minutes at 100˚C .
- Add 10 ml of monoethanolamine (MEA) acting as stabilizer in above solution. We obtained milky and homogeneous solution, followed by continued stir at 60˚C for 90 minutes
- Now leave the solution for gelation for 24 Hrs.
- Spin coating is performed on glass substrate at following rpm:
  - i) 10*100 rpm for 1min
  - ii) 20*100 rpm for 1min
  - iii) 30*100 rpm for 1min
- Annealing was performed at 100˚C for 1Hrs.

- Based upon the above procedure, we have developed the sample series of undoped Zinc Oxide thin films by changing the parameters as follows:
- On the same parameters as stated above develop - 5 samples for each series.
- By varying the 3rd stage spinning speed at 30*100 rpm for 2min, 25*100 rpm for 1min, 25*100 rpm for 2min develop - 5 samples of each series
- By varying the annealing at, 150˚C , 200˚C - 5 samples of each series

3.3.4 Sample Series-4 Sn-doped Zinc Oxide thin films

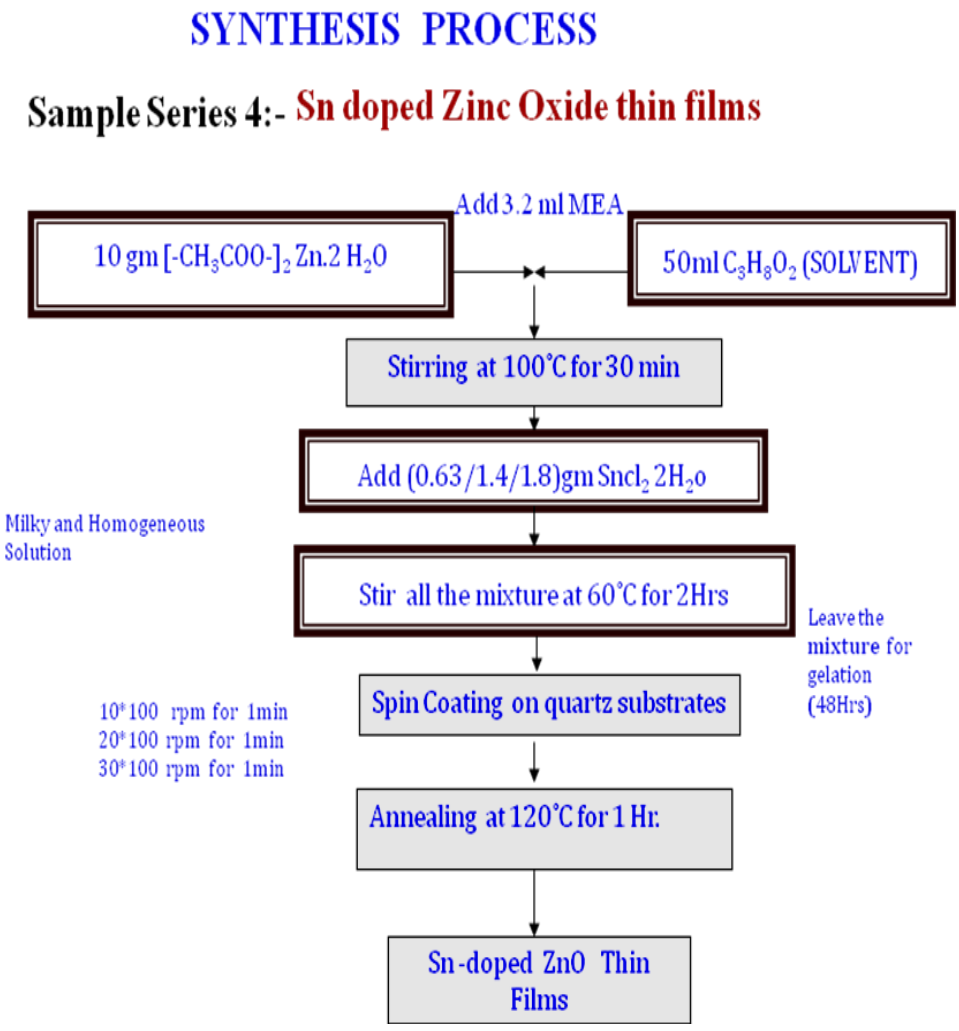

Fig.3.7: Synthesis Process of Sample Series 4: Sn-doped ZnO Thin Films

- 10 gm Zinc Acetate dehydrates ([-CH_3COO-]$_2$ Zn.2 H_2O) was first dissolved in a mixture of 50ml 2-methoxyethanol (solvent) and 3.2ml of monoethanolamine (MEA) acting as stabilizer. This mixture is prepared using magnetic stirrer for 30 minutes at 100˚C.

- Add 0.63/1.4/1.8 gm $SnCl_2$ $2H_2O$ as tin resource in above solution. We obtained milky and homogeneous solution, followed by continued stir at 60˚C for 2Hrs.
- Now leave the solution for gelation 48Hrs.
- Spin coating is performed on glass substrate at following rpm:
  i) 10*100 rpm for 1min
  ii) 20*100 rpm for 1min
  iii) 30*100 rpm for 1min
- Annealing was performed at 120˚C for 1Hr.
- Based upon the above procedure, we have developed the sample series of Sn doped Zinc Oxide thin films by changing the parameters as follows:
- On the same parameters as stated above develop - 5 samples for each series.
- By varying the 3rd stage spinning speed at 30*100 rpm for 2min, 25*100 rpm for 1min, 25*100 rpm for 2min develop - 5 samples of each series
- By varying the annealing at, 150˚C, and 200˚C - 5 samples of each series.

All the above sample series were characterized for structural and surface morphology. Unfortunately the results were not satisfactory due to some restrictions, like weak adhesion, hardly control over porosity, and low wearing resistance. So, despite so many advantages, sol-gel technique also has some disadvantages and that is the reason it never attains at its full industrial potential. Specifically, the point of confinement of the maximum coating thickness is 0.5 mm when the break free property is an imperative necessity. The caught materials with the thick covering regularly brings about disappointment amid thermal process. The substrate–layer expansion bungle restrains the wide utilization of sol-gel procedure.

Therefore, to overcome the above limitations a polymer embedded approach has been adopted to explore interesting physics of self-assembly and study the properties of these oxide structures. In polymer embedded metal-oxide thin films, polymer controls viscosity and binds the metal-oxide ions, resulting in their homogeneous distribution in the film. These uniform, flexible and crack-free metal-oxides-polymer films can be synthesized on much larger scale, in bigger dimensions and for variety of applications [179]. PVA plays the active role in the system and by considering the critical tunneling regime; it increased the surface area of the nanocomposite. Moreover, it is the hydrophobic feature inside PVA matrix,

anisotropy and surface tension that plays an important role on the sub-microrod crystal growth [180]. The effect of concentration of SnO_2 colloidal particles on the kinetics of gelation of hydrolysis containing PVA was analyzed by dynamic rheological measurements [181]. Khorami et al. [182] report the synthesis of SnO_2/ZnO/PVA composite nanofibers via electro-spinning method and showed high sensitivity, quick response and recovery times at optimum temperature of 368 ^oC. Hence, it is important to address the issue of polymer embedded metal oxides, understand the interesting science there in and explore its technological importance.

Surface modification does not change the initial geometry of polymer-metal matrix which can be utilized for gas sensing applications. It was established that the surface modification by noble metals could really be accompanied by effects such as the increase of sensitivity, the shift of sensor response maximum in the region of lower operating temperatures and the decrease of response time [183-184]. Among the metal additives to SnO_2, Ag has also been used for gas sensing application. For example, Ag doped SnO_2 thin films have been developed which show good selectivity for H_2S detection. The Ag-SnO_2 film presents better sensitivity as compared to pure SnO_2, due to distribution of Ag_2O particles in grain boundaries of nanocrystalline SnO_2 and the formation of p-n heterojunction [185].

Therefore, in this thesis the sample series 5 and 6 for SnO_2 embedded in PVA by chemical route with silver as a noble metal additive have been successfully synthesized.

3.3.5 Sample Series-5 Ag-doped Tin Oxide Thin Films with PVA using $SnCl_4$

These thin films were deposited on silica substrate via spin coating process and annealed at different temperatures as follows:

- 7gm $[-CH_2CHOH-]_n$ PVA was first dissolved in a 63ml H_2O (distilled water) adding PVA very slowly. This mixture is prepared using magnetic stirrer for 2Hrs at 100˚C temperature.
- We get a clear, transparent and homogeneous solution and allow to cool at room temperature, now add 1.5gm $SnCl_4$ $5H_2O$ + 2ml H_2O and stir the mixture for 1 Hr at room temperature, milky and homogenous solution obtained.

SYNTHESIS PROCESS

Sample Series 5:- **Ag-doped Tin Oxide thin films using $SnCl_4$**

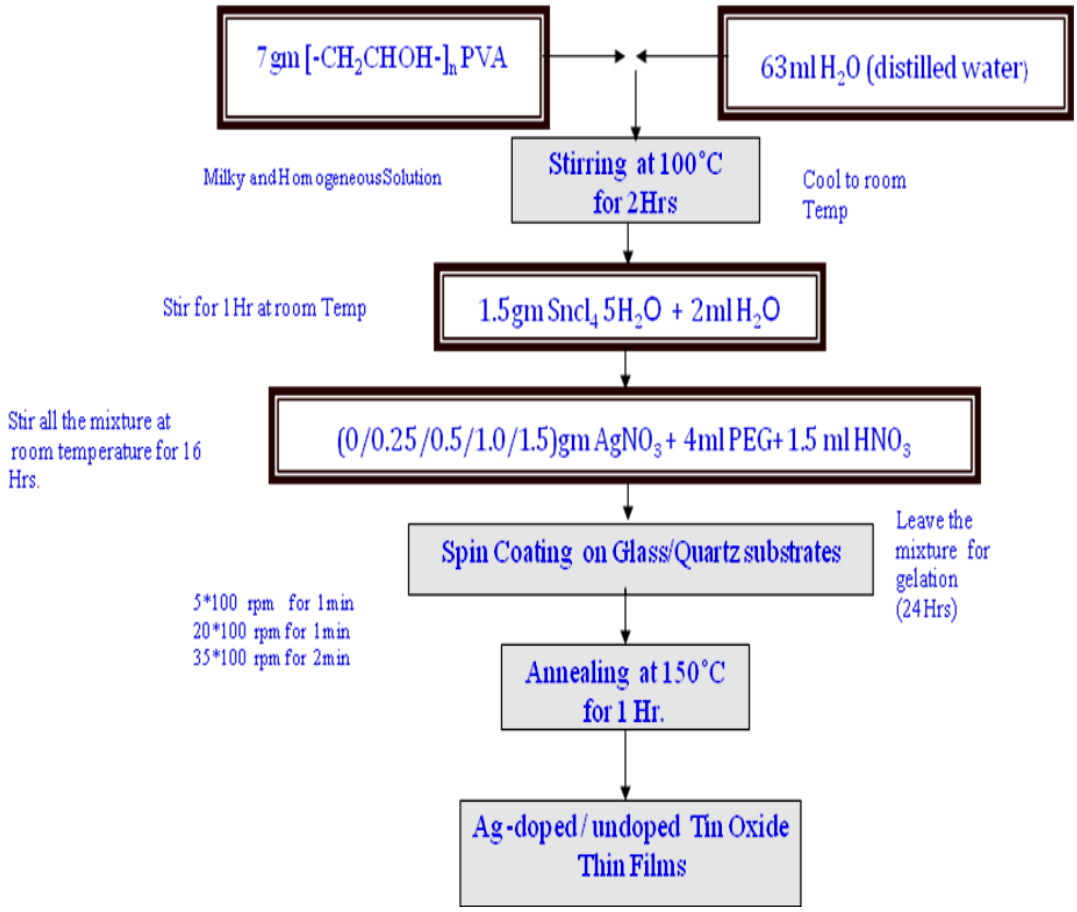

Fig.3.8: Synthesis Process of Sample Series 5: Ag-doped SnO_2 Thin Films with PVA using $SnCl_4$

- Now add the different proportion of Ag (doping) i.e. (0/0.25/0.5/1.0/1.5)gm $AgNO_3$ + 4ml PEG+1.5 ml HNO_3 and followed by continued stir at room temperature for 16 hrs. Now left the solution for gelation 24hrs.
- Spin coating is performed on glass/quartz substrates at following rpm:
  - i) 10*100 rpm for 1min
  - ii) 20*100 rpm for 1min
  - iii) 30*100 rpm for 1min
- Annealing was performed at 150˚C for 1Hrs.
- Based upon the above procedure, we have developed the sample series of Ag doped Tin Oxide thin films by changing the parameters as follows:
- On the same parameters as stated above develop - 5 samples of each series.

- By varying the 3rd stage spinning speed at 30*100 rpm for 2min, 25*100 rpm for 1min, 25*100 rpm for 2min develop - 5 samples of each series
- By varying the annealing at, 150˚C, and 200˚C - 5 samples of each series

3.3.6 Sample Series-6 Ag-doped Tin Oxide Thin Films with PVA using $SnCl_2$

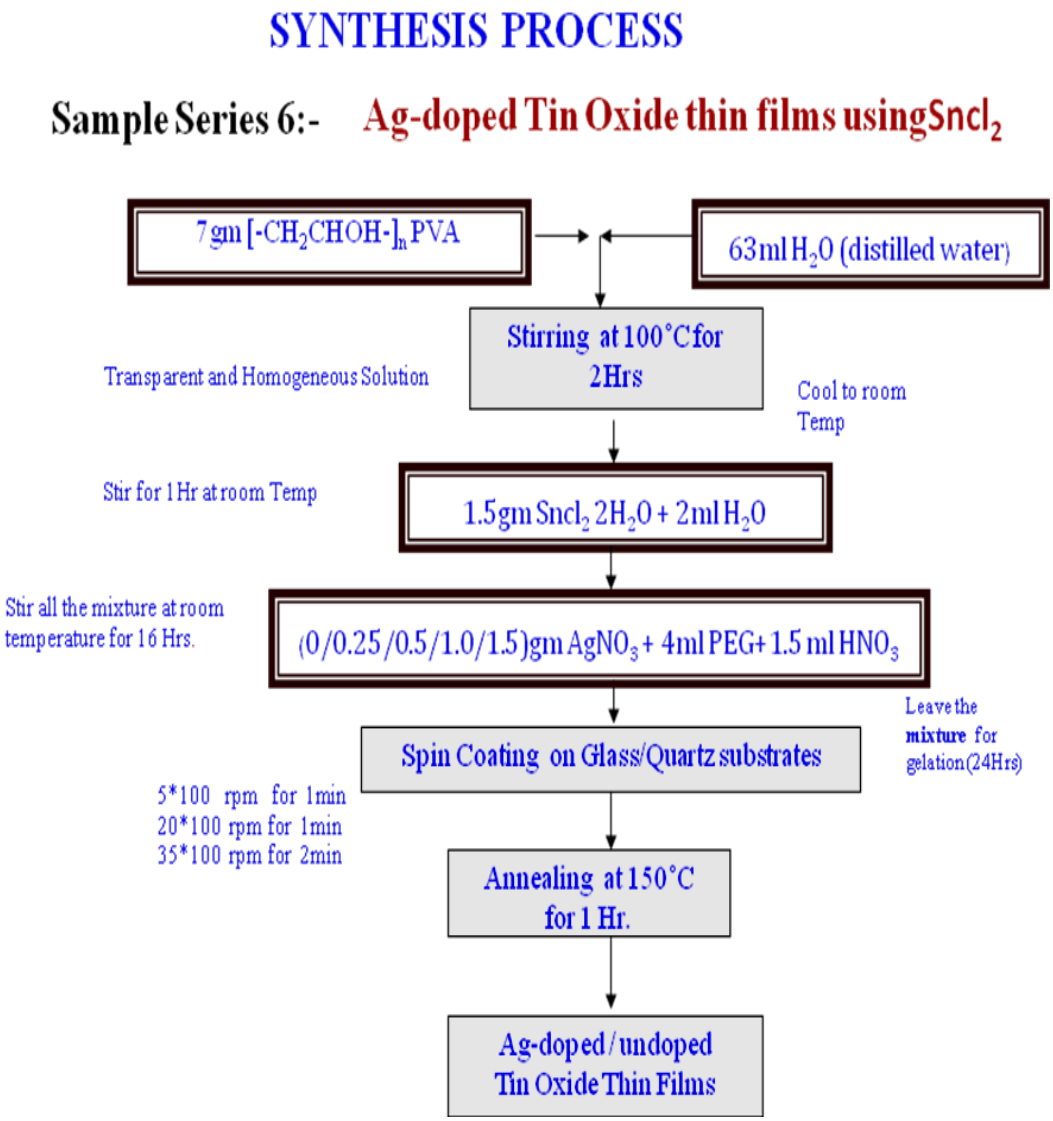

Fig.3.9: Synthesis Process of Sample Series 6: Ag-doped SnO_2 Thin Films with PVA using $SnCl_2$

- 7gm $[-CH_2CHOH-]_n$ PVA was first dissolved in a 63ml H_2O (distilled water) adding PVA very slowly. This mixture is prepared using magnetic stirrer for 2Hrs at 100˚C temperature.
- We get a clear, transparent and homogeneous solution and allow to cool at room temperature, now add 1.5gm $SnCl_2$ $2H_2O$ + 2ml H_2O and stir the

mixture for 1 Hr. at room temperature, milky and homogenous solution obtained.

- Now add the different proportion of Ag (doping) i.e. (0/0.25/0.5/1.0/1.5)gm $AgNO_3$ + 4ml PEG+1.5 ml HNO_3 and followed by continued stir at room temperature for 16 hrs. Now left the solution for gelation 24hrs.
- Spin coating is performed on glass substrate at following rpm:
    i) 10*100 rpm for 1min
    ii) 20*100 rpm for 1min
    iii) 30*100 rpm for 1min
- Annealing was performed at 150˚C for 1Hrs.
- Based upon the above procedure, we have developed the sample series of Ag doped Tin Oxide thin films by changing the parameters as follows:
- On the same parameters as stated above develop - 5 samples of each series.
- By varying the 3rd stage spinning speed at 30*100 rpm for 2min, 25*100 rpm for 1min, 25*100 rpm for 2min develop - 5 samples of each series
- By varying the annealing at, 100˚C, and 200˚C - 5 samples of each series

3.3.7 Sample Series-7 ZnO-SnO_2 Based Composite Thin Films with PVA

- 7gm $[-CH_2CHOH-]_n$ PVA was first dissolved in a 70 ml H_2O (distilled water) adding PVA very slowly. This mixture is prepared using magnetic stirrer for 2Hrs at 80˚C temperature.
- We get (PVA) a clear, transparent and homogeneous solution and then allow it to cool at room temperature.
- Now 03 gm Zinc Acetate dehydrates (Zn $[-CH_3COO-]_2$. 2 H_2O) was first dissolved in 5 gm $SnCl_4$. $5H_2O$ and add to the as processed PVA. This mixture is prepared using magnetic stirrer for 2 Hrs. at 120˚C.
- After this, stir the above mixture for 16 Hrs. at room temperature. Homogeneous milky white solution has been obtained.
- Now left the solution for gelation 24hrs.
- Spin coating is performed on glass substrate at following rpm:
    iv) 10*100 rpm for 1min
    v) 20*100 rpm for 1min

vi) 35*100 rpm for 2min

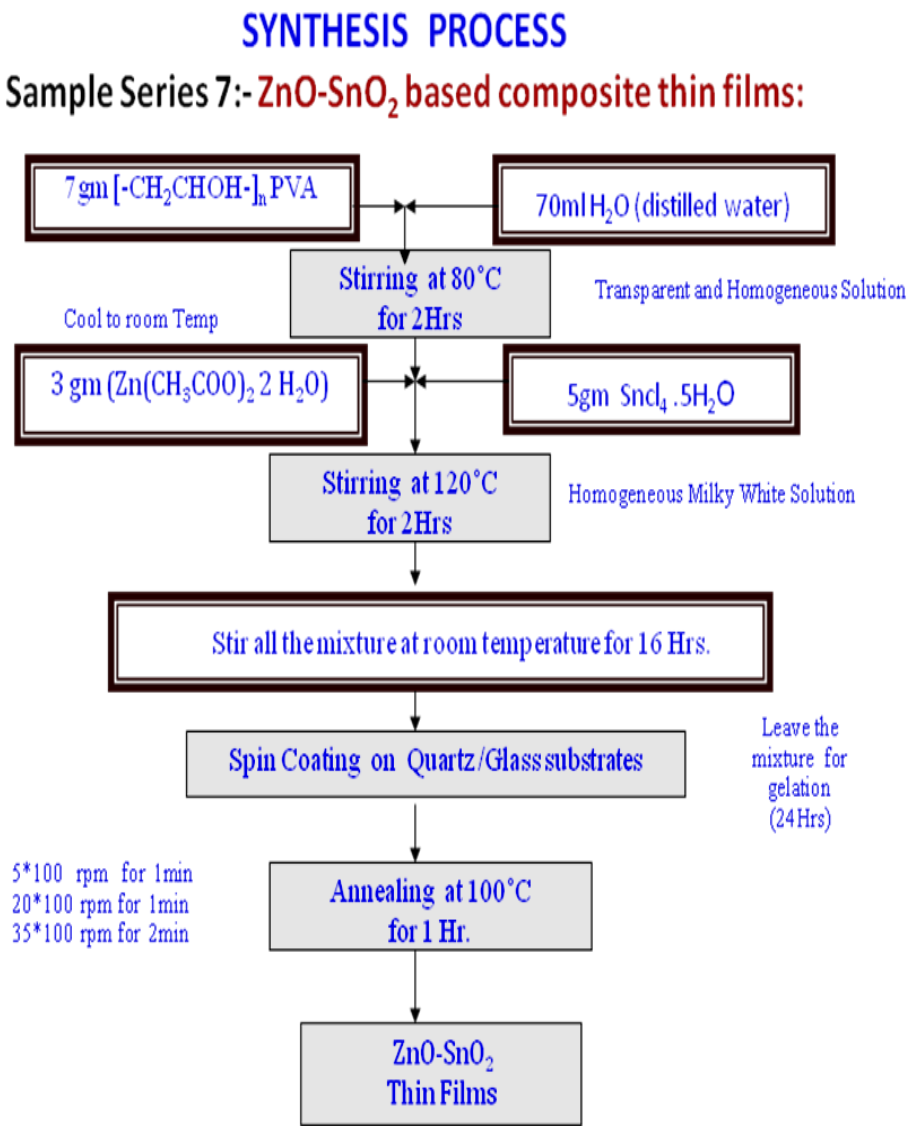

Fig.3.10: Synthesis Process of Sample Series 7: ZnO-SnO_2 Composite Thin Films with PVA

- Annealing was performed at 100˚C for 1Hrs.
- Based upon the above procedure, we have developed the sample series of ZnO-SnO_2 composite thin films by changing the parameters as follows:
- On the same parameters as stated above develop - 5 samples of each series.
- By varying the 3rd stage spinning speed at 35*100 rpm for 1min, 30*100 rpm for 2min, 25*100 rpm for 2min develop - 5 samples of each series
- By varying the annealing at 150˚C, and 200˚C - 5 samples of each series.

3.4 Pulsed Laser Deposition Technique

Pulse laser Deposition (PLD) is further reassuring method for the deposition of thin film. This procedure relies on upon fast vanishing by the usage of high power laser shot and then condensation of vaporized material on the substrate. The PLD is also fast, basic and to an extraordinary high adaptable framework to develop the thin films of various materials. In 1987, when YBaCuO prepared the superconducting thin films using PLD, this technique open the space for epitaxial films and controlled stoichiometric. The PLD advancement can be further utilized used in the development of single crystals and multicomponent nanostructured materials. Laser ablation cannot be approximated theoretically because of various unsafe conditions involved in it and basically it is microscopic technique. The high photon flux gives fundamentally prompt warming of the material, at times to temperatures near the critical point. The material evaporate at this temperature. The particles in the radiated gas can in like manner interface with the laser photons, which warm the gas.

A laser beam is involved at low pressure in the presence of a gas onto the target material put in a high-vacuum chamber. So by thermal ejection and photochemical ejection the photon density on the target material surface causes the ejection of neutral and ionized material. There are a couple of main factors to be decided for PLD process like the pulse duration, their intensity, temperature and the selection of laser wavelength. Occasionally it is fundamental to utilize a gas to pick up the right composition in the film. The temperature of the plasma depends on pulse duration and its intensity. The background gas in the chamber is used for better interaction of laser ablation. Plasma conditions are controlled by Langmuir probes and optical spectroscopy and to monitor the film growth optical reflectometry is used.

The deposition of oxide thin films using PLD usually requires a background O_2 gas pressure in the growth chamber. This background gas serves two purposes. First, the requirement of reactive species for deposition of oxide (atomic oxygen) thin film is provided by the background oxygen gas. Secondly, the background gas pressure helps in reducing the kinetic energy of the ablated species. When a laser beam of sufficient energy is focused on a target, the target material goes into vapour state directly without melting. The vaporized species in front of the target are seen as glowing plasma, called the plume. The plume interacts with the processing gas (generally reactive gas) available in the deposition chamber and the ablated matter is

condensed on the surface of the substrate as a thin film. If the laser beam is intense enough, it can ablate the hardest and most heat resistant material also [186]. In the present study, oxygen has been used as the processing gas for deposition of the sensing layer. Stoichiometry of the oxide thin films deposited by the PLD technique is very close to that of the ablated target and hence it is possible to prepare stoichiometric thin films. This is termed as the "stoichiometry transfer", which has made the PLD technique useful for the growth of complex and multi-element systems. The advantage of PLD technique is the requirement of small sized targets (10 to 25 mm diameter) which could be prepared in the laboratory by conventional ceramic processing technique. Therefore, fabrication of thin films of composite or multilayered structure and introduction of any new dopant in thin film is very convenient using PLD technique and has a fast turn-around time in comparison to other deposition techniques.

To attain the objectives of this research work the following sample series have been prepared by the PLD technique:

3.4.1 Sample Series 8:- Undoped and Cu-doped ZnO Oxide Thin Films

EXPERIMENTAL PROCEDURE

- Pulsed laser deposition technique was used for the deposition of undoped ZnO and varying Cu concentration ranging from (1 to 5 %) Cu-doped ZnO thin films.
- Quartz substrates with pre-deposited interdigitated electrode pattern of platinum were used for the film deposition and the substrates were ultrasonically cleaned in acetone and in methanol for 3 minutes each.
- The chamber was evacuated by a turbo molecular pump to a base pressure of 1×10^{-6} Torr.
- Pure and Cu-doped ZnO targets were used for thin film deposition.
- A KrF excimer laser (λ=248 nm) with beam energy of 250 mJ/pulse at a repetition rate of 5 Hz was used for ablating the target.
- Thin films of about 300 nm thickness were deposited at a substrate temperature of 300 °C with 300 m torr oxygen pressures in the chamber.

3.4.2 Sample Series 9:- Undoped and Li doped ZnO Oxide Thin Films

- Pulsed laser deposition technique was used for the deposition of undoped ZnO and varying Li concentration ranging from (1 to 8 %) Li-doped ZnO thin films.
- Quartz substrates with pre-deposited interdigitated electrode pattern of platinum were used for the film deposition and the substrates were ultrasonically cleaned in acetone and in methanol for 3 minutes each.
- The chamber was evacuated by a turbo molecular pump to a base pressure of 1×10^{-6} Torr.
- Pure and Li-doped ZnO targets were used for thin film deposition.
- A KrF excimer laser (λ=248 nm) with beam energy of 250 mJ/pulse at a repetition rate of 5 Hz was used for ablating the target.
- Thin films of about 300 nm thickness were deposited at a substrate temperature of 300 °C with 300 m torr oxygen pressures in the chamber.
- Film thickness of as deposited films were obtained using AMBIOS XP-100 thickness profilometer.

The structural and surface morphology of the as deposited films were characterized by complementary techniques such as XRD, SEM and AFM etc. in the next chapter of this thesis.

Chapter 4 Thin Film Characterization Techniques and Result Discussions

4.1 Introduction

Before using any material for some application it is relevant to find out its properties. The properties of a material can be found using techniques like X-Ray Diffraction (XRD), Scanning Electron Microscopy (SEM), and Atomic Force Microscopy (AFM). XRD is a versatile investigation technique with which one can easily identify the material, find out the crystallinity, crystallite size, lattice constants, phases, etc. and by using SEM and AFM the morphology of the film, particle size, porosity etc. of the material can be determined. To interpret the results obtained out of these investigations it is very important to understand the basics of these characterization methods.

In this chapter the fundamentals of these techniques have been explained briefly. The films that have been developed will be subjected to these investigations to understand them thoroughly before applying them as thin film sensors. In this thesis we have fabricated nanostructured undoped and doped Tin/Zinc oxide thin films as gas sensors. To study the sensing response of these films it is quite important to have sensor testing unit ready before hand. This unit comprises of many important components, without them it is impossible to investigate the sensing beahviour of the material. These integral parts and their results are explained in the following sections.

4.2 Thin Film Characterization Techniques

4.2.1 X-Ray Diffraction

The X-Rays gets diffracted from the reticular planes forming the atoms with in crystal and this phenomena of diffraction of X-rays is used in XRD [187]-[188]. The X-ray after passing through crystal gets diffracted at specific angles. The diffracted beam angles depend on the crystal orientation, structure of the crystal and wavelength of the X-ray. The constructive interference of diffracted rays at a specific wavelength occurs, when the path difference between two diffracted rays from atomic planes surfaces become an integral number of wavelength. This condition is depicted by the Bragg law:

$$2d \sin \theta = n \lambda, \qquad (4.1)$$

Where n is an integer, λ is the wavelength of the radiation, d is the spacing between surfaces, and θ is the angle between the radiation and the surfaces. The equation (4.1) shows that constructive interference effects are detected only when wavelength of the radiation is approximately of the same size as that of physical dimensions interaction size of radiations. Thus diffraction techniques need radiation of beams of neutrons or electrons or X-Rays with wavelength in the range of the electromagnetic spectrum where it (wavelength) is comparable with the distances between ions or atoms (of the order of 10^{-10}m (1Å)). Thus, through X-beam spectra one can recognize and investigate any crystalline matter.

The nature and quality of the acquired result will depend on the crystallinity level or order. Keeping in mind the end goal to do this, a diffractometer is required. Fundamentally, an X-Ray diffractometer comprises of an X-beam generator and detector (such as movable proportional counter or a photographic film), a goniometer and a test holder. X Rays are produced using X ray tubes. In X ray tubes the X Rays are produced by shelling a metal focused with high energy (10-100keV) electrons that thump out center electrons. An X-ray photon is emitted when an electron from outer shell jumps and fills the hole in the inner shell. For strong Kα X-ray generation at 0.71073 and 1.5418 Å, Mo and Cu, are commonly used targets respectively.

In X-ray generation beside the desired line, other undesired lines also appear in the spectra which have to be removed for understanding of the desired spectra. Crystal monochromators are used to suppress undesired lines. In this thesis work the investigation of polycrystalline materials and mainly of thin films is done using the X-ray diffraction methods. XRD gives rise to a large number of diffraction cones which help to find all the possible orientations of the small crystals, each one corresponding to a family of planes satisfying the Braggs law, in case of powder/film. For expansive grains, rings are intermittent and shaped by little spots. As the grain's size reduces, the spots become nearer and for an ideal size a persistent ring is formed. For lines in a photographic register or graphic registers this ring is transformed into a peak. The clarity of rings is lost and wide peaks or bands are formed for lower grain sizes. The intensity of the different rings and along each ring is not uniform, when the crystals are preferentially oriented and not randomly oriented.

A sealed gas proportional counter or scintillation counter is used as X-rays are detector by a radiation detector. The accepting opening get together and the indicator

is coupled together and move around a circle so as to output a scope of 2 θ (Bragg) points. A different diffraction diagram is produced by each crystalline powder, which is the premise for a subjective investigation by X-beam diffraction. Distinguishing proof is essentially constantly joined by the orderly examination of the acquired range with a standard one (an example), taken from any X-beam powder information document inventories, distributed by the American Culture for Testing and Materials (JCPDS). Each of the individual crystalline substances present has diffraction profiles of a mixture of crystalline specimens. By performing in-situ XRD analysis or analyzing samples treated at different annealing temperatures, an accurate analysis of phase transitions in SGS materials can be also carried out. Quantitative examination of diffraction profiles can be differing. We will portray quickly the measure of grain size in polycrystalline examples that, as already examined, is a pivotal parameter in metal oxide gas sensors.

Scherrer formula is used to determine the size of the crystals in the film. Scherrer demonstrated that the normal measurement of the crystalline structure that make a crystalline powder is connected with the profile of the top by method for the condition:

$$D = \frac{K\lambda}{\beta Cos\theta} \tag{4.2}$$

Where

K = Proportionality constant approximately similar to the unit.

β = FWHM of the peak in radians (theoretically corrected from the instrumental broadening). This is the most common and basic condition that permits to assess grain size.

4.2.2 Scanning Electron Microscopy (SEM)

Because seeing is considered to be believed and understanding, for thin film and coating characterization the SEM (Scanning Electron Microscopy) is the most commonly used equipment [189]. Zworykin first proposed the idea to image surface topography of materials by using the secondary emission formed by a focused electron probe. SEM uses electron beam to scan the surface of a sample and produces images by knowing the electronic interactions with the sample interface. The surface of a thick sample, which is electron transparent, is scanned by an electron probe

formed by the focusing action of a strong convergent lens. In the process of scanning secondary electrons produced. These electrons are sent to a scintillator where they produce current in the detector. The photocurrent generated with respect to the position of the probe is amplified and recorded. The current is used for recording the image of the scanned surface. It is usual in scanning electron microscopy to employ incident electron beams in the range 0.5-40 keV. The principal modes of contrast depend upon the detection of two categories of electrons. First, the reflected primary or back scattered electrons, with energies >50eV, which are scattered from atoms within a shallow depth in the specimen (~1mm), and second, emitted secondaries with energies 50eV but greater than the work function of the specimen surface. The last ones are obtained as an ionization product and because of their relatively low energies must be formed at very shallow depths (~0.1mm). As electrons are scattered by the atomic potential V(r), determined by the nuclear and electron cloud Coulomb potentials, it is clear that the characteristics of both reflected and secondary electrons are sensitive to variations in atomic number (hence composition) and topography. However, the reflective mode is much more efficient in detecting atomic number contrast while the emissive mode is used when topographical information is required. When used in the emissive mode topographic contrast is so strong that it may dominate any other contrast mechanism.

The SEM's resolution is dependent on amount of current induced in electron probe which further depends on the size of the electron probe. Current induced in electron probe is limited by the diffraction limitation as well as chromatic and spherical aberrations .Beam spreading and the interaction of the probe with the sample are responsible for deterioration of resolution of SEM. At high emission voltages (20-30kV), the resolution limitation is more evident as these high voltages are require for sufficient brightness in conventional electron sources. For resolution less than 1nm lower voltages of the range from 1KV to 5 KV can be used with high-brightness field emission sources. Nevertheless, in a conventional SEM a difference in resolution between the two modes arises because the secondary (typically d~10nm) and reflected (typically d~100nm) electrons originate from different depths in the specimen.

Here in this research work the surface morphology of the as deposited thin films were obtained by using JEOL Carry Scope. It is a compact and portable SEM

that utilizes a standard tungsten filament. It is to be used for inspecting and measuring samples processed in the clean room. The Carry Scope is capable of imaging from 8X to 300,000X and up to 5nm resolution. Accelerating voltage can be varied from 500V to 20kV and the beam diameter can also be adjusted. It features manual XYZ stages with full 360° rotation and -10° to 90° tilt and can hold a full 4″ wafer.

4.2.3 Atomic Force Microscope (AFM)

Atomic Force Microscope (AFM) is another equipment for analyzing the surface morphology of thin films and AFM designed by G. Binnig in 1986 [190]. AFM finds the forced interaction between the surface and a sharp tip. AFM can be used with insulators also as the forced interaction is not dependent on tips and electrically conducting samples. A probe tip is mounted on a cantilever-type spring for measuring the forces. When sample and tip approach each other the forced interaction between them causes the deflection in cantilever following Hooke's law:

$$F = c.\ \Delta z \tag{4.3}$$

Where

c is the spring constant of the tip

Δz is the deflection.

Laser beam deflection is amongst one of the various techniques to sense the deflection. In this optical deflection method laser beam is reflected from the back side of cantilever and the displacement of cantilever gives a measure of laser beam deflection and its detection. A position-sensitive photodiode array is used to find the direction of the reflected laser beam.

The force sensor (cantilever and tip) of the AFM needs to fulfill certain conditions to work:

- Small spring constant to allow detection with even small forces.
- High resonant frequency to minimize sensitivity to mechanical vibrations and for high scan speeds.
- Small effective radius of curvature of sharp tips for atomic resolution studies.

For increasing the cantilever's resonant frequency, its mass must be reduced. Therefore, silicon oxide, silicon nitride or pure silicon using photolithographic techniques are used for micro fabricating AFM cantilevers. The V-shaped cantilevers are preferred over rectangular cantilevers due to their increased lateral stiffness. V-

shaped cantilevers does not lead to lateral bending of the cantilever due to its reduced sensitivity to lateral (frictional) forces. AFM images can be degraded to a great extent due to this lateral bending. Moreover the surface structure measurements are provided with the help of the lateral forces measurement. Due to different interactions between the tip and the sample, the AFM operates as "noncontact mode or attractive" and "contact mode or repulsive". Contact AFM is used to acquire images captured in this work, we will briefly discuss it next.

4.2.3.1 Contact AFM

In contact AFM mode, the tip is brought in contact with the specimen surface at a certain value of the force. This force is conserved to constant value with the help of a feedback system that reverses the tip as soon the measured force is found above the stipulated value, and approaches it when the force falls below a lower value. Different AFM images are produced by two feedback modes and these images can be easily distinguished from each other [191].

As the tip is scanned over the surface then the force is kept constant along the z position at each point of the tip by the feedback mechanism. The feedback system responds very fast to small changes in the applied force. For a slowly responding feedback system, average force (and height) is kept constant only. Variations are caused in the set value by surface features on the force.

4.2.3.2 Advantages & Disadvantages of AFM over SEM

As compared to scanning electron microscope (SEM), AFM has many advantages over it. AFM gives three dimensional surface profile of a sample, while scanning electron microscope gives a two-dimensional image or a two-dimensional projection. Further, samples viewed by AFM do not need any metal or carbon coatings while in SEM these coatings can irreversibly damage or change the sample. AFM modes can work perfectly well in ambient air or even in humidity atmosphere, whereas SEM requires costly vacuum conditions for proper operation. As AFM has higher resolution than SEM thereby making it possible to study even living organisms and biological macromolecules. AFM gives actual atomic resolution in ultra-high vacuum, and high resolution AFM performance resolution is comparable to Transmission Electron Microscopy and Scanning Tunneling Microscopy in liquid environments.

Image size is one of the disadvantage AFM has as compared to SEM. The AFM images a largest elevation of the order of micrometers and a maximum 150×150 μm scanning area where as SEM can image maximum loftiness on the order of millimeter and millimeters by millimeters area.

Another disadvantage is that image artifacts can occur due to wrong choice of tip for the resolution required. Traditionally the speed of scanning of AFM is not fast as compared to SEM. AFM needs several minutes for a typical scan, while a SEM is scans at very fast speeds of the order of real-time for a poor quality image. Due to this AFM scanned images does not give accurate measurement of distances and it also gives rise to thermal drift. To phase out the image distortions due to thermo drift, various techniques are suggested. Scanned images of AFM are distorted by cross-talk between the (x, y, z) axes and hysteresis of the piezoelectric material that will require filtering and software enhancement. Filtering can "spread out" actual topographical features. However, real-time correction software or closed-loop scanners are used in newer AFMs that practically remove all such issues. Orthogonal scanners (as opposed to a single tube) are used in few AFM to remove cross-talk problems. Therefore both the techniques are complementary to each other.

4.3 Structural and Morphological Studies of as Deposited Thin Films

In order to achieve the objective 1, the as prepared thin film sample series of undoped and doped SnO_2/ZnO were characterized by complementary techniques such as X-ray diffraction (XRD), scanning electron microscopy (SEM), and atomic force microscopy (AFM) from the following Labs:-

- CEERI- Pilani (Rajasthan), Dr. K. J. Rangra
- AIRF- JNU (New Delhi Campus), Dr. Manoj Partap Singh
- Puerto Rico- USA, Department of Physics, Dr. R.S. Katiyar
- IIT-Delhi- Physic Dept., Thin Film Division, Dr. M.C. Bhatnagar
- Thapar University- (Patiala), SAI LAB, Dr. Sushil Mittal
- KU-Kurukshetra, Esc. Department, Dr. Dinesh Gupta

4.3.1 XRD Analysis of Undoped SnO_2 Powder

The XRD pattern of the 1st sample of this work i.e. undoped SnO_2 powder obtained by sol-gel via precipitation method and annealed at 200°C is shown in Fig. 4.1.

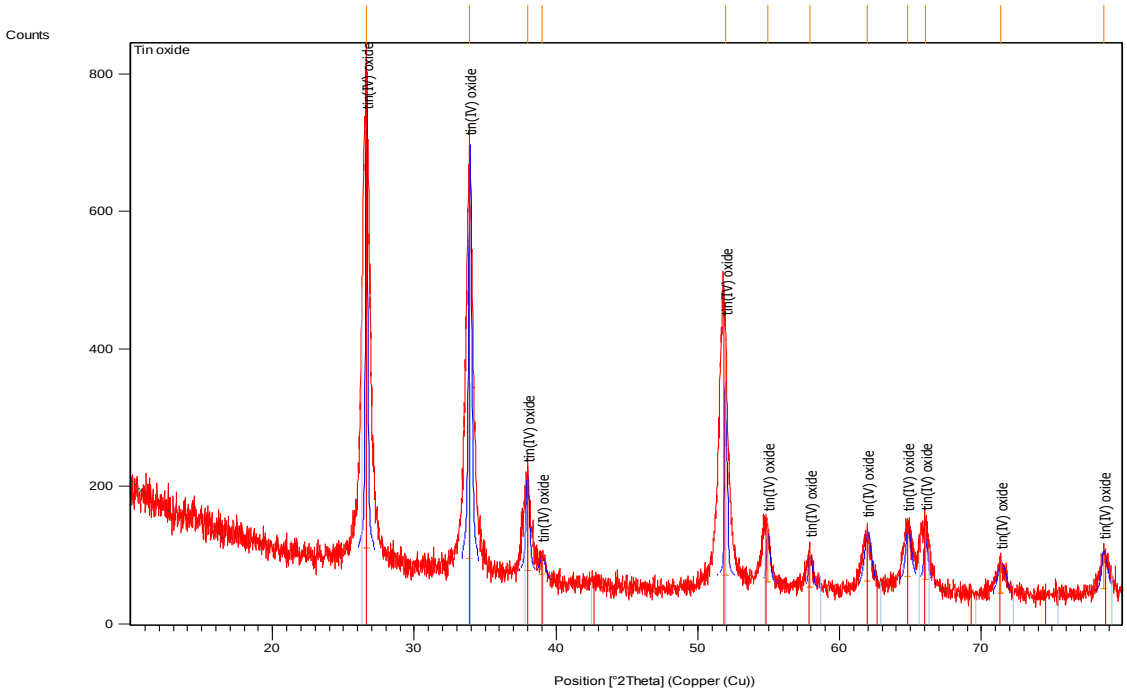

Fig. 4.1: XRD pattern of Undoped SnO_2 powder

The structural analyses of undoped SnO_2 powder obtained by sol-gel via precipitation method and annealed at 200°C are carried out with the help of an X-ray diffraction pattern. The diffraction peaks are quite similar to those of bulk tin oxide which can be indexed at 2θ= 26.61º (110), 33.91º (101), 51.91º (211), 54.93º (220) and 57.90º (002) corresponds to tetragonal structure of SnO_2. The crystalline size in the prepared undoped SnO_2 powder is obtained using Scherer formula as shown in the following Table 4.1.

The Sherrer diffraction formula was used to estimate the crystalline domain size (D): $D = k\lambda / \beta_{FWHM} Cos\theta$ where k=0.9, λ=1.54056 Å (X-ray wavelength for CuK_α), β_{FWHM} is line broadening at half the maximum intensity (FWHM) in radians and θ is the diffraction angle. The crystalline domains sizes correspond to the different peaks of tin oxide positioned are found as follows: i.e. 53 nm at (26.61º), 33 nm at (33.91º), 29.0 nm at (37.97º), 18 nm at (38.99 º), and 55 nm at (51.94 º).

Table 4.1: Crystalline size of undoped SnO_2 powder prepared by Sol-Gel process

Pos. [°2Th.]	Height [cts]	FWHM [°2Th.] β	d-spacing [Å]	Rel. Int. [%], size
26.6117	704.57	0.1535	3.34972	**100.00, D= 53nm**
33.9100	592.70	0.2303	2.64363	**84.12, D= 33nm**
37.9708	135.66	0.2558	2.36973	**19.25, D= 29nm**
38.9975	25.36	0.4093	2.30967	**3.60, D= 18nm**
51.9463	355.29	0.1279	1.76033	**50.43, D= 55nm**
54.9336	81.69	0.2047	1.67146	11.59
57.9021	50.83	0.2558	1.59264	7.21
61.9431	70.01	0.4605	1.49809	9.94
64.8088	73.30	0.3582	1.43861	10.40
66.0347	78.71	0.2047	1.41484	11.17
71.3718	41.82	0.6140	1.32159	5.94
78.6128	48.40	0.3120	1.21600	6.87

The average crystalline size is found to be ≈36 nm. It is observed that there is no additional peak in the XRD spectra which indicates high crystalline behaviour of the prepared undoped SnO_2 powder.

4.3.2 XRD Analysis of Undoped and Ag-Doped SnO_2 Thin Films

XRD patterns of undoped & Ag-doped Tin Oxide thin films samples (prepared via chemical route with PVA and using spin coating unit) at RT and annealed at different temperatures (300º C, 350º C, 400º C, 450º C and 500º C) are shown in Fig. 4.2. Among the metal additives to SnO_2, Ag has also been used for gas sensing application [192]. Therefore in this thesis, we successfully synthesized SnO_2 embedded in PVA by chemical route with silver as a noble metal additive. Thin film was deposited on silica substrate via spin coating process and annealed at different temperatures. The thin film samples of silver doped tin oxide were characterized by elementary techniques such as X-ray diffraction (XRD) and scanning electron microscopy (SEM). However, the effect of variation of the sintering temperature on the silver doped tin oxide thin film is not yet attempted.

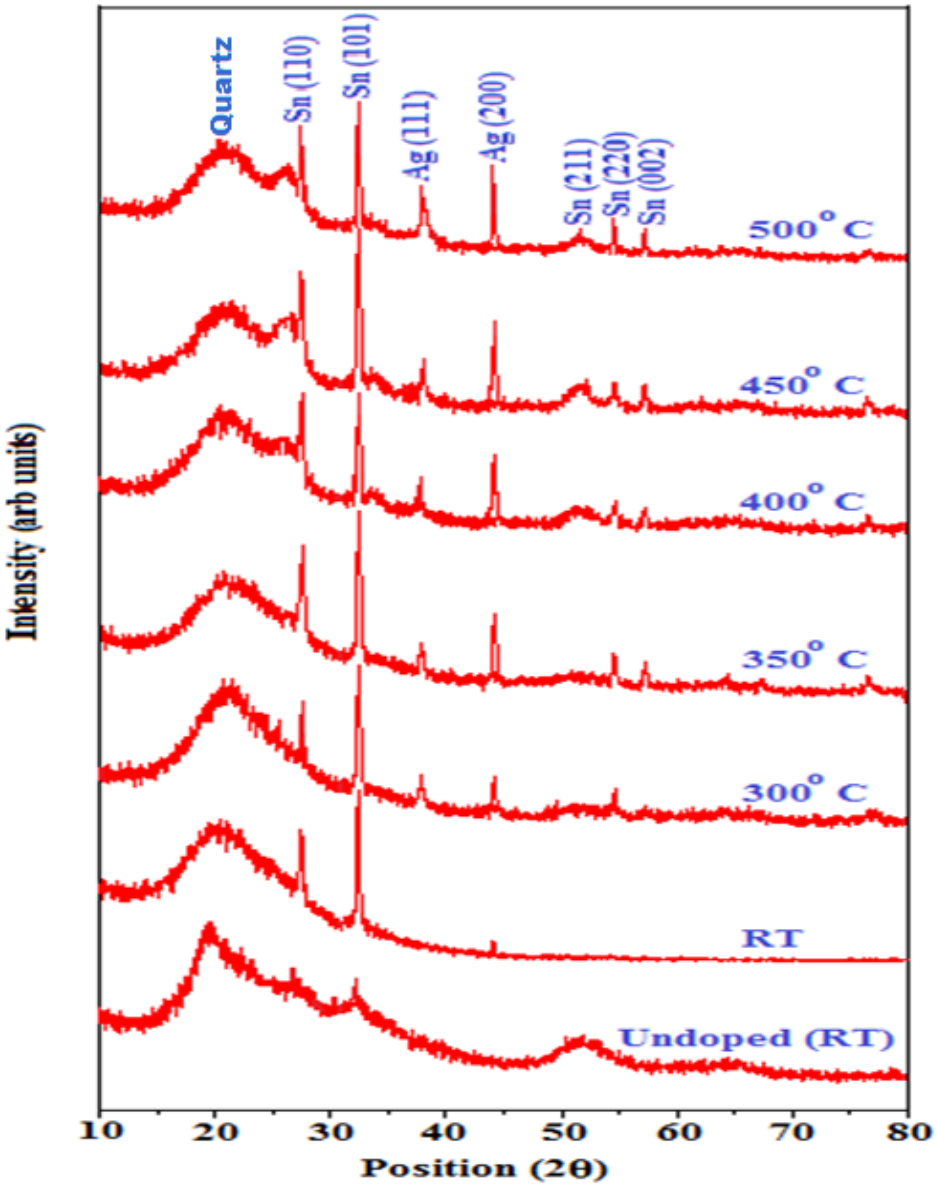

Fig.4.2: XRD pattern of undoped & Ag-doped Tin Oxide thin films at RT and annealed at different temperatures (300º C, 350º C, 400º C, 450º C and 500º C).

The diffraction peaks are quite similar to those of bulk tin oxide [185] which can be indexed at 2θ= 27.30º (110), 32.46º (101), 51º (211), 54.5º (220) and 57º (002) corresponds to tetragonal structure of SnO_2. This is actually in a good agreement with the JCPDS file of SnO_2 (JCPDS: 41-1445). The broad peak at 2θ corresponds to quartz substrate.

In addition to this, peaks observed at 2θ= 38º (111) and 44º (200) are assigned due to silver (JCPDS: 4-783). Indeed, no additional peaks were observed, indicating the high purity of the thin films. Furthermore, the intensities of various peaks are very weak for undoped sample. However, for all annealed samples, the appearance of

sharp peaks and the similarities in terms of the peak positions and the half peak width indicate a well-developed crystallinty, whereas there is no second phase appears for these annealed samples, implying that the dopant segregation does not occur during high temperature annealing. The Sherrer diffraction formula was used to estimate the crystalline domain size (D): $D = k\lambda / \beta_{FWHM} Cos\theta$ where k=0.9, λ=1.54056 Å (X-ray wavelength for CuK_{α}), β_{FWHM} is line broadening at half the maximum intensity (FWHM) in radians and θ is the diffraction angle. The crystalline domains sizes correspond to the most prominent peak of tin oxide (101) positioned at 32.46º were found to be 16.0 nm (RT), 17.25 nm (300 ºC), 18.0 nm (350 ºC), 19.50 nm (400 ºC), 20.0 nm (450 ºC) and 21.0 nm (500 ºC). In short, average crystalline size was found to be 18.62 nm. It is observed that there is no considerable difference among the half peak widths in the XRD profiles of the annealed thin film samples. Furthermore, the phenomena certify that the difference among the crystalline size of all the annealed samples is slight. The main feature of the spectra is, with increasing annealing temperature, crystalline size increases which indicates the enhancement of high crystalline behaviour and hence the sensitivity of the films increased [193]. These results agree well with the conclusion that tin oxide nanoparticles exhibit a lattice expansion with reduction in the particle size [194]. Therefore, a programme of annealing temperature (300ºC - 500ºC) was undertaken and we observed that thin film samples could be good candidate for sensing applications.

4.3.3 XRD Analysis of Undoped and Cu-Doped ZnO Thin Films

XRD pattern of undoped and 3% Cu-doped ZnO films sample (prepared by PLD technique) are shown in Fig 4.3. As shown in Fig. 4.3 a dominant (002) peak and weaker (100) and (101) peaks of ZnO with slight shift due to Cu doping are observed, which indicates that both the films have strong preferred c-axis orientation. Using Sherrer diffraction formula ($D = k\lambda / \beta_{FWHM} Cos\theta$ where k=0.9, λ=1.54056 Å (X-ray wavelength for Cu K_{α}), β_{FWHM} is line broadening at half the maximum intensity (FWHM) in radians and θ is the diffraction angle) the crystallite size of most intense peaks corresponding to (002) plane are 52.59nm and 41.45nm for undoped and 3% Cu doped ZnO thin films respectively.

Though, we have developed a complete sample series of undoped ZnO and varying Cu concentration ranging from (1 to 5 %) in host ZnO matrix. As for doping concentration up to 3 % Cu, no CuO phase was found.

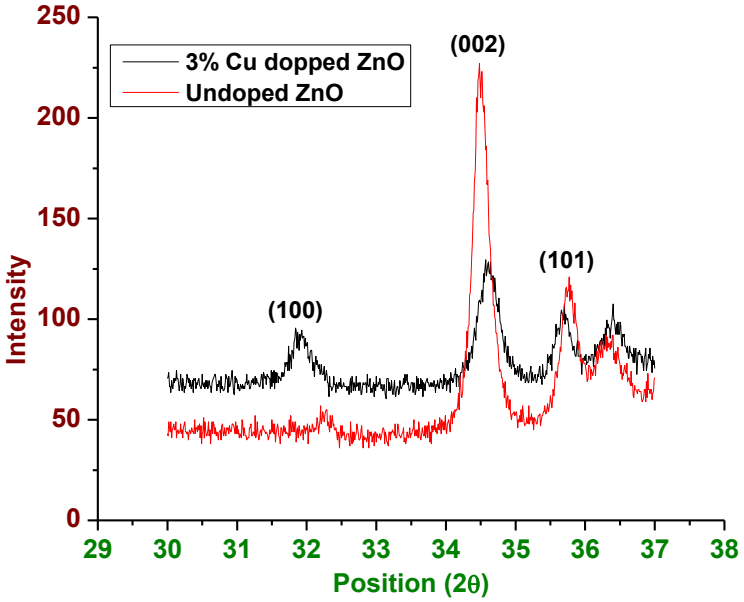

Fig. 4.3: XRD graph of undoped and 3% Cu-doped ZnO films

Though, we have developed a complete sample series of undoped ZnO and varying Cu concentration ranging from (1 to 5 %) in host ZnO matrix. As for doping concentration up to 3 % Cu, no CuO phase was found. It implies that copper atoms replace zinc in the hexagonal lattice and/or copper segregate to the non-crystalline region in the grain boundary. But weak CuO phase appeared from 5 % Cu doping. It may indicate that the solid solubility of Cu in ZnO has been exceeded. Moreover, it is found that there is slight increase in lattice parameters up to 5% Cu doping, as compared with the undoped ZnO. The slight increase in lattice parameter revealed that the ionic size of tetrahedrally coordinated Cu^{2+} is larger than Zn^{2+}. The reason of increment may be due to the non uniform substitution of Cu ion into the Zn site as the radius of Cu^{2+} ion is smaller than the Zn^{2+} ion.

Such kind of results may be due to the growth conditions like deposition technique, doping procedure, substrate temperature, oxygen pressure, energy of laser radiation, etc. and also agree with previous reports [102], [103] and [195]. Q.A. Drmosh *et al.* [195] reported the structural properties of Cu-doped ZnO thin films for different concentration of Cu and found that 3 wt% Cu-doped ZnO film show the

more significant shift in (002) peak in comparison with 1wt% Cu and 2wt% Cu-doped ZnO thin films.

Moreover, Shewale *et al.* [103] reported that a structural parameter like dislocation density shows a decreasing trend with the Cu doping concentration from 1 wt% to 3 wt% while for further increase in Cu concentration i.e. at 4 wt% the dislocation density increases, which leads to increase the concentration of lattice imperfections. So, in order to achieve higher sensitivity at lower operating temperature we need to utilize the active film with minimum number of dislocation in the crystalline structure. More recently, L. Chow *et al.* [102] also reported the similar structural results in ZnO peaks with increasing Cu concentration from 0 to 3 wt%. Here, such kind of results may be due to the fact that moderate quantity of Cu atoms (≈3 wt %) could be considered to exist as interstitials that shared the oxygen with Zn atoms and excess Cu doping atoms (>3 wt %) can be energetically favorable to coalesce into metallic copper clusters [196].

Furthermore, Fig.4.3 clearly shows the effect of 3% Cu doping in ZnO lattice: it does not lead to phase segregation, thus we can conclude that Cu ions did not change the hexagonal wurtzite structure in Cu-doped ZnO film and that is an important issue for gas sensing applications. Therefore, 3% Cu doping corresponds to the better crystallization of the doped ZnO thin films. Consequently we have chosen 3% of copper doping in host ZnO for this thesis.

4.4 Raman Analysis of Undoped and 3% Cu-Doped ZnO Thin Films

Raman spectroscopy of undoped and 3% Cu-doped ZnO films sample (prepared by PLD technique) are shown in Fig 4.4. This graph shows the Raman shifts between 200 to 1200 per cm. Raman scattering is inelastic scattering, typically weak than Raleigh scattering but have advantage over IR spectroscopy. It provides the information regarding microscopic structure, vibration, rotational, and other frequency modes in this range of as deposited thin films. We obtain E_2 (high) modes of high intensity at 437 Cm^{-1} along with additional modes (AM) at 577 Cm^{-1} of lower intensity in 3% Cu doped ZnO thin films hinting towards minimum defects and E_2 (high) is a symbol of wurtzite phase of ZnO.

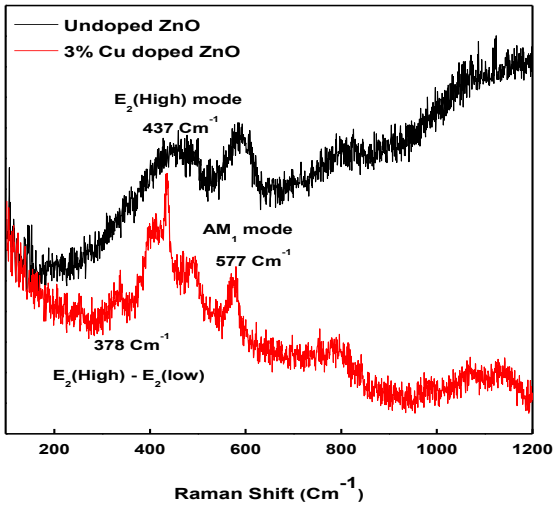

Fig. 4.4: Raman spectroscopy of undoped and 3% Cu-doped ZnO thin film

4.5 SEM Analysis of Undoped and Ag-Doped SnO_2 Thin Films

Control on size, morphology and distribution of nanoparticles play a vital role in the properties on nanocomposites. Thus in orders to get a real idea what are happening inside the material, SEM micrographs were taken into account. The surface morphology of 1.0g Ag doped SnO_2 nanocomposite thin films and undoped SnO_2 film (prepared by chemical route with PVA and using spin coater) at room temperature are shown in Fig.4.5 (a) and Fig. 4.5(a) inset respectively.

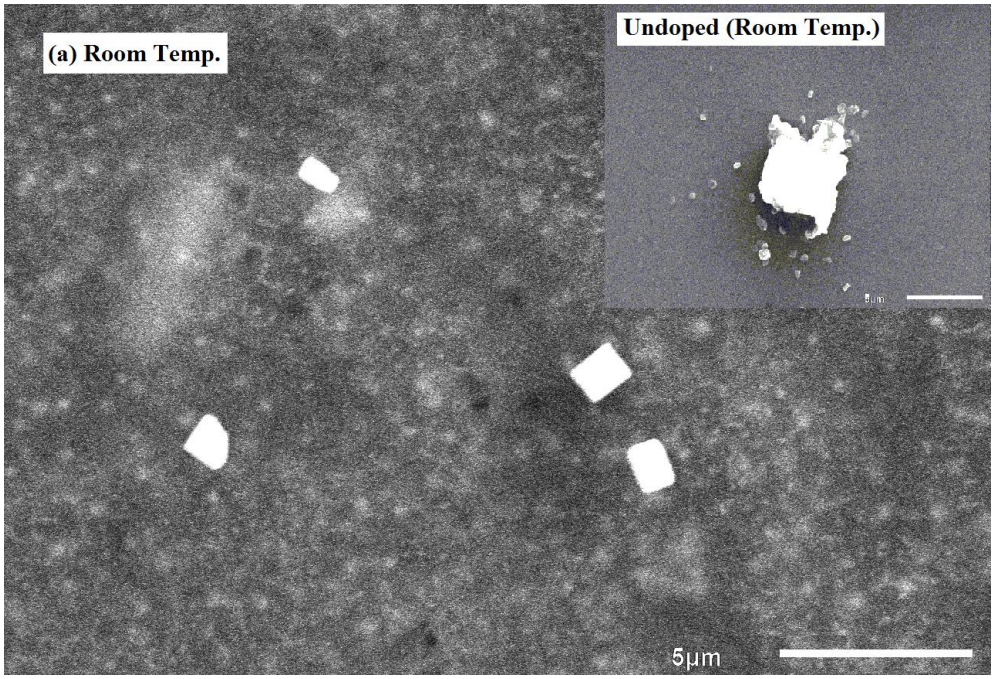

Fig. 4.5 (a): 1.0g Ag doped and undoped (inset) SnO_2 thin film at room temperature

In Fig. 4.5(a) four aggregates of size ≈ 1μm are observed for 1.0g Ag doped SnO_2 film at room temperature and additionally small particles of less resolution can also be seen in the micrograph. The surface morphology of 1.0g Ag doped SnO_2 films annealed at different temperatures (300 ºC, 350 ºC, 400 ºC, 450 ºC and 500 ºC) are shown in Fig. 4.5 (b-f).

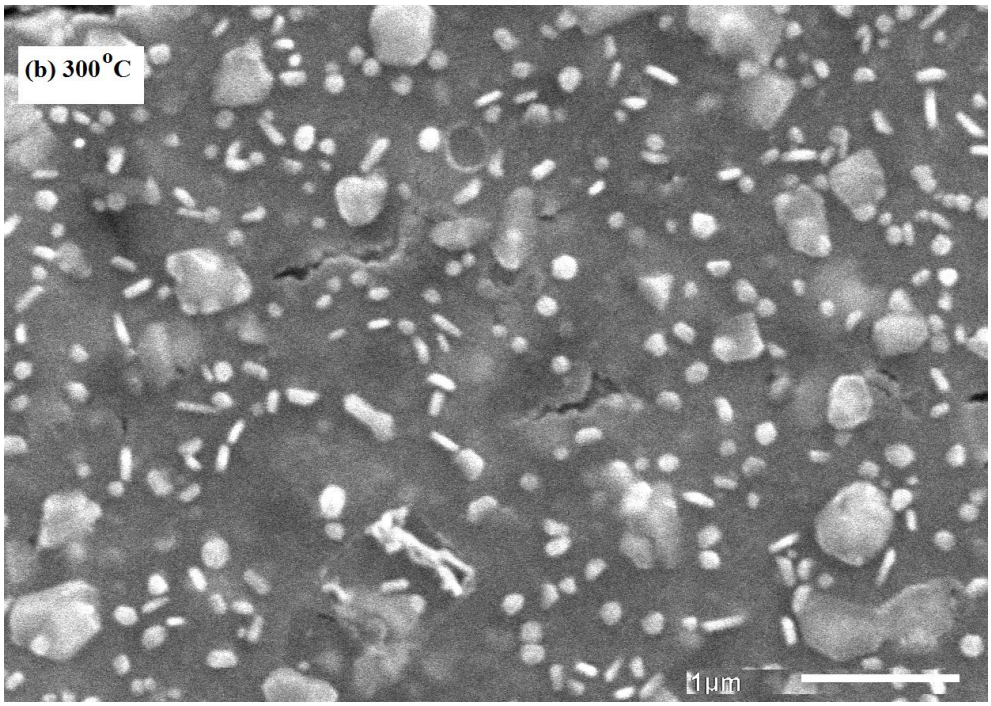

Fig. 4.5 (b)

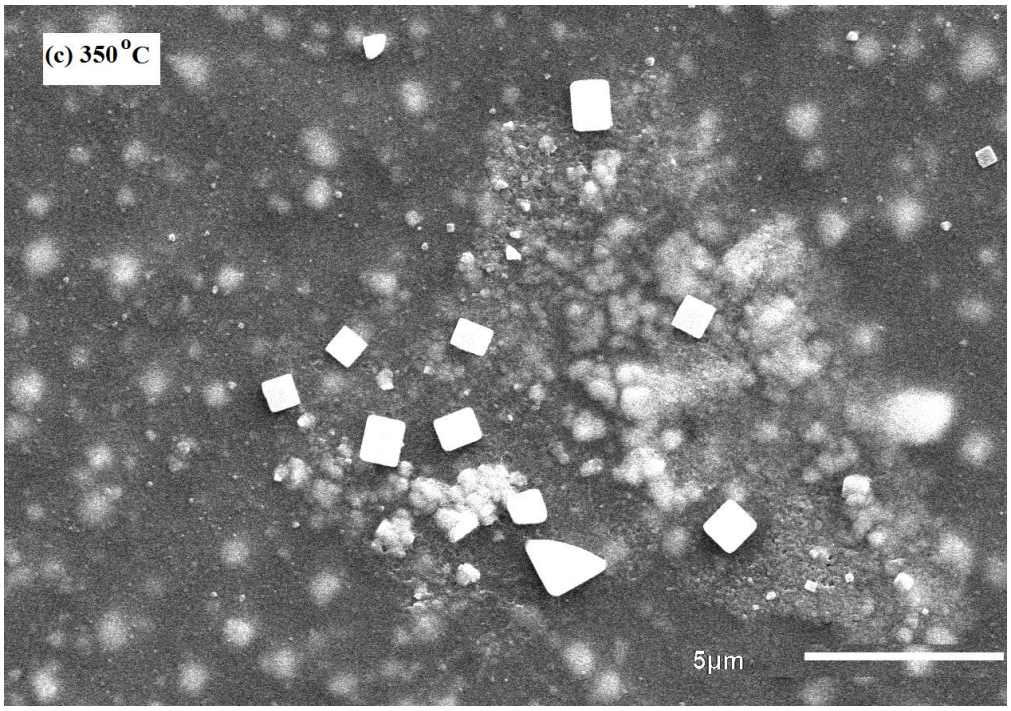

Fig. 4.5 (c)

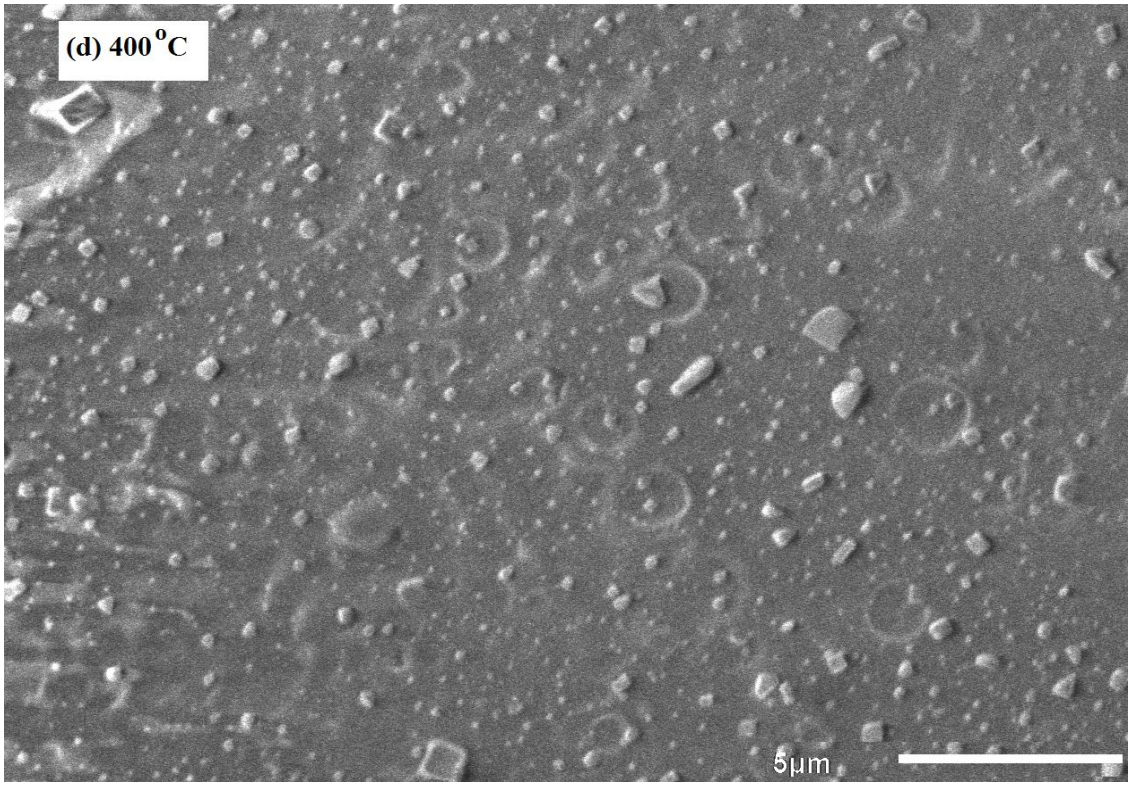

Fig. 4.5 (d)

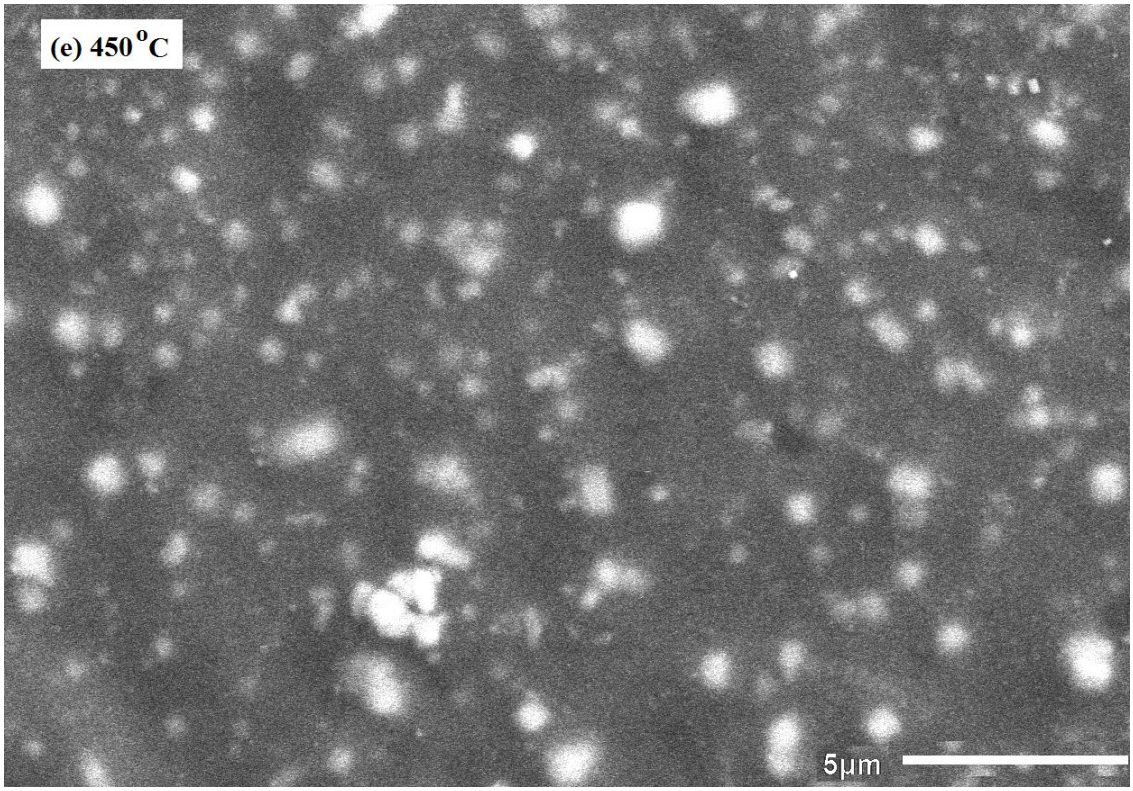

Fig. 4.5 (e)

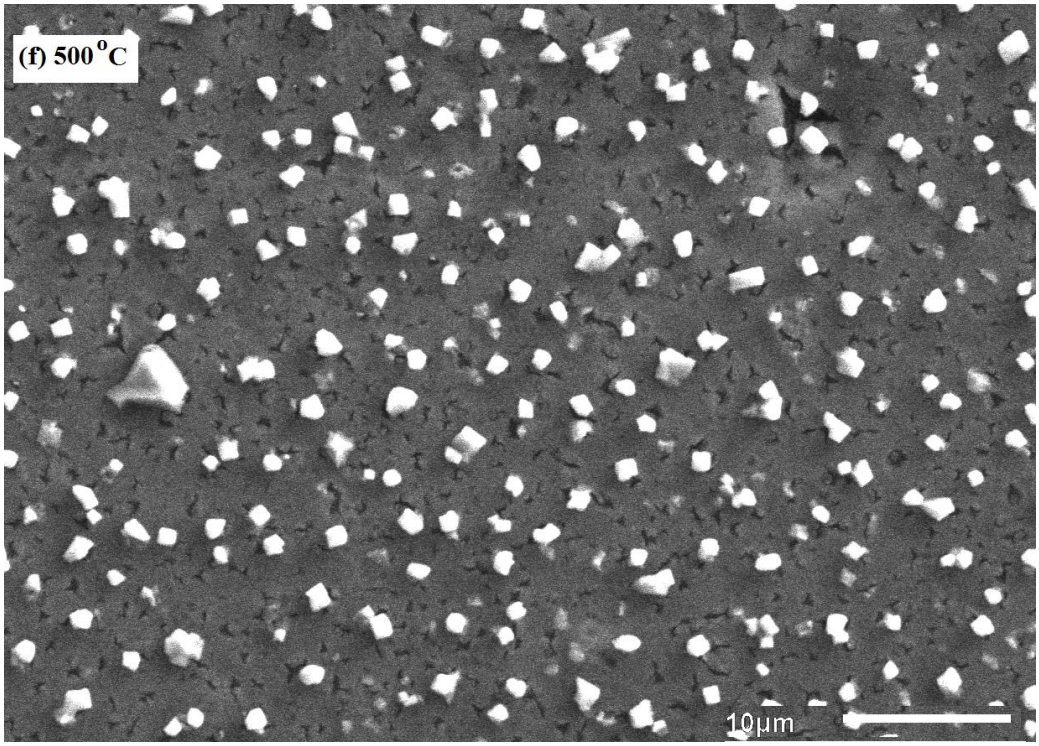

Fig. 4.5 (f)

Fig. 4.5(b-f): Surface morphology of 1.0g Ag doped SnO_2 films annealed at different temperatures (300 ºC, 350 ºC, 400 ºC, 450 ºC and 500 ºC)

From image 4.5 (b) the small rod and spherical shape particles in silver doped SnO_2 film are also observed; besides a mixture of smaller and larger aggregates can also be seen in the film treated at 300 ºC. In Fig 4.5 (d) small spherical/rectangular shaped particles are observed for the film treated at 350ºC. In this image, some agglomeration along with the individual particles is also seen, while in blurred image 4.5 (e) the particles with smaller aggregates also being observed. In Fig. 4.5(f), the film appears to be smooth relative to the other images and the particles with larger diameter are also observed; additionally, in this image the superficial cracks appear on the surface of the film as the film shrinks due to grain growth during the calcinations process. In the SEM micrographs of silver doped SnO_2 films, we cannot separate silver clusters and the SnO_2 grains. Therefore, we do not have possibilities to estimate the real size of Ag clusters. However, taking into account that synthesized precipitates include silver and SnO_2, one can suppose that due to the bigger silver density of the presence of additional oxygen atoms in SnO_2 compound, the average size of the silver clusters must be smaller than the size of the SnO_2-silver precipitates. Therefore, distribution of the particle size and the average particle size were obtained by using a public domain software i.e. ImageJ (It is Java-based image processing programme

developed by Wayne Rasband at national institute of health) and the results were shown in Fig. 4.6(a-e) with histograms.

The distribution of the particle size of 1.0g Ag doped SnO_2 films annealed at different temperatures (300 ºC, 350 ºC, 400 ºC, 450 ºC and 500 ºC) are shown in Fig. 4.6 (a-e).

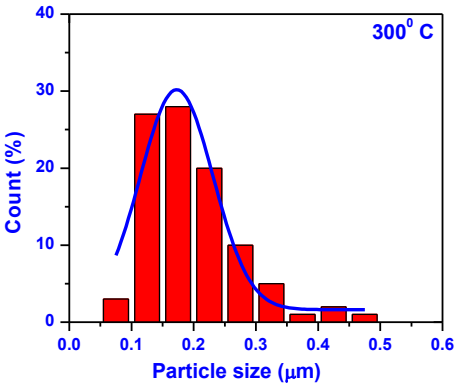

Fig. 4.6(a)

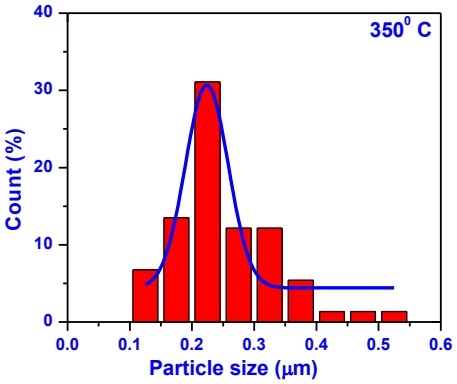

Fig. 4.6(b)

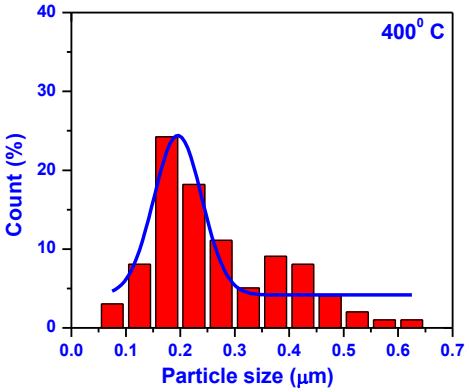

Fig. 4.6(c)

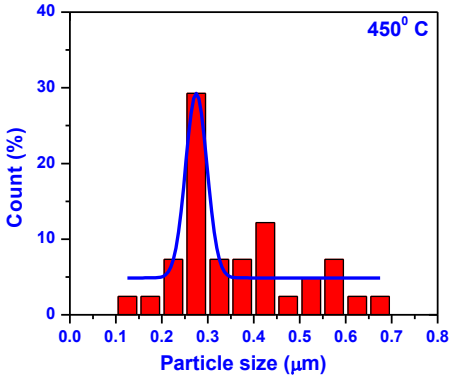

Fig. 4.6(d)

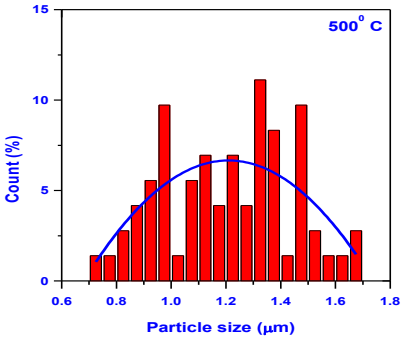

Fig. 4.14(e)

Fig. 4.6(a-e): Distribution of the particle size of 1.0g Ag doped SnO_2 films annealed at different temperatures (300 ºC, 350 ºC, 400 ºC, 450 ºC and 500 ºC)

The average particle sizes were calculated as 0.275 μm (Fig. 4.6a), 0.325 μm (Fig. 4.6b), 0.350 μm (Fig. 4.6c), 0.400 μm (Fig. 4.6d) and 1.2 μm (Fig. 4.6e) for films annealed at temperatures 300 ºC, 350 ºC, 400 ºC, 450 ºC and 500 ºC for one hour, respectively. In these figures, solid lines give the Gaussian fit to the particle size distribution (histogram) and it is observed that the particle size distribution became broader for the film annealed at 500 ºC (Fig. 4.6(e)), while in figures 4.6 (a-d) particle size distribution is nearly uniform. Consequently, as shown in the above figures, the temperature effect on the particle size is evident. These observations were consistent with that reported by Jin et al. on sol-gel formed nanocrystalline tin oxide film [197]. Namely, at relatively high annealed temperatures the particle sizes itself and its distribution in the film appeared to become larger. The SEM images were also consistent with the trend observed from the XRD i.e. increase in crystalline size with increase in annealing temperature.

4.6 SEM Analysis of Undoped ZnO and Li-Doped ZnO Thin Films

The surface morphology of the undoped ZnO (a), 2% Li-doped ZnO (b), and 8% Li-doped ZnO (c) thin films (developed by PLD technique) are shown in Fig. 4.7.

It can be observed that the particles are mono-dispersed, closely packed and well distributed on the quartz substrate. Small broken hexagonal crystals are detected in 8% Li-doped ZnO films i.e. Fig. 4.7 (c) exhibits a rougher surface morphology of ZnO thin film than Fig. 4.7 (a) and Fig. 4.7 (b). Though, smooth surface and uniform morphology are obtained for 2% Li- doped ZnO film and causes a high resistivity due to substitution of smaller lithium ions at Zn sites. Conversely, high doping of 8% Li leads to a lower resistivity reason likely involves the formation of Li interstitial defects, which have a donor nature and the excess of lithium employed as carrier [198]. Accordingly, the control of grain size, morphology and distribution of nanoparticles play a vital role in the gas sensing properties of the films [199].

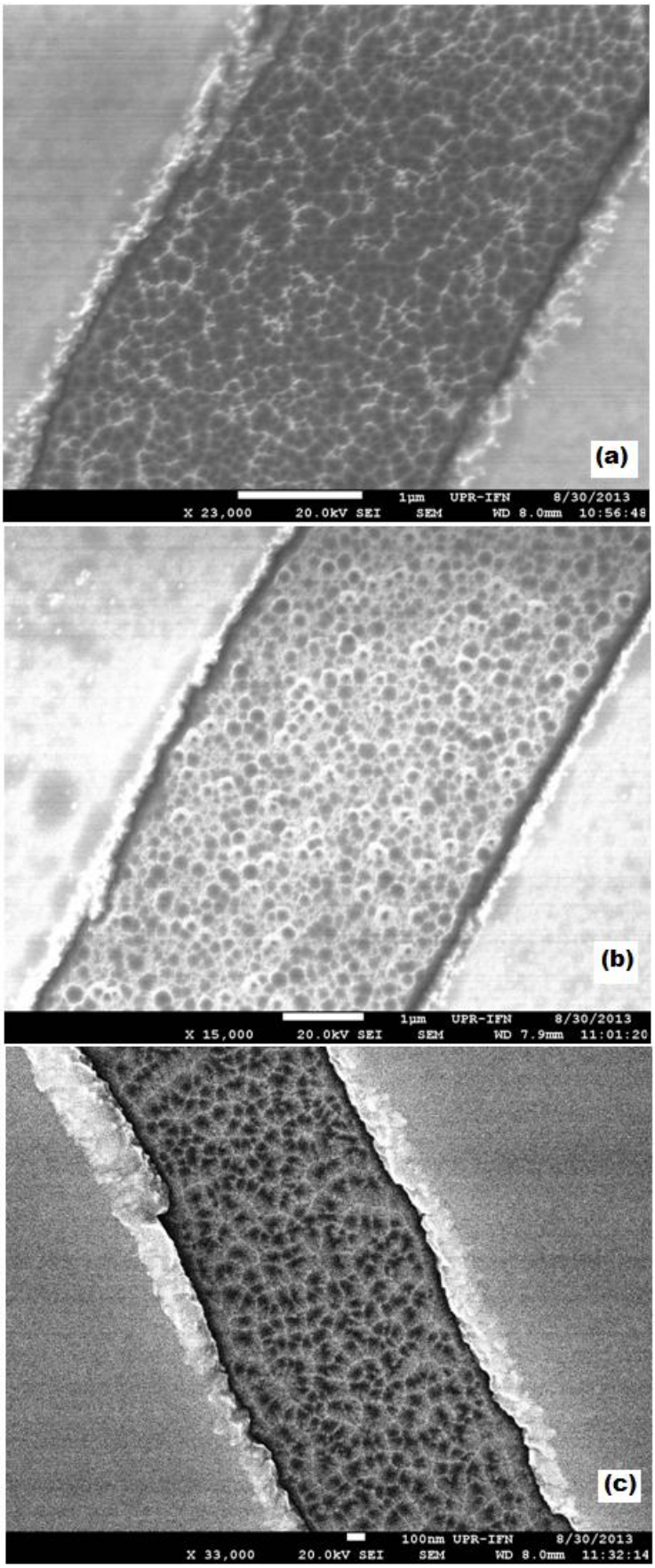

Fig. 4.7: SEM images of (a) pure ZnO, (b) 2% Li-doped ZnO, and (c) 8% Li-doped ZnO

4.7 AFM Analysis of Undoped and 3% Cu-Doped ZnO Thin Films

The surface topography (a) and (c) of the undoped ZnO, and (b) and (d) of 3% Cu-doped ZnO thin films (developed by PLD technique) were investigated by AFM in 2D and 3D respectively as shown in Fig. 4.

It can be seen that the particles are mono-dispersed, closely packed and well distributed on the quartz substrate. The root mean square (rms) of the surface roughness of films showed no significant difference in its value, which was about 18 ± 2 nm. Topography, control of grain size, morphology and distribution of nanoparticles play a vital role in the gas sensing properties of the films.

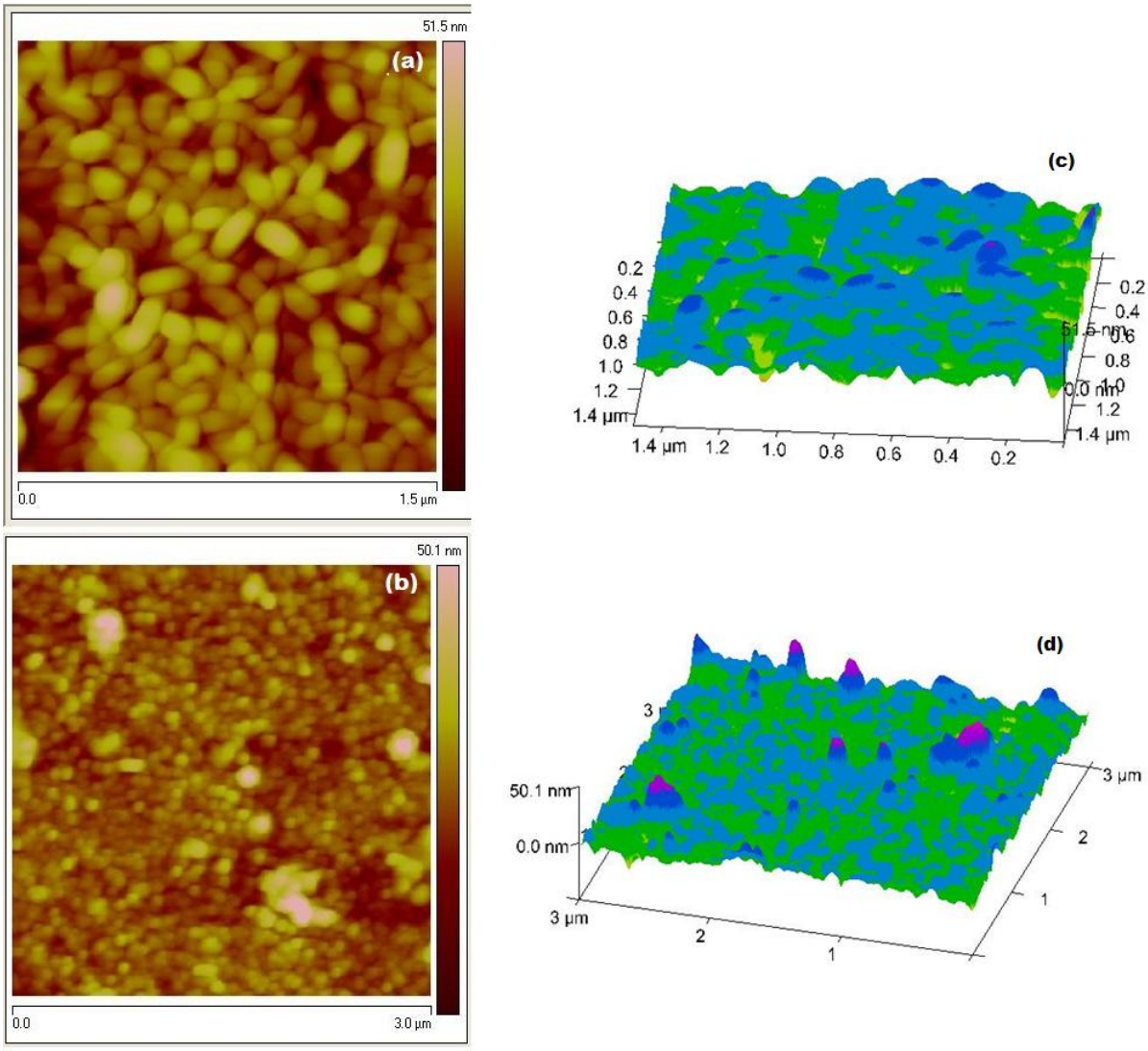

Fig.4.8: AFM images (a) and (c) of undoped ZnO, (b) and (d) of 3% Cu-doped ZnO thin films in 2D and 3D

It is clear from the above structural and morphological studies that undoped and doped ZnO thin films deposited by PLD techniques have shown the better crystalline structure and surface morphology as compared to undoped and doped SnO_2 thin films developed by chemical route. As good crystalline structure and surface morphology of the thin films are the mandatory requirements to be used for gas sensing. Therefore in the next chapter undoped ZnO, Cu-doped ZnO, and Li-doped ZnO thin films were tested for various gas sensing parameters.

Chapter 5 Gas Sensing Properties of as Deposited Thin Films

Undoped and doped-ZnO thin film based sensor structures prepared by PLD technique have been exploited for H_2 gas sensing. Deposition parameters of the developed sensors have been optimized to yield enhanced response characteristics towards different concentrations for H_2 gas. Undoped and varying quantity of Copper (Cu) and Lithium (Li) were deposited over ZnO thin films, and their responses behaviour towards H_2 and CH_4 are studied. The sensing response with varying H_2 gas concentration at three operating temperatures viz. 50 ºC, 100 ºC and 150 ºC and cross selectivity of the developed sensor structure towards methane (CH_4) gas is also studied in this work.

5.1 3%Cu-doped ZnO Thin Film Gas Sensor for H_2 and CH_4 gases

5.1.1 Introduction

For achieving the 2nd and 3rd objectives highly sensitive and selective gas sensor for hydrogen gas has been developed utilizing copper doped zinc oxide (Cu-ZnO) thin films. These films were deposited using PLD technique with various parameters on quartz substrates with predeposited interdigitated platinum electrodes. The as deposited films were characterized by XRD and AFM. The novelty of this sensor is that the sensitivity for methane and hydrogen gases can be completely reversed if measurements are performed at 150 ^{0}C as compared to 50 or 100 ^{0}C.

As discussed in the chapter 2 under gaps in the literature review that the major problems associated with ZnO based hydrogen gas sensor are their high operating temperature (normally between 250 ºC to 400 ºC) and poor selectivity (as shown in Table 2.1). However, high working temperature of such gas sensors is energy intensive, increases operating cost and requires high operational safety measures in an environment with explosive gases like H_2. Therefore, our aim is to reduce the operating temperature of ZnO based hydrogen gas sensor for safety in industrial and household environments. Copper is known as a preferable dopant in ZnO due to its advanced attributes such as low toxicity, source abundance, similar ionic radius as that of Zn^{2+} ion, electronic shell structure, and many physical and chemical properties similar to those of Zn [169]. ZnO thin films doped with Cu are known to have higher electrical resistance and improved gas sensing properties [200]-[201]. The electrical resistivity of ZnO was increased by doping Cu indicating the acceptor like behaviour

of the Cu dopant. The co-ordinated Zn^{2+}, Cu^{1+} and Cu^{2+} cations have ionic radii of 0.06, 0.06 and 0.057nm respectively, with stable electronic configuration, Zn^{2+} ($3d^{10}$), Cu^{2+} ($3d^{9}$) and Cu^{1} ($3d^{10}$). The increase in film resistivity can be explained in terms of electron trapping by Cu 3d hole states of Cu^{2+}. The copper dopant in the ZnO films can be in the form of copper oxide. CuO (Cu^{2+}) has a Cu 3*d*9 4*s*0 O 2*p*6 valence band configuration (neglecting hybridization) and may therefore trap electrons with the Cu 3*d* hole state [202]. So resistivity is increased. Consequently, in the present work, we have chosen 3% Cu-doped ZnO thin films (as discussed in chapter 4 under XRD Analysis of Undoped and 3% Cu-Doped ZnO Thin Films) for investigating the hydrogen gas sensing properties, as there are very few reports available in literature for the same.

5.1.2 Experimental Detail

Although, there are several methods for the deposition of ZnO thin films; yet, PLD technique has been considered as an important promising technique for the growth of high quality films because of its ability to maintain the expedient control of the stoichiometry of the target material in the film and a relatively higher deposition rate in controllable oxygen partial pressure. Consequently, undoped ZnO and 3% Cu-doped ZnO thin films were successfully grown by PLD technique. The chamber was evacuated by a turbo molecular pump to a base pressure of 1×10^{-6}Torr. Quartz substrates with pre-deposited interdigitated pattern of platinum were used for film deposition as shown in Fig. 5.1.

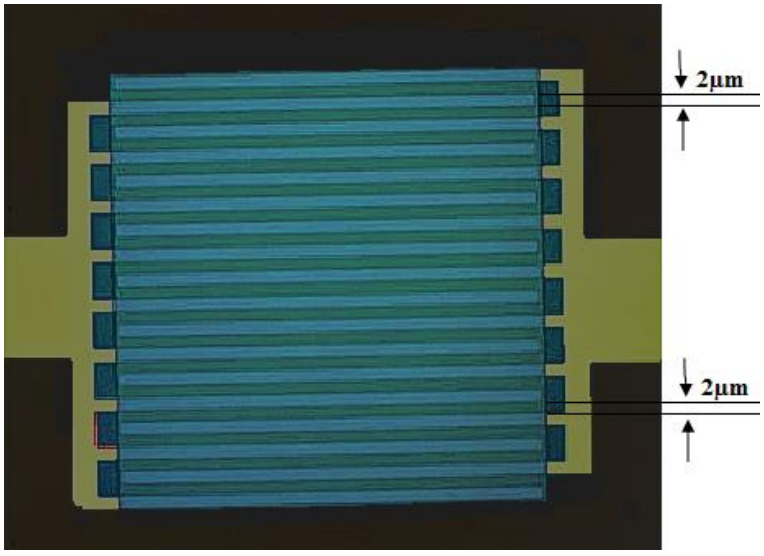

Fig. 5.1: ZnO film deposited on interdigitated electrode pattern

The substrates were ultrasonically cleaned in acetone and in methanol for 3 minutes. We have used a pure and Cu-doped ZnO target for thin film deposition. A KrF excimer laser (λ=248 nm) with beam energy of 250 mJ/pulse at a repetition rate of 5 Hz was used for ablating the target. Thin films of about 300nm thickness were deposited at a substrate temperature of 300 ºC with 300mTorr oxygen pressure in the chamber.

Crystalline structure and surface topography of the as deposited films as discussed in chapter 3 were characterized by X-ray diffraction (Rigaku Ultima III instrument) and atomic force microscopy (Nanoscope V), respectively. The gas sensing parameters of as grown thin films were studied by I-V measurement technique using a custom made gas sensing setup as shown in Fig. 5.2.

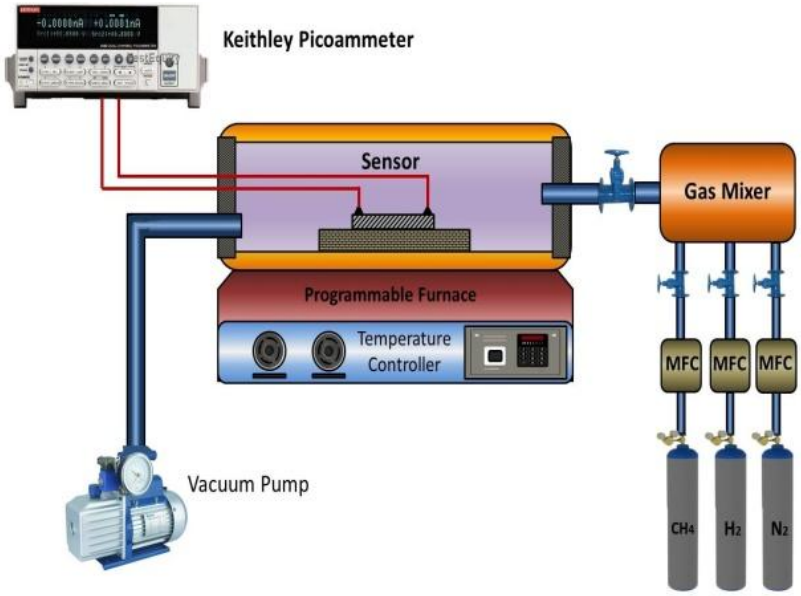

Fig. 5.2: Gas sensing setup-1

The gas sensing measurements were performed by a PC connected to a Keithley 2401 low voltage source, picoammeter through GPIB interface and lab view v8.5 software. As deposited sensor was placed inside a test chamber fitted with programmable heating arrangement. The hydrogen (H_2) and methane (CH_4) gases were allowed to flow through the test chamber using Sierra mass flow controllers and the measurements were obtained for different gases concentration ranges from 10 ppm to 1000 ppm at three operating temperatures i.e. 50 ºC, 100 ºC, and 150 ºC.

5.1.3 Gas Sensing Mechanism

It is accepted that the sensitivity of metal oxide gas sensors is attributed to the chemisorption of oxygen on the oxide surface and the subsequent reaction between adsorbed oxygen and test gas, which cause the resistance of the film to change. Gas sensing mechanism of as deposited Cu-doped ZnO thin films depend on the sensor temperature and adsorbed species of oxygen ions (O_2^-, O^-, O^{2-}) on the surface. Different species of oxygen ions are stable at different temperatures viz. O_2^- below 100 ºC, O^- between 100 ºC and 300 ºC and O^{2-}above 300 ºC [16]. Oxygen molecules from the ambient atmosphere are initially adsorbed at the Cu-doped ZnO surface. The electrons are extracted from the conduction band of the zinc oxide and subsequently the sensor resistance increases according to the following mechanism:

$$O_2\,(gas) + 2e^- \rightarrow 2O^-_{ads} \qquad (5.1)$$

The adsorbed oxygen in the form O^-_{ads} makes the thin films more sensitive because this O^-_{ads} is the most reactive species among the three. When hydrogen gas is exposed to this Cu-doped ZnO sensor, the hydrogen molecules react with O^-_{ads} and re-inject the trapped electrons back to the conduction band according to the following reactions [203]:

$$H_{2\,(ads)} + O^-_{(ads)} \rightarrow H_2O_{\,(gas)} + e^- \qquad (5.2)$$

The electron concentration of Cu-doped ZnO film thus increases which in turns decrease the resistance of the film and hence sensor response increases. We have actually observed higher sensitivity of Cu- doped ZnO thin films at 150 ºC in support of this interpretation.

5.1.4 Gas Sensing Properties

The hydrogen gas sensing properties of 3% Cu-doped ZnO thin films were measured in three steps as follows.

1) By Varying the Sensor Operating Temperature (50 - 150 ºC) and Keeping the Gas Concentration Fixed: Cu-doped ZnO sensor response measured at 50 ºC, 100 ºC and 150 ºC for 10 ppm of hydrogen gas is shown in Fig. 5.3. The sensor currents measured at 1 volt are 0.5mA, 0.72mA and 1.05mA for 50 ºC, 100 ºC and 150 ºC respectively.

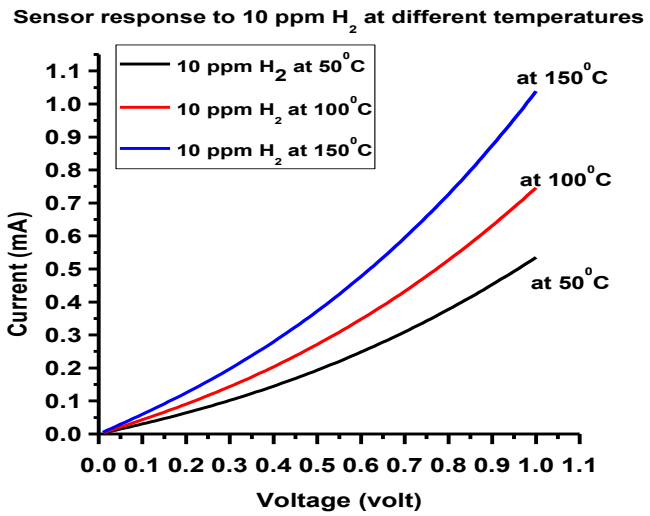

Fig. 5.3: 3% Cu-doped ZnO sensor response to 10 ppm of hydrogen gas at different temperatures

At all temperatures the resistance of the film decreases when they are exposed to the same concentration of hydrogen gas (10 ppm). As the temperature is increased to 100 ºC sensor response improves. On further increasing the temperature to 150 ºC the sensor response is considerably enhanced. The presence of nano-sized particles in the highly resistive 3% Cu-doped ZnO film [168] may also be the important reason for the hydrogen response at very low temperature of 50 ºC even for a very low concentration (10 ppm) of hydrogen gas.

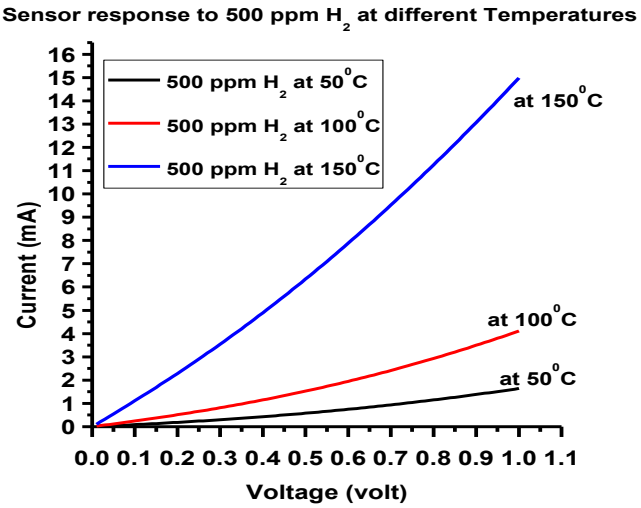

Fig. 5.4: 3% Cu-doped ZnO sensor response to 500 ppm of hydrogen gas at different temperatures

Now the hydrogen gas concentration was increased to 500 ppm and the resulting sensor response characteristics is shown in Fig. 5.4. The sensor currents measured at 1 volt are 1.2mA, 4.0mA and 15mA for 50 ºC, 100 ºC and 150 ºC

respectively. It is evident from Fig.5.4 that sensor response improves as the temperature is increased from 50 ºC to 150 ºC. Accordingly the inference is that if we increase the concentration of hydrogen gas from 10 ppm to 500 ppm, there is significant enhancement in the sensor response at 150 ºC. The increase in the sensor current with increase in the operating temperature can be attributed to the fact that the thermal energy was high enough to overcome the activation energy barrier of the reaction between the hydrogen molecules and adsorbed oxygen species [16], [204].

2) By Varying the Gas Concentration (10 – 1000 ppm) and Keeping the Operating Temperature Fixed: The operating temperature of the sensor was fixed at 50 ºC and the resulting sensor response characteristics for 10 ppm, 500 ppm, 750 ppm, and 1000 ppm of hydrogen gas is shown in Fig.5.5. The sensor currents measured at 1 volt for 10 ppm, 500 ppm, 750 ppm, and 1000 ppm of hydrogen gas are 0.5mA, 1.2mA, 3.3mA, and 6.5mA respectively. The increase in sensor currents with increasing of hydrogen concentration may be due to the fact that more hydrogen molecules react with more adsorbed oxygen species on the film grain surface.

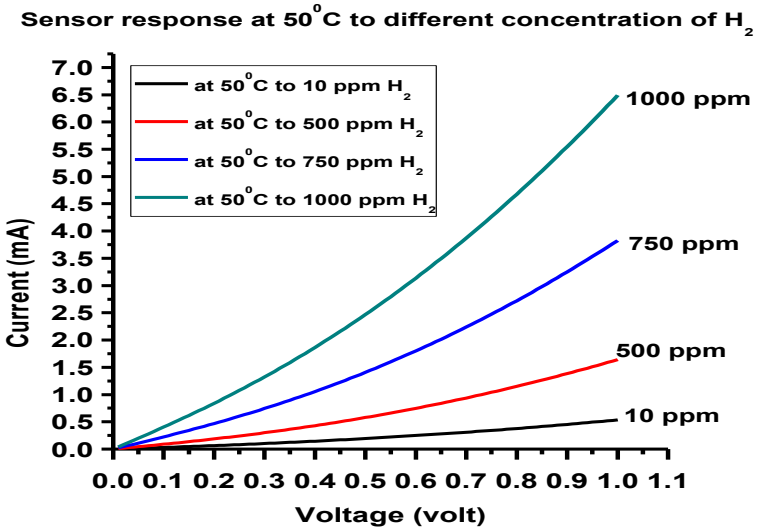

Fig. 5.5: 3% Cu-doped ZnO sensor response to different concentration of H_2 gas at 50 ºC

3) Selectivity Study for Hydrogen and Methane Gases for Three Concentrations (500, 750, and 1000 ppm) at Three Temperatures (50, 100, and 150 ºC): For selectivity study the sensor response was measured at 50 ºC and 100 ºC for 500 ppm of hydrogen and methane gases as shown in Fig.5.6. The sensor currents measured at 1 volt for 500 ppm of hydrogen gas are 1.2mA (at 50 ºC), and 4.0mA (at

100 ºC). The sensor currents for methane gas are 5.5mA (at 50 ºC), and 10.0mA (at 100 ºC).

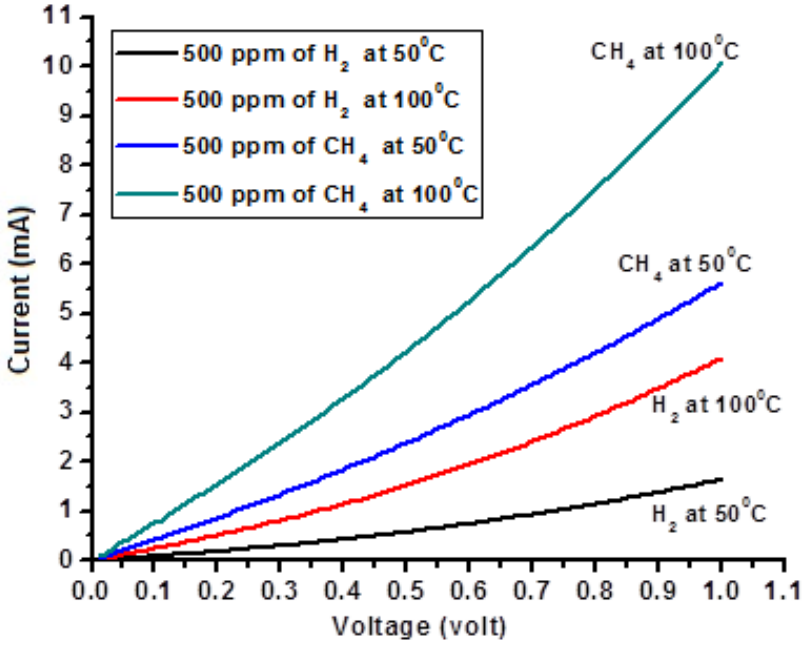

Fig. 5.6: 3%Cu-doped ZnO sensor response to 500 ppm hydrogen and methane gases at 50 ºC and 100 ºC temperatures

It is evident from Fig.5.6 that sensitivity of the sensor for methane is more than two to three times as compared to hydrogen at both the temperatures (50 ºC and 100 ºC). Such higher responses even at very low temperatures may be due to the presence of nano-sized particles in the 3% Cu-doped ZnO thin film.

Next, the sensor operating temperature was increased to 150 ºC and the resulting sensor response characteristics for 750 ppm and 1000 ppm are shown in Fig. 5.7. The sensor currents measured at 1 volt for 750 ppm, and 1000 ppm of hydrogen gas are 20.0mA and 25.0mA respectively, whereas for methane gas the sensor currents are 12.0mA and 15.0mA respectively. It is clear from Fig.5.7 that the sensitivity of the sensor is more than 1.5 times for hydrogen gas as compared to methane gas.

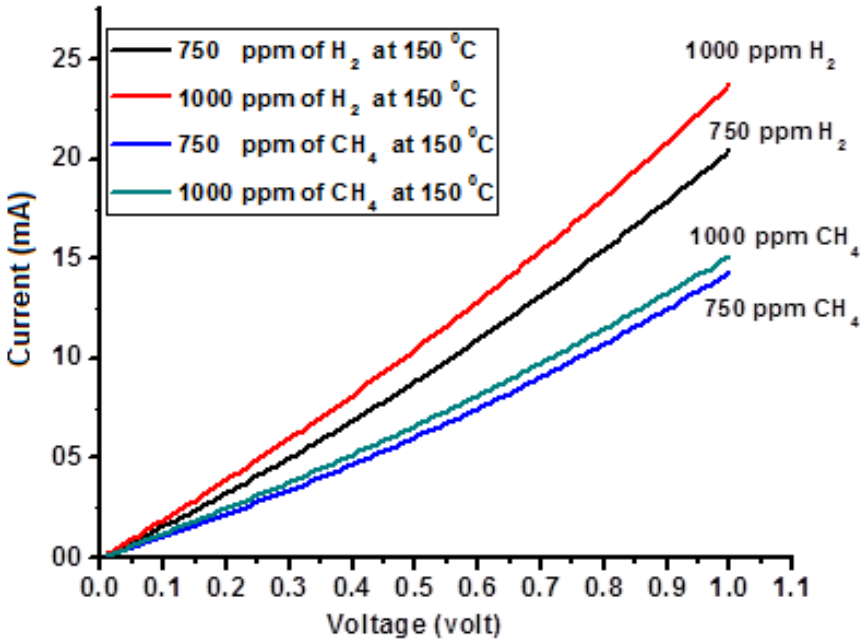

Fig. 5.7: 3% Cu-doped ZnO sensor response at 150 ºC for different concentration of hydrogen and methane gases

5.1.5 Sensitivity Responses

The sensitivity responses of as deposited 3% Cu-doped ZnO thin films were studied by measuring the conductance change of the sensing film in the presence and absence of hydrogen gas. The variation of sensitivity response of the developed sensor as a function of operating temperature for different concentration of hydrogen gas is shown in Fig. 5.8. The sensitivity response S (%) was determined by the following equation:

$$\text{Sensitivity, S (\%)} = [\frac{R_a - R_g}{R_a}] \times 100 \qquad (5.3)$$

where R_a and R_g are the resistances of the sensor in pure nitrogen atmosphere and hydrogen gas respectively. As discussed in introduction part that most of the ZnO based hydrogen sensors operate normally between 250 ºC to 400 ºC and such high temperatures are not suitable for explosive gases like hydrogen. Accordingly in the present study we selected three temperatures of 50 ºC, 100 ºC and 150 ºC in order to find an optimum or critical temperature in this range.

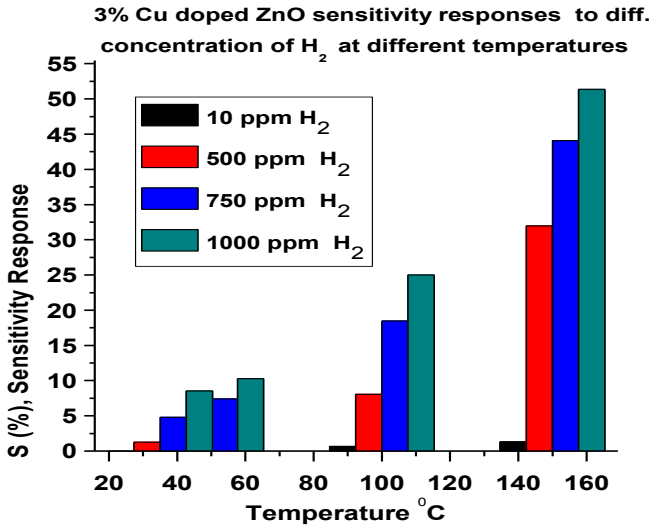

Fig. 5.8: 3%Cu-doped ZnO sensitivity responses to different concentration of hydrogen gas at different temperatures

It is evident from Fig. 5.8 that sensitivity response of the developed sensor shows the linear dependence on hydrogen gas concentrations and operating temperatures. We were able to achieve maximum sensitivity of 51% for 1000 ppm of hydrogen gas at 150 ºC. So, the developed sensor shows better sensitivity at substantially reduced operating temperatures i.e. 150 ºC, which is lower than that reported by other authors (Table 5.1). It may be due to the fact that, the Cu atoms are weakly bonded with the oxygen gas, and the resulting complex is readily dissociated at relatively low temperature and the oxygen atoms are produced. Thus, for 3% Cu-doped ZnO films, the optimum operating temperature is 150 ^{o}C. Consequently, this temperature (150ºC) was considered as optimum/critical temperature for all the experiments in this work and authors feel that there was no need to go beyond this temperature.

The enhanced response of the 3% Cu-doped ZnO film can be attributed to the formation of highly reactive species according to the reaction

$$O_2 + Cu_2 \leftrightarrow 2Cu{:}\ O \qquad (5.4)$$

These created atoms migrate along the surface of the grains. This migration is induced by the catalyst atoms and is known as spillover of the gas ions. The oxygen atoms capture electrons from the surface layer and acceptor surface states are formed. On exposure to hydrogen gas of 3% Cu-doped ZnO film, the H_2 molecules react with adsorbed oxygen in the same manner as described in Eqn. (5.2) i.e.

$$H_{2\,(ads)} + O^-_{(ads)} \rightarrow H_2O_{\,(gas)} + e^-$$

The amount of oxygen adsorbed on the surface would depend on the number of Cu or CuO misfits to adsorb the oxygen which in turn would reduce the exposed gas. When the optimum amount of 3% Cu is incorporated on the surface of the ZnO film, Cu or CuO species would be distributed uniformly throughout the surface of the film. As a result the initial resistance of the film is high and this amount would also be sufficient to promote the catalytic reaction effectively and the overall change in the resistance on the exposure of hydrogen gas leading to an increase in the sensitivity. When the amount of Cu or CuO on the surface of the film is less than the optimum, the surface dispersion may be poor and the sensitivity of the film is observed to be decreased since the amount may not be sufficient to promote the reaction more effectively. When the amount of Cu or CuO on the surface of the films is more than the optimum, the Cu or CuO species would be distributed more densely. Therefore the initial resistance of the films would change and the overall change in the resistance on the exposure of H_2 gas would be smaller leading to lower response.

Hence, the uniqueness of this work is that we could achieve higher sensitivity of 51% at substantially reduced temperature i.e. 150 ºC. Transient response of 3% Cu-doped ZnO film at 150 °C for 1000 ppm of hydrogen gas is shown in Fig. 5.9. The response time of the developed sensor as calculated from the Fig. 5.9 is about 65 seconds and recovery time is about 250 seconds.

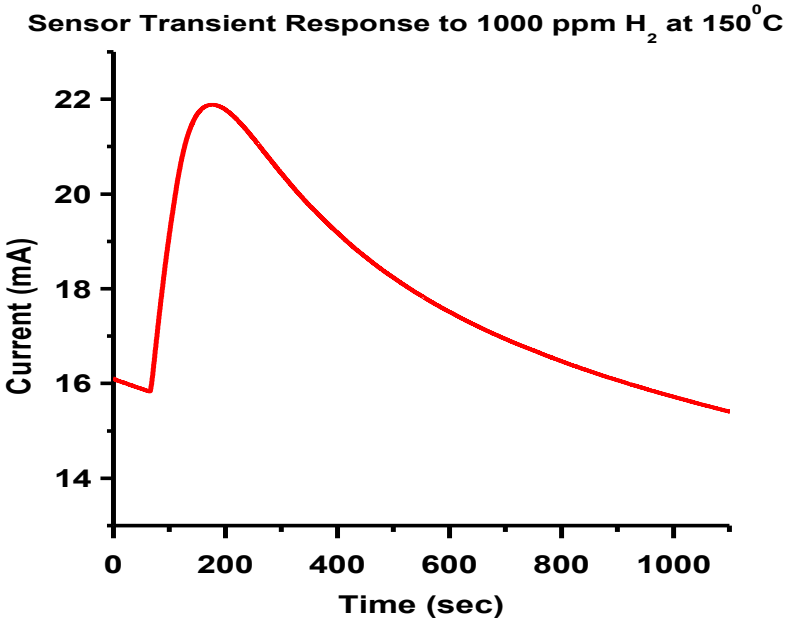

Fig. 5.9: 3% Cu-doped ZnO sensor transient response to 1000 ppm hydrogen gas at 150 ºC

In Table 5.1, we have compared the hydrogen sensing parameters (e.g. test gas concentration, operating temperature and sensitivity response %) of 3% Cu-doped ZnO thin films (i.e. present work) with those reported for other undoped and doped semiconducting metal oxide thin film based sensing elements.

Table 5.1: Comparison for Hydrogen Sensing Parameters of Present Sensor with other Semiconducting Metal Oxide Based Sensors

Thin film	Deposition Techniques	H_2 Concentration	Oper. Temp (ºC)	Sensitivity Response S (%)	Ref.
$Mg_{0.1}Zn_{0.9}O$	PLD Technique	500 (ppm)	300	50 (R_a/R_g)	[122]
ZnO	RF-Sputtering	1000 (ppm)	400	8 (Z_a/Z_g)	[133]
Sn-ZnO/TiO_2	Hydro-thermal Process	1% of H_2 in air	160	1.48 (I_g/I_a)	[101]
CuO/ZnO sensor	Solid state synthesis route	4000 ppm	400	4.9 (I_g/I_a)	[151]
3% Cu-ZnO rod	Hydro-thermal Process	200 ppm	150	44 ((R_a-R_g)/R_g) *100	[48]
CuO	DC Sputtering	6%	250	4 (R_g/R_a)	[205]
CuO-$Cu_xFe_{3-x}O_4$	RF-Sputtering	0.125%	280	37 ((R_g-R_a)/R_a)	[206]
$Mg_{0.5}Zn_{0.5}Fe_2O_4$	Spin Coating Process	1660 (ppm)	250	75 ((R_a-R_g)/R_a)	[207]
WO_3	Thermal Process	10000 (ppm)	150	11 ((R_a-R_g)/R_g)	[208]
3% Cu doped ZnO	PLD Technique	1000 (ppm)	150	51 ((R_a-R_g)/R_g) *100	Present Work

It is evident from Table 5.1 that the hydrogen sensing characteristics of the present work is better than most of the other investigated materials i.e. developed sensor shows better sensitivity at substantially reduced operating temperatures of 150 ºC.

5.1.6 Selectivity Responses

Selectivity or specificity is defined as the ability of a sensor to respond to certain gas in the presence of other gases. Percent selectivity of one gas over others is defined as the ratio of the maximum response of other gas to the maximum response of the target gas at optimum temperature. It is possible to improve the sensors selectivity by varying the sensor operating temperature [38], [40], and [209]. 3% Cu doped ZnO sensor's selective response for 750 ppm of hydrogen and methane gases at

different temperatures is shown in Fig.5.10. The sensitivity responses of the order of ~ 7.4 and ~ 11.8 for the 750 ppm of hydrogen and methane gases were obtained at 50 ºC temperature. However, the sensitivity responses of the order of ~ 44.1 and ~ 32.6 were obtained for the same concentration of hydrogen and methane gases at 150 ºC temperature as shown in Fig. 5.10. As a result our developed sensor (3% Cu-doped ZnO thin film) with the same sensitive material operated at different temperatures show a completely different response to hydrogen and methane gases.

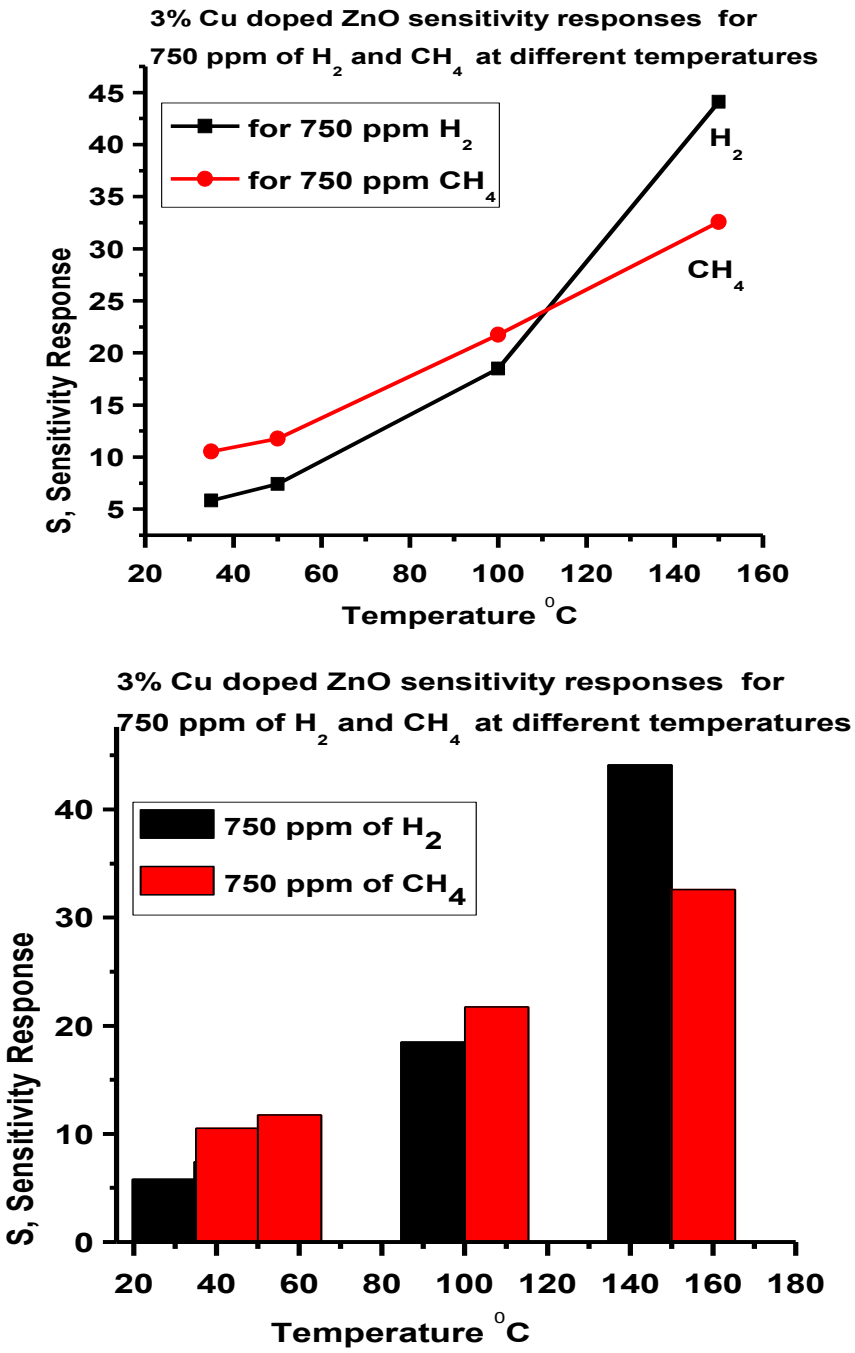

Fig. 5.10: 3% Cu-doped ZnO sensor selective response for 750 ppm of H_2 and CH_4 gases at different temperatures

The response to particular gas can be greatly improved by adding a catalytic metal to the oxide and the grain size of the oxide also affects the response and selectivity to specific gases because grain boundaries are acting as electron scattering centers [52], [77], [118], and [172]. In contrast to H_2 (hydrogen) gas, the overall reducing reactions between CH_4 (methane) gas and chemisorbed oxygen species (O^- and O^{2-}) are given by:

$$CH_4 + 4O^-(ads) \rightarrow 2H_2O + CO_2 + 4e^- \quad (5.5)$$

$$CH_4 + 4O^{2-}(ads) \rightarrow 2H_2O + CO_2 + 8e^- \quad (5.6)$$

Moreover, it is obvious from Fig.5.8 and Fig.5.10 that 3% Cu doping in the host ZnO matrix can simultaneously enhance both the response and selectivity for hydrogen gas at substantially reduced operating temperature i.e. 150 ºC, which is better than the previous reports as shown in Table 5.1. The sensor shows higher sensitivity to methane as compared to hydrogen under identical conditions up to 100 ºC. It may be due to the fact that different pollutants have characteristic optimum oxidation and reduction temperatures and therefore give rise to characteristic resistance-temperature profiles. Hence, by varying the operation temperature of the sensor it is possible to increase or decrease its sensitivity and selectivity towards specific gases. Accordingly the inference is that the sensitivity for methane and hydrogen are completely reversed if measurements are performed at 150 ^{0}C as compared to 50 ^{0}C or 100 ^{0}C.

5.1.7 Result and Discussions

- As most of the ZnO based hydrogen sensors operate normally between 250 ºC to 400 ºC and such high temperatures are not suitable for explosive gases like hydrogen. Accordingly in the present study we selected the three temperatures of 50 ºC, 100 ºC and 150 ºC in order to find an optimum or critical temperature in this range.
- We were able to achieve maximum sensitivity of 51% for 1000 ppm of hydrogen gas at 150 ºC.
- It is evident that the hydrogen sensing characteristics of the present work is better than most of the other investigated materials i.e. the developed sensor shows the better sensitivity at substantially reduced operating temperatures of 150 ºC.

- Moreover, it is apparent that 3% Cu doping in the host ZnO matrix can simultaneously enhance both the response and selectivity for hydrogen gas at substantially reduced operating temperature i.e. 150 ºC.
- The sensor shows the higher sensitivity to methane as compared to hydrogen under the identical conditions up to 100 ºC.
- The sensitivity responses of the order of ~ 7.4 and ~ 11.8 for the 750 ppm of hydrogen and methane gases were obtained at 50 ºC temperature. However, the sensitivity responses of the order of ~ 44.1 and ~ 32.6 were obtained for the same concentration of hydrogen and methane gases at 150 ºC temperature.
- Accordingly the inference is that the sensitivity for methane and hydrogen are completely reversed if measurements are performed at 150 ^{0}C as compared to 50 ^{0}C or 100 ^{0}C.
- Our developed sensor (3% Cu-doped ZnO thin film) with the same sensitive material operated at different temperatures show a completely different response to hydrogen and methane gases.

5.2 Li-doped ZnO Thin Films Gas sensor for H_2 sensing

5.2.1 Introduction

In order to achieve the 2nd and 3rd objectives, we have also studied undoped ZnO, and varying Li doping from 1 to 8% in the host ZnO thin film sample series for hydrogen sensing. Thin films were deposited by using PLD technique on interdigitated quartz substrate with various parameters (as discussed in chapter 3), and these films were characterized by XRD and SEM (as discussed in chapter 4). It has been observed that Li plays a very important role in hydrogen gas sensing properties of ZnO thin films at reduced operating temperature i.e. between 50 ºC to 150 ºC.

In this work, fast response hydrogen gas sensors operated at sustainably reduced operating temperature were fabricated from lithium (Li) doped zinc oxide (ZnO) thin films. As ZnO is the most promising candidate for gas sensing applications because of its chemical sensitivity to toxic and combustible gases, high chemical stability, suitability to doping, non-toxicity, abundance in nature, and low cost. In fact, ZnO is a direct wide band gap (3.37eV) semiconductor used for the sensing of gases in industrial, urban and domestic settings [3], [27]. Hydrogen (H_2) gas is considered as one of the best resources of clean energy, as burning of the H_2 is water, which is decomposed again into hydrogen and oxygen [161]. It is the ultimate fossil fuel candidate, with high heat of combustion (142kJ/g), low minimum ignition energy (0.017 mJ) and wide flammable range (4-75%), as well as high burning velocity [163]. As a matter of fact, H_2 is a tasteless, colorless, odorless, inflammable, and explosive gas, so it cannot be detected by human beings. Therefore, a reliable and cost-effective hydrogen gas sensor needs to be developed to save human lives as well as safety component in the future hydrogen based economy.

However, most of the zinc oxide (ZnO) based hydrogen gas sensors operate at high temperature, normally between 250°C to 450°C (as shown in Table 2.1). Such a high operating temperature is energy intensive, increases the operating cost and requires high operational safety measures in an environment with explosive gases like hydrogen etc. Thus, it is urgent to reduce the operating temperature of the ZnO thin film based hydrogen gas sensors. In order to overcome this drawback, considerable research and development are underway. Consequently, a reliable and cost-effective ZnO thin films based hydrogen gas sensor operates at low temperature, needs to be developed.

One critical approach is to modify the surface of the ZnO thin film by suitable materials doping. Since the resistivity of ZnO thin films can be controlled by doping [200]-[202]. Hence, depending on the applications, ZnO thin films have been subjected to various types of doping; like, Aluminum, Indium, Copper, Iron, Gallium, Manganese, Tin and Lithium etc. [55], [122], [166], [168], and [210]. Here, in the present work, the effects of lithium on hydrogen gas sensing behaviour in ZnO thin films were studied at reduced operating temperature. In general, Li substituting for Zn theoretically possesses shallower acceptor levels [211]. Besides, most of the Li-doped ZnO films were either n-type or semi-insulating because Li incorporation occurs at interstitial sites as well as at substitution sites [212]-[213]. Recently there have been a number of efforts to characterize the Li-related defect structure sensitive properties, such as impurity diffusion [214], and electrical measurements [210]. Thus, in the present thesis, undoped ZnO, and varying Li concentration ranging from (1 to 8 %) Li-doped ZnO thin films were successfully grown by PLD on interdigitated quartz substrate at 300 °C to understand the hydrogen sensing behaviour of these films at reduced operating temperature. To the best of our knowledge, no reports are available in the literature on Li-doped ZnO thin films for hydrogen gas sensing applications. The dynamic gas sensing measurements were performed from 50 ºC to 150 ºC for 50 sccm (standard cubic centimeters per minute) to 150 sccm flow of pure hydrogen gas.

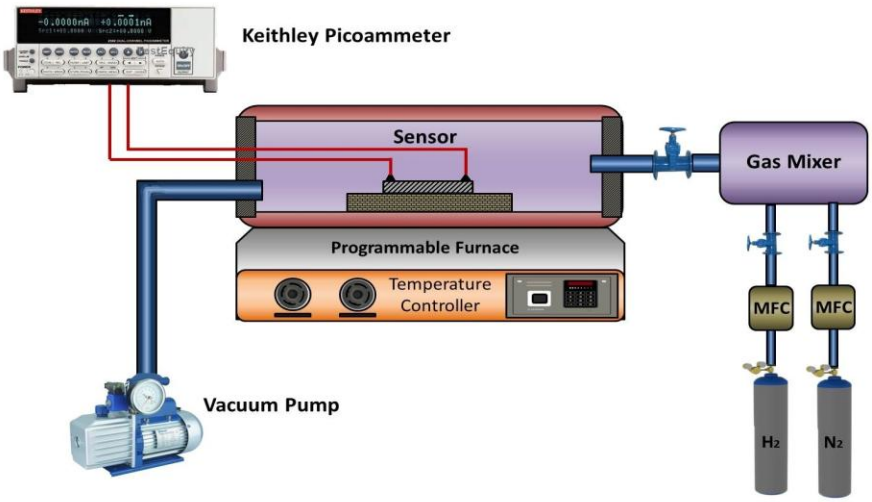

Fig. 5.11: Gas sensing setup-2

The gas sensing parameters of as grown thin films were studied by I-V measurement technique by using a custom made gas sensing setup as shown in Fig. 5.11. The gas sensing measurements were performed with the help of a PC connected to a low voltage source Keithley 2401 through GPIB interface and lab view v8.5 software. As deposited sensor was placed inside an enclosed test chamber fitted with programmable heating arrangement that would maintain a uniform temperature inside the chamber. Hydrogen gas was allowed to flow to the test chamber through a Sierra mass flow controller.

5.2.2 Gas Sensing Mechanism

The hydrogen gas sensing mechanism of as deposited Li-doped ZnO thin films depends on the sensor temperature and adsorbed species of oxygen ions (O_2^-, O^-, O^{2-}) on the surface. Oxygen molecules from the ambient atmosphere are initially adsorbed at the Li-doped ZnO surface. Electrons are extracted from the conduction band of the Li-doped zinc oxide material and subsequently the sensor resistance increases according to the following equation i.e.

$$O_2\,(gas) + 2e^- \rightarrow 2O^-_{ads}.$$

Lithium doping in ZnO is usually carried out to control electrical properties [210]. Each zinc atom can provide two 4s electrons to Oxygen atom to fill up the 2p states while Li can only provide one single 2s electron. Hence, the LiZn center is an acceptor and p conduction is observed in ZnO [211]. Meanwhile, Li can also lose its outmost electron behaving as a donor and n conduction is observed in ZnO, as a result Li incorporation occurs at interstitial sites as well as at substitution sites [213]. When hydrogen gas is exposed to this Li-doped ZnO sensor, hydrogen molecules react with O^-_{ads} and re-inject the trapped electrons back to the conduction band according to the following reaction i.e.

$$H_{2(ads)} + O^-_{(ads)} \rightarrow H_2O_{(gas)} + e^-.$$

The electron concentration of Li-doped ZnO film, thus, increases which, in turns, decreases the resistance of the film and hence sensor response improves. We have actually observed higher sensitivity of 2% Li- doped ZnO films at 150 °C in support of this interpretation.

5.2.3 Gas Sensing Properties

The hydrogen (H_2) gas sensing properties of low doped (i.e.2%) Li-doped ZnO and high doped (i.e. 8%) Li-doped ZnO thin films were measured in two steps as follows:

1) By Varying the Sensor Operating Temperature (50 - 150 ºC) and Keeping the Gas Concentration Fixed:

Both 2% Li-doped ZnO and 8% Li-doped ZnO sensors show identical behaviour of higher sensitivity responses at higher operating temperature i.e. 150 °C. Therefore, this temperature (150°C) is considered as an optimum or critical temperature for all the experiments in this work.

2) By Varying the Gas Concentration (50 – 150 sccm) and Keeping the Operating Temperature Fixed:

Below 50 sccm of hydrogen flow the sensor response is very weak. Accordingly, we have decided to use 50 sccm or more in this work.

5.2.3.1 I-V Characteristic of 2% Li-doped ZnO Thin Films

I-V characteristics of 2% Li-doped ZnO sensor response measured at 50 ºC, 100 ºC and 150 ºC for 50 sccm of hydrogen flow through the gas chamber is shown in Fig. 5.12(a). The sensor currents measured at 1 volt for 50 sccm flow of hydrogen are 0.3µA, 0.82µA and 11.05µA for 50 ºC, 100 ºC and 150 ºC respectively. At all temperatures, the resistance of the film decreases when they are exposed to the same flow of low concentration hydrogen i.e. 50 sccm. Below 50 sccm of hydrogen flow the sensor response is very weak. Accordingly, we have decided to use 50 sccm or more in this study. As the temperature is increased to 100 ºC, sensor response improves. On increasing the temperature to 150 ºC the sensor response considerably enhanced in the range 0-1 volt. The increase in the sensor current with increase in the operating temperature can be attributed to the fact that the thermal energy was high enough to overcome the activation energy barrier of the reaction between the hydrogen molecules and adsorbed oxygen species [133].

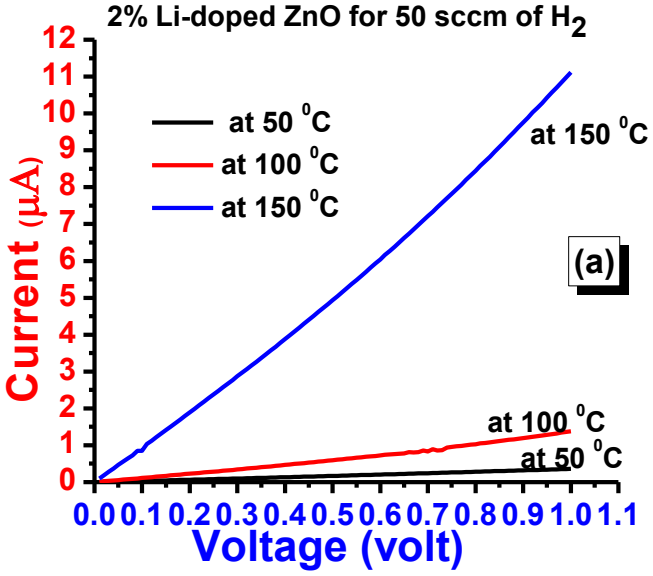
2% Li-doped ZnO for 50 sccm of H2
Current (μA)
Voltage (volt)
at 50 °C
at 100 °C
at 150 °C
(a)

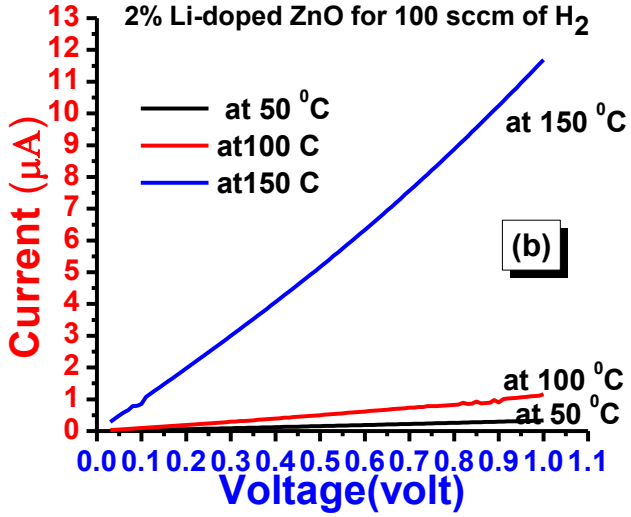
2% Li-doped ZnO for 100 sccm of H2
Current (μA)
Voltage(volt)
at 50 °C
at100 C
at150 C
(b)

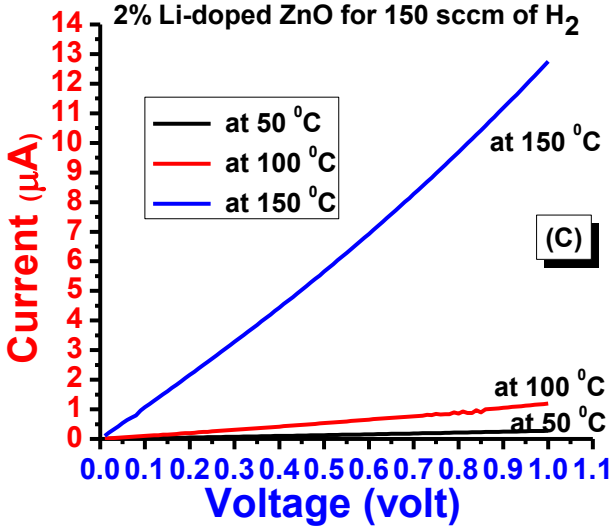
2% Li-doped ZnO for 150 sccm of H2
Current (μA)
Voltage (volt)
at 50 °C
at 100 °C
at 150 °C
(C)

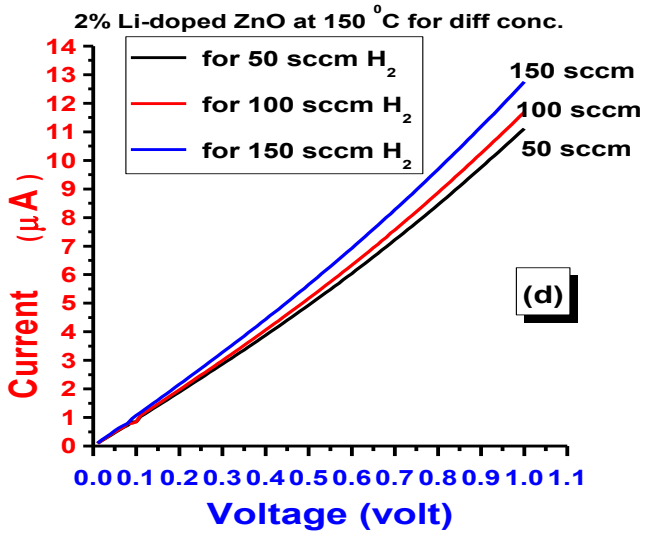

Fig. 5.12: 2% Li-doped ZnO sensor responses at different operating temperature for (a) 50sccm of H_2, (b) 100sccm of H_2, (c) 150sccm of H_2 flow, and (d) combined sensor response at 150 °C for different concentrations of H_2 flow

Accordingly, significant increase in electron concentration resulted from the sensing reaction and hence raises the sensor current. 2% Li-doped ZnO sensor responses to the 100 sccm and 150 sccm of hydrogen flow in the gas chamber measured at 50 ºC, 100 ºC and 150 ºC are shown in Fig. 5.12(b) and Fig. 5.12(c) respectively.

It is evident from the figures that the response is not much different from that of the same sensor at 50sccm of hydrogen flow. So the inference is that if we increase the flow rate of hydrogen from 50sccm to 100sccm or 150sccm, there is no pronounced effect in the sensor resistance. However, there is a trivial rise in the sensor current at 150 ºC for different concentration of hydrogen flow as shown in the Fig. 5.12(d). Here, more hydrogen molecules may react with more adsorbed oxygen species on the film grain surface and may cause the decrease of barrier height leading to the reduction of electrical resistance, and, hence a little increase in the sensor current.

5.2.3.2 I-V Characteristic of 8% Li-doped ZnO thin films

I-V characteristics of 8% Li- doped ZnO sensor response measured at 50 ºC, 100 ºC and 150 ºC for 50 sccm of hydrogen flow through the gas chamber is shown in Fig. 5.13.

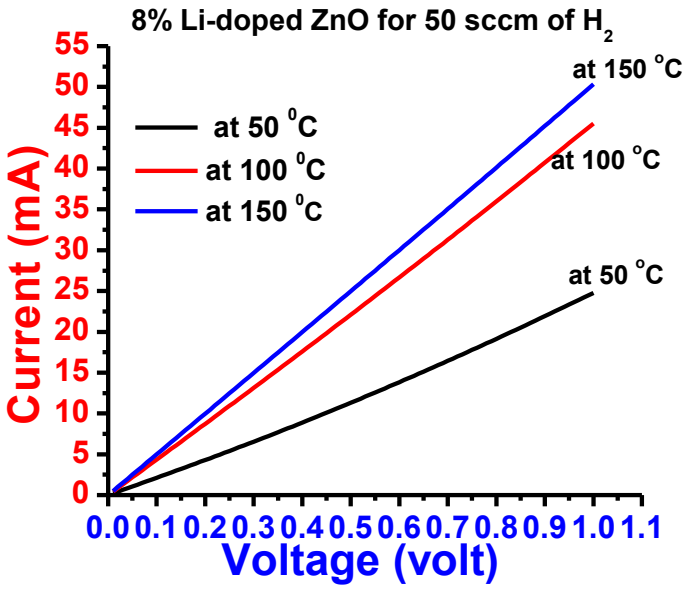

Fig. 5.13: 8% Li-doped ZnO sensor response to 50 sccm hydrogen flow at different temperatures

From the result of the 2% Li-doped ZnO, we know that the optimum parameters for sensor operation are 50 sccm of hydrogen flow at 150 °C. So, we used 50 sccm of hydrogen flow to study the sensor response of 8% Li-doped ZnO films at three different temperatures. Rather, 8% Li-doped ZnO films, currents measured at 1 volt for 50 sccm flow of hydrogen are 22.5mA, 46.32mA and 51.05mA for 50 ºC, 100 ºC and 150 ºC respectively. Fig. 5.13 shows that, although the response increases with temperature as in the 2% Li-doped ZnO films, however, 8% Li-doped ZnO films show sufficient response to 50 sccm of hydrogen at 50 °C in voltage range of 0-1volt. The presence of nano-sized particles in the highly sensitive 8% Li-doped ZnO film may also be another reason for the hydrogen response at very low temperature of 50 ºC even for a low concentration i.e. 50 sccm flow of hydrogen .

5.2.4 Sensitivity Responses

The gas sensing performance of as deposited Li-doped ZnO films were studied by measuring the conductance change of the sensing film in the presence and absence of hydrogen. The variation of sensitivity responses of sensor as a function of operating temperature for 50sccm flow of hydrogen is shown in Fig. 5.14(a) 2% Li-doped ZnO, Fig.5.14(b) 8% Li-doped ZnO, and Fig. 5.14(c) combined sensitivity response for both doping. Transient response of 2% Li-doped ZnO film at 150 °C for

50sccm flow of hydrogen is shown in Fig. 5.14 (d). The sensitivity response S (%) for the as deposited sensors was determined using equation (5.3).

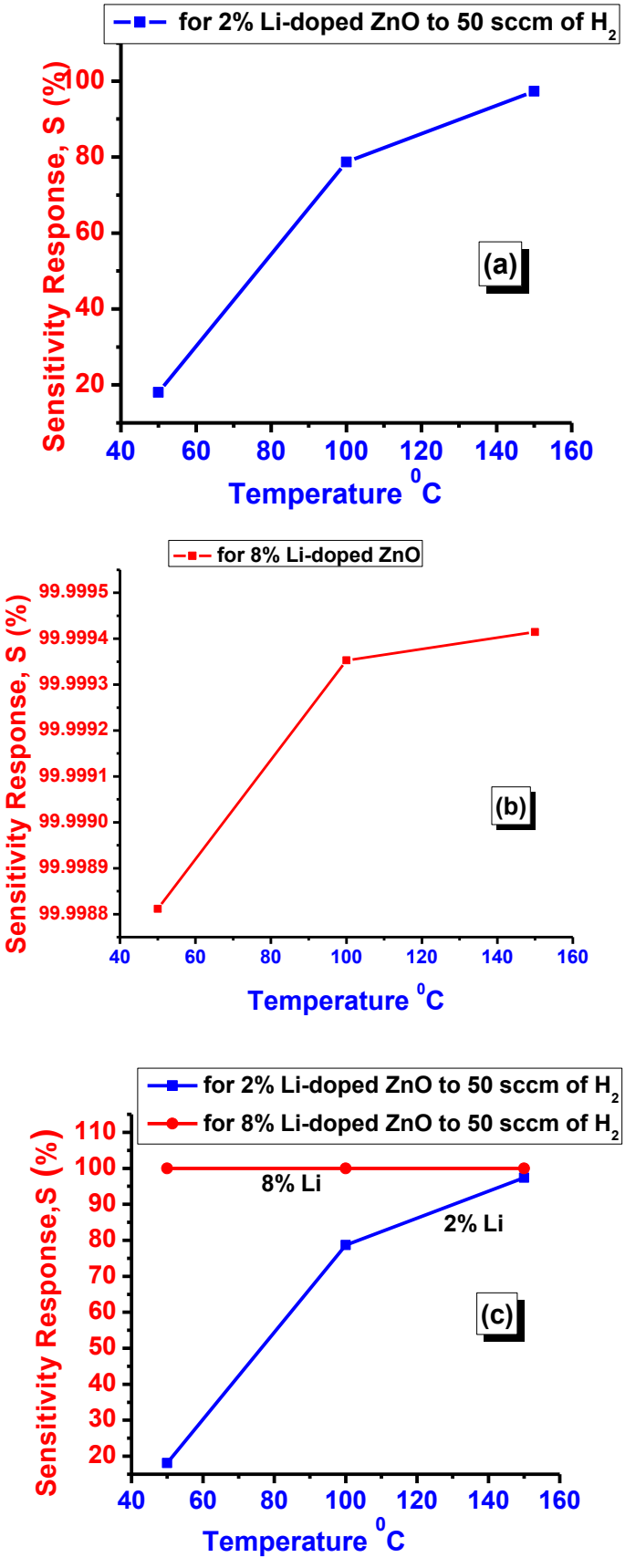

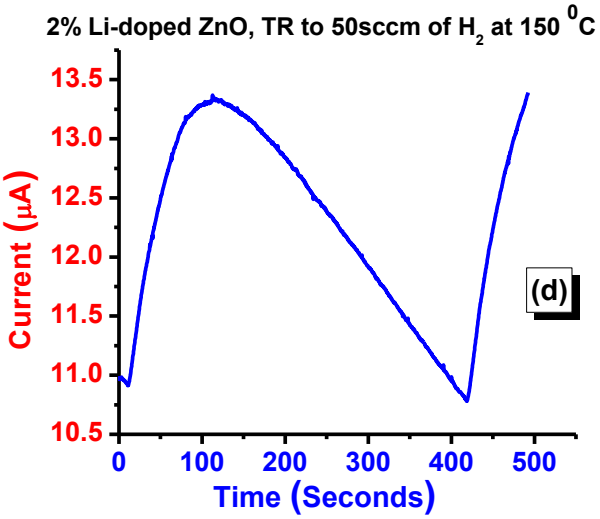

Fig. 5.14: Sensitivity Response S (%) to 50sccm of H_2 flow at different operating temperature for (a) 2% Li-doped ZnO, (b) 8% Li-doped ZnO, (c) combined sensitivity response for both doping, and (d) transient response at 150 °C

Both 2% Li-doped ZnO and 8% Li-doped ZnO sensors show identical behaviour of higher sensitivity responses, S (%) ≈ 98-99.9% at higher operating temperature i.e. 150 °C. Therefore, this temperature (150°C) is considered as an optimum or critical temperature for all the experiments in this work. However, 8% Li-doped ZnO sensor shows the higher sensitivity response in comparison to 2% Li-doped ZnO even at low operating temperature of 50 °C. This behaviour may be attributed to the fact that 2% Li-doped ZnO film possesses high resistivity due to Li substituting for Zn and as lithium doping amount were increased (8% Li-doped ZnO) resistivity decreases because excess of lithium was employed as a carrier [215]. These results also show the good agreement with other authors that lithium does not predominantly substitute on the Zn sites and it preferentially formed interstitial defects upon diffusion into ZnO [216]. However, Jeong et al. [215] also reported that low lithium doping content in ZnO (i.e. 2% Li-doped ZnO) shows better and uniform morphology in comparison to high lithium doping content in ZnO (i.e.8% Li-doped ZnO). We have actually observed the similar results from SEM images as discussed in chapter 4 and shown in Fig. 4.15. Whereas, it is well-known that increasing the carrier density via doping or oxygen vacancies is self-limiting because the increase of the number of free carriers decreases the mobility of carriers due to carrier-carrier scattering. Therefore, there is a trade-off relation between the carrier density and the carrier mobility for obtaining low resistivity. Accordingly, the inference is that

depending on the application, lithium doping in ZnO can be varied for hydrogen sensing. The response time as calculated from the Fig. 5.14(d) is about 55 seconds and recovery time is about 220 seconds. Thus, Li plays a very important role in the hydrogen sensing at reduced operating temperatures i.e. 50 ºC to 150 ºC, which is lower than that obtained other reports as shown in Table 5.1. Hence, the novelty of this developed sensor is that it works at substantially reduced temperatures range i.e. 50 ºC to 150 ºC and it shows better sensitivity towards the hydrogen gas.

5.2.5 Result and Discussions

- 8% Li-doped ZnO sensor shows the higher sensitivity response in comparison to 2% Li-doped ZnO even at low operating temperature of 50 °C. It may be attributed to the fact that 2% Li-doped ZnO film possesses high resistivity due to Li substituting for Zn and as lithium doping amount were increased (8% Li-doped ZnO) resistivity decreases because excess of lithium was employed as a carrier.
- However on increasing the carrier density via doping or oxygen vacancies is self-limiting because the increase of the number of free carriers decreases the mobility of carriers due to carrier-carrier scattering.
- Therefore, there is a trade-off relation between the carrier density and the carrier mobility for obtaining low resistivity. Accordingly, the inference is that depending on the application, lithium doping in ZnO can be varied for hydrogen sensing.
- Hence, the novelty of this developed sensor is that it works at substantially reduced temperatures range i.e. 50 ºC to 150 ºC and it shows better sensitivity towards the hydrogen gas.

Chapter 6 Conclusions

- We have demonstrated that highly sensitive and selective gas sensor for hydrogen gas can be developed by 3% copper doping in the ZnO host matrix.
- It is concluded that for 3% Cu-doping the optimum parameters are 1000 ppm of hydrogen gas at 150 ºC in the voltage range of 0-1volt.
- We could achieve higher sensitivity of 51% at substantially reduced operating temperature i.e. 150 ºC. More importantly this sensor responds to 10 ppm of hydrogen gas even at low operating temperature i.e. 50 ºC.
- The novelty of this sensor is that the sensitivity for methane and hydrogen gases can be completely reversed if measurements are performed at 150 ^{0}C as compared to 50 or 100 ^{0}C.
- As a result our developed sensor (3% Cu-doped ZnO thin film) with the same sensitive material operated at different temperatures show a completely different response to hydrogen and methane gases.
- Low and high lithium doping of 2% and 8% in the host ZnO were studied for hydrogen sensing properties of ZnO thin films at reduced operating temperature.
- It has been observed that for low lithium doping (2%) the optimum parameters are 50 sccm of hydrogen flow at operating temperature 150 °C in the voltage range of 0-1volt.
- For high lithium doping (8%) the sensor is quite sensitive at reduced operating temperature 50 °C to the same flow of hydrogen of 50 sccm.
- As a result, we have concluded that Li plays a very important role in hydrogen gas sensing properties of ZnO thin films at substantially reduced operating temperature i.e. between 50 ºC to 150 ºC.

  Therefore all the three objectives of this thesis have been achieved.

Future Scope in the Field of Metal Oxide Gas Sensors:

Nowadays, investigation is directed, rather than to new sensors, to increase the characteristics of existing gas sensors. As we have discussed in the thesis that ideal gas sensors should present: - high sensitivity towards target gas; - high selectivity (low cross sensitivity); - high stability; - low sensitivity to humidity and temperature; - high reproducibility and reliability; - short reaction and recovery time; - be robust and durable; - easy calibration; - small dimensions (portability). Most of these characteristics are dependent not only on the used material, but also on the method used for its synthesis, and especially on the additives present on the material surface and the method used for their addition.

As gas sensor technology is an interdisciplinary indeed, so the collaboration among people working in broadly different disciplines would be necessary to open new frontier. However from the extensive research work/review reports it is observed that for future work on metal oxide based gas sensors the following major problems have to be overcome:

i) Metal oxide gas sensors are not selective. So by some modifications of the film properties it may possible to intensify its sensitivity to target gas.

ii) There is no universal verdict for simultaneous optimization of all sensors parameters. Therefore, one should always seek a compromise between high sensitivity, high stability and high selectivity of the designed devices.

iii) Finally, challenging spirit is a backbone of every successful researcher. It greatly depends upon the researcher's capability to select correctly necessary combination of additives, composite sensors and method of structural engineering for optimal result attainment.

References:

[1] W.H. Brattain, J. Bardeen, "Surface properties of germanium," *Bell. Syst. Tec. J.*, vol.1, pp.1–41, 1953.

[2] A. Bielanski, J. Deren and J. Haber, "Electric conductivity and catalytic activity of semiconducting oxide catalysts," *Nature*, vol. 179, pp. 668–669, 1957.

[3] T. Seiyama, A. Kato, K. Fujiishi and M. Nagatani, "A new detector for gaseous components using semiconductive thin films," *Anal. Chemistry*, vol. 34, pp.1502-1503, 1962.

[4] N. Taguchi, Japanese Patent 45-38200, 1968.

[5] V.E. Henrich, P.A. Cox, The Surface Science of Metal Oxides; Cambridge University Press: Cambridge, UK, 1994.

[6] G. Korotcenkov, "Metal Oxides for Solid-State Gas Sensors: What Determines Our Choice?"*Mater. Sci. Eng. B*, vol. 139, pp.1-23, 2007.

[7] M. Batzill, and U. Diebold, "The surface and materials science of tin oxide," *Prog. Sur. Sci*., vol. 79, pp. 47-154, 2005.

[8] Z.L. Wang, "Zinc oxide nanostructures: growth, properties and applications," *J. Phys. Condens. Matter*, vol. 16, pp. 829-858, 2004.

[9] T. K. Subramanyam, B. Srinivasulu Naidu, S. Uthanna, "Physical Properties of Zinc Oxide Films Prepared by dc Reactive Magnetron Sputtering at Different Sputtering Pressures," *Cryst. Res. Technol*. vol. 35, pp. 1193–1202, 2000.

[10] C. Klingshirn, "ZnO: from basics towards applications," *Phys. Status Solidi B*, vol. 244, pp. 3027-3073, 2007.

[11] Ü. Özgür, Y.I. Alivov, C. Liu, A. Teke, M. A. Reshchikov, S. Doğan, V. Avrutin, S. J. Cho, H. Morkoçd, "A comprehensive review of ZnO materials and devices," *J. Appl. Phys.*, vol. 98, pp. 041301-041404, 2005.

[12] P. Kumar, H.K. Malik, A. Ghosh, R. Thangavel, K. Asokan, "Bandgap tuning in highly c-axis oriented Zn_{1-x} Mg_xO thin films," *Appl. Phys. Lett.*, vol. 102, pp. 221903-221908, 2013.

[13] J.B. Lee, H. J. Lee, S. H. Seo, J. S. Park, "Characterization of undoped and Cu-doped ZnO films for surface acoustic wave applications," *Thin Solid Films*, vol. 398/399, pp. 641-646, 2001.

[14] J.G.E. Gardeniers, Z.M. Rittersma, G.J. Burger, "Preferred orientation and piezoelectricity in sputtered ZnO films," *J. Appl. Phys.*, vol. 83, pp. 7844-7854, 1998.

[15] S. Dutta, H. E. Jackson, J. T. Boyd, F. S. Hickernell, R. L. Davis, "Scattering loss reduction in ZnO optical waveguides by laser annealing," *Appl. Phys. Lett.*, vol. 39, pp. 206-210, 1981.

[16] M. Takata, D. Tsubone, and H. Yanagida, "Dependence of electrical conductivity of ZnO on degree of sintering," *J. Am. Ceram. Soc.*, vol. 59, pp. 4-8, 1976.

[17] A. Mandelis, and C. Christofides C., Physics, Chemistry, and Technology of Solid State Gas Sensor Devices, John Wiley and Sons, 1993.

[18] M.E. Franke, T.J. Koplin, and U. Simon, "Metal and Metal Oxide Nanoparticles in Chemiresistors: Does the Nanoscale Matter," *Small,* vol. 2, pp.36-50, 2006.

[19] C. Xu, J. Tamaki, N. Miura and N. Yamazoe, "Grain size effects on gas sensitivity porous SnO_2-based elements," *Sens.Actuators B:* vol. 3, pp. 147-155, 1991.

[20] D.R. Miller, S.A. Akbar, and P.A. Morris, "Nanoscale metal oxide-based heterojunctions for gas sensing: A review," *Sens. Actuators B*, vol. 204, pp. 250-272, 2014.

[21] A. Rothschild, Y. Komem, "The effect of grain size on the sensitivity of nanocrystalline metal-oxide gas sensors,"*J. Appl. Phys.*, vol. 95, pp. 6374–6380, 2004.

[22] C.N.R. Rao, G.U. Kulkarni, P.J. Thomas, and P.P. Edwards, "Size-Dependent Chemistry: Properties of Nanocrystals," *Chem. Eur. J.* vol. 8, pp. 28-35, 2002.

[23] W. Kim, M. Choi, and K. Yong, "Generation of oxygen vacancies in ZnO nanorods/films and their effects on gas sensing properties," *Sens. Actuators B,* vol. 209, pp. 989-996, 2015.

[24] Y.F. Sun, S.B. Liu, F.L. Meng, J.Y. Liu, Z. Jin, L.T. Kong and J.H. Liu, "Metal Oxide Nanostructures and Their Gas Sensing Properties sensors: A Review," *Sensors,* vol. 12, pp. 2610-2631, 2012.

[25] S. H. Choi, G. Ankonina, D.Y. Youn, S. G. Oh, J. M. Hong, A. Rothschild, I. D. Kim, "Hollow ZnO nanofibers fabricated using electrospun polymer templates and their electronic transport properties," *ACS Nano*, vol. 3, pp. 2623–2631, 2009.

[26] L. J. Bie, X. N. Yan, J. Yin, Y. Q. Duan, Z. H. Yuan, "Nanopillars ZnO gas sensor for hydrogen and ethanol," *Sens. Actuators B*, vol. 126, pp. 604–608, 2007.

[27] X.L. Cheng, H. Zhao, L.H. Huo, S. Gao, J.G. Zhao, "ZnO nanoparticulate thin film: preparation, characterization and gas-sensing property," *Sens. Actuators B*, vol. 102, pp. 248-252, 2004.

[28] G. Korotcenkov, V. Brinzari, M. Ivanov, A. Cerneavschi, J. Rodriguez, A. Cirera, A Cornet, and J. Morante, "Structural Stability of Indium Oxide Films Deposited by Spray Pyrolysis during Thermal Annealing," *Thin Solid Films*, vol. 479, pp. 38-51, 2005.

[29] M.C. Carotta, A. Cervi, V. Natale, S. Gherardi, A. Giberti, V. Guidi, D. Puzzovio, B. Vendemiati, G. Martinelli, M. Sacerdoti, D. Calestani, A. Zappettini M. Zha, L. Zanotti, "ZnO gas sensors: a comparison between nanoparticles and nanotetrapods-based thick films," *Sens. Actuators B*, vol. 137, pp. 164–169, 2009.

[30] D. Gruber, F. Kraus, J. Muller, "A novel gas sensor design based on $CH_4/H_2/H_2O$ plasma etched ZnO thin films," *Sens. Actuators B*, vol. 92, pp. 81–89, 2003.

[31] V. Kobrinsky, A. Rothschild, V. Lumelsky, Y. Komem, Y. Lifshitz, "Tailoring the gas sensing properties of ZnO thin films through oxygen non-stoichiometry," *Appl. Phys. Lett.*, vol. 93, pp. 113502-113505, 2008.

[32] N. Yamazoe, "Toward innovations of gas sensor technology," *Sens. Actuators B*, vol.108, pp. 2–14, 2005.

[33] N. Barsan, D. Koziej, U. Weimar, "Metal oxide-based gas sensor research: How to?," *Sens. Actuators B*, vol.121, pp. 18–35, 2007.

[34] P.B. Weisz, "Effect of electronic charge transfer between adsorbate and solid on chemisorption and catalysis," *J. Chem. Phys.*, vol. 21, pp. 1531–1538, 1953.

[35] N. Yamazoe, J. Fuchigami, M. Kishikawa9j, and T. Seiyama, "Interactions of tin oxide surface with O_2, H_2O and H_2," *Surf. Sci.*, vol. 86, pp. 335-344, 1979.

[36] Y. Shimizu, T. Maekawa, Y. Nakamura, M. Egashira, "Effects of gas diffusivity and reactivity on sensing properties of thick film SnO_2-based sensors," *Sens. Actuators B*, vol. 46, pp. 163–168, 1998.

[37] N. Yamazoe, N. Miura, "Some basic aspects of semiconductor gas sensors," *Chemical Sensor Technology,* Kodansha Ltd., Tokyo, Japan, vol. 4, pp. 19-42, 1992.

[38] A.P. Lee, B.J. Reedy, "Temperature modulation in semiconductor gas sensing," *Sens. Actuators B,* vol. 60, pp. 35–42, 1999.

[39] G.Wedler, Lehrbuch der physikalischen Chemie, 4th ed., Wiley-VCH, Weinheim, 1997.

[40] Y. Kato, K. Yoshikawa, M. Kitora, "Temperature-dependent dynamic response enables the qualification and quantification of gases by a single sensor," *Sens. Actuators B,* vol. 40, pp. 33–37, 1997.

[41] W.M. Sears, K. Colbow, F. Consandori, "General characteristics of thermally cycled tin oxide gas sensors," *Semicond. Sci. Technol.*, vol. 4, pp. 351-359, 1989.

[42] S. Nakata, M. Nakasuji, N. Ojima, M. Kitora, "Characteristic nonlinear responses for gas species on the surface of different semiconductor gas sensors," *Appl. Surf. Sci.*, vol. 135, pp. 285-292, 1998.

[43] K.J. Choi, H.W. Jang, "One-dimensional oxide nanostructures as gas-sensing materials: Review and issues" *Sensors,* vol.10, pp.4083–4099, 2010.

[44] G. Korotcenkov, V. Brinzari, V. Golovanov, Y. Blinov, "Kinetics of gas response to reducing gases of SnO_2 films deposited by spray pyrolysis," *Sens. Actuators B,* vol. 98, pp. 41-45, 2004.

[45] G. Korotcenkov, "Gas response control through structural and chemical modification of metal oxide films: state of the art and approaches," *Sens. Actuators B,* vol. 107, pp. 209-232, 2005.

[46] S. Semancik, T.B. Fryberger, "Model studies of SnO_2-based gas sensors: Vacancy defects and Pd additive effects," *Sens. Actuators B,* vol. 1, pp. 97-102, 1990.

[47] A. Cabot, A. Vila, J.R. Morante, "Analysis of the catalytic activity and electrical characteristics of different modified SnO_2 layers for gas sensors," *Sens. Actuators B,* vol. 84, pp. 12-20, 2002.

[48] I. Matko, M. Gaidi, J.L. Hazemann, B. Chenevier, M. Labeau, "Electrical properties under polluting gas (CO) of Pt- and Pd-doped polycrystalline SnO_2 thin films: analysis of the metal aggregate size effect," *Sens. Actuators B,* vol. 59, pp. 210-215, 1999.

[49] A. Chowdhuri, S. K. Singh, K. Sreenivas, V. Gupta, "Contribution of adsorbed oxygen and interfacial space charge for enhanced response of SnO_2sensors having CuO catalyst for H_2S gas," *Sens. Actuators B,* vol. 145, pp. 155-166, 2010.

[50] D. Haridas, A. Chowdhuri, K. Sreenivas, V. Gupta, "Effect of thickness of platinum catalyst clusters on response of SnO_2thin film sensor for LPG," *Sens. Actuators B,* vol. 153, pp. 89-95, 2011.

[51] N. Yamazoe, "New approaches for improving semiconductor gas sensors," *Sens. Actuators B,* vol. 5, pp. 7–19, 1991.

[52] S.R. Morrison, "Selectivity in semiconductor sensors," *Sens. Actuators*, vol. 12, pp. 425-440, 1987.

[53] D. Haridas, V. Gupta, "Enhanced response characteristics of SnO_2 thin film based sensors loaded with Pd clusters for methane detection," *Sens. Actuators B,* vol. 166-167, pp. 156-164, 2012.

[54] Y. Zhao, X. He, J. Li, X. Gao, J. Jia, "Porous CuO/SnO_2 composite nanofibers fabricated by electro-spinning and their H_2S sensing properties," *Sens. Actuators B,* vol. 165, pp. 82-87, 2012.

[55] N. Yamazoe, Y. Kurokawa, T. Seiyama, "Effects of additives on semiconductor gas sensors," *Sens. Actuators B,* vol. 4, pp. 283-289, 1983.

[56] J.W. Gardner, P.N. Bartlett, "A Brief History of Electronic Noses," *Sens. Actuators B,* vol. 18, pp. 210–211, 1994.

[57] E. Schaller, J.O. Bosset, F. Escher, "Electronic Noses and Their Application to Food," *Food Science and Technology*, vol. 31, pp. 305-316, 1998.

[58] A. Hierlemann, M. Schweizer-Berberich, U. Weimar, G. Kraus, A. Pfau, W. Göpel, "Pattern Recognition and Multicomponent Analysis" in H. Baltes, W. Göpel and J. Hesse (Eds.), Sensors (Update), Weinheim, VCH, vol. 2, pp.119-180, 1996.

[59] C. Xu, J. Tamaki, N. Miura and N. Yamazoe, Relationship between gas sensitivity and microstructure of porous SnO_2, *J. Electrochem. Soc. Jpn.,* vol. 58, pp. 1143-1148, 1990.

[60] G. Korotcenkov, V. Brinzari, M. DiBattista, J. Schwank, A. Vasiliev, "Peculiarities of SnO_2 thin film deposition by spray pyrolysis for gas sensor application," *Sens. Actuators B,* vol. 77, pp. 244 -252, 2001.

[61] N. Yamazoe, N. Miura, in: S. Yamauchi (Ed.), Chemical Sensor Technology, 4, Kodansha, Tokyo, pp. 19–42, 1992.

[62] D.E. Williams, K.F.E. Pratt, "Classification of reactive sites on the surface of polycrystalline tin dioxide," *J. Chem. Soc.*, vol. 94, pp. 3493 – 3500, 1998.

[63] T. Wolkenstein, Electronic processes on semiconductor surfaces during chemisorption, Consultants Bureau, New York, 1991.

[64] N. Barsan, U. Weimar, "Understanding the fundamental principles of metal oxide based gas sensors; the example of CO sensing with SnO_2 sensors in the presence of humidity," *J. Phys. Condens. Matter,* vol. 15, pp. 813–839, 2003.

[65] N. Barsan, U. Weimar, "Conduction Model of Metal Oxide Gas Sensors," *J. Electroceram.*, vol. 7, pp. 143–167, 2001.

[66] V. Brinzari, G. Korotcenkov, J. Schwank, in: S. Buettgenbach (Ed.), Optimization of thin film gas sensors for environmental monitoring through theoretical modeling Chemical Micro-sensors and Applications II, Proceedings of SPIE vol. 3857, pp. 186–197, 1999.

[67] V. Lantto, T.S. Rantala, "Equilibrium and non-equilibrium conductance response of sintered SnO_2 samples to CO," *Sens. Actuators B,* vol. 5, pp. 103-107, 1991.

[68] V. Brynzari, G. Korotchenkov, S. Dmitriev, "Theoretical study of semiconductor thin films gas sensors: Attempt to consistent approach," *J. Electron. Technol*., vol. 33, pp. 225-235, 2000.

[69] T. Hyodo, N. Nishida, Y. Shimizu, M. Egashira, "Preparation and gas-sensing properties of thermally stable mesoporous SnO_2," *Sens. Actuators B,* vol. 83, pp. 209-215, 2002.

[70] Y. Shimuzu, T. Maekawa, T. Nakamura, M. Egashira, "Effects of gas diffusivity and reactivity on sensing properties of thick film SnO_2-based sensors," *Sens. Actuator B,* vol. 46, pp. 163–168, 1998.

[71] T. Hyodo, S. Abe, Y. Shimuzu, M. Egashira, "Gas-sensing properties of ordered mesoporous SnO_2 and effects of coatings thereof," *Sens. Actuators B,* vol. 93, pp. 590-600, 2003.

[72] Y. Shimizu, Y. Nakamura, M. Egashira, "Effects of diffusivity of hydrogen and oxygen through pores of thick film SnO_2-based sensors on their sensing properties," *Sens. Actuators B,* vol. 13-14, pp. 128-131, 1993.

[73] N. Yamazoe, N. Miura, in: G. Sberveglieri (Ed.), Gas Sensors, Kluwer Academic Publishers, The Netherlands, 1992.

[74] N. Yamazoe, J. Fuchigami, M. Kishikawa, T. Seiyama, "Interactions of tin oxide with O_2, H_2O and H_2," *Surf. Sci.*, vol. 86, pp. 335-344, 1979.

[75] N. Yamazoe, S. Matsushima, T. Maekawa, J. Tamaki, N. Miura, "Control of Pd dispersion in SnO_2-based sensors," *Catal. Sci. Technol.*, vol. 1, pp. 201- 205, 1991.

[76] G. Sakai, N. Matsunaga, K. Shimanoe, N. Yamazoe, "Theory of gas-diffusion controlled sensitivity for thin film semiconductor gas sensor," *Sens. Actuators B*, vol. 80 pp. 125- 131, 2001.

[77] N. Yamazoe, "New approaches for improving semiconductor gas sensors," *Sens.Actuators B*, vol. 5, pp. 7-19, 1991.

[78] S. Abe, U.S. Choi, K. Shimanoe, N. Yamazoe, "Influences of ball-milling time on gas-sensing properties of Co_3O_4-SnO_2 composites," *Sens. Actuators B* vol. 107, pp. 516-522, 2005.

[79] C. Xu, J. Tamaki, N. Miura, N. Yamazoe, "Grain size effects on gas sensitivity of porous SnO_2-based elements," *Sens. Actuators B*, vol. 3, pp. 147-155, 1991.

[80] A. Dieguez, A. Romano-Rodry´guez, J.L. Alay, J.R. Morante, N. Barsan, J. Kappler, U. Weimar, W. Gopel, "Parameter optimisation in SnO_2 gas sensors for NO_2 detection with low cross-sensitivity to CO: sol-gel preparation, film preparation, powder calcination, doping and grinding," *Sens. Actuators B*, vol. 65, pp. 166-168, 2000.

[81] J. Arbiol, F. Peiro, A. Cornet, J.R. Morante, J.A. Pe´rez-Omil, J.J. Calvino, "Computer image HRTEM simulation of catalytic nanoclusters on semiconductor gas sensor materials supports," *Mater. Sci. Eng. B*, vol. 91- 92, pp. 534-536, 2002.

[82] A. Cabot, A. Dieguez, A. Romano-Rodriguez, J.R. Morante, N. Barsan, "Influence of the catalytic introduction procedure on the nano-SnO_2 gas sensor performances - Where and how stay the catalytic atoms?"*Sens. Actuators B*, vol. 79, pp. 98-106, 2001.

[83] A. Cirera, A. Cornet, J.R. Morante, S.M. Olaizola, E. Castano, J.R. Gracia, "Comparative structural study between sputtered and liquid pyrolysis nanocrystalline SnO_2," *Mater. Sci. Eng. B*, vol. 69-70, pp. 406-410, 2000.

[84] G.G. Mandayo, E. Castano, F.J. Gracia, A. Cirera, A. Cornet, J.R. Morante, "Strategies to enhance the carbon monoxide sensitivity of tin oxide thin films," *Sens. Actuators B*, vol. 95, pp. 90-96, 2003.

[85] G. Korotcenkov, "The role of morphology and crystallographic structure of metal oxides in response of conductometric-type gas sensors," *Mater. Sci. Eng*., vol.61, pp. 1-39, 2008.

[86] G. Korotcenkov, V. Golovanov, A. Cornet, V. Brinzari, J. Morante, M. Ivanov, "Distinguishing feature of metal oxide films' structural engineering for gas sensor applications," *J. Phys.: Confer. Series (IOP)*, vol. 15, pp. 256-261, 2005.

[87] G. Korotcenkov, A. Cornet, E. Rossinyol, J. Arbiol, V. Brinzari, Y. Blinov, "Faceting characterization of tin dioxide nanocrystals deposited by spray pyrolysis from stannic chloride water solution," *Thin Solid Films*, vol. 471, pp. 310-319, 2005.

[88] G. Korotcenkov, V. Macsanov, V. Tolstoy, V. Brinzari, J. Schwank, G. Faglia, "Structural and gas response characterization of nano-size SnO_2 films deposited by SILD method," *Sens. Actuators B*, vol. 96, pp. 602-609, 2003.

[89] G. Korotcenkov, M. DiBattista, J. Schwank, V. Brinzari, "Structural characterization of SnO_2 gas sensing films deposited by spray pyrolysis," *Mater. Sci. Eng.*, vol. 77, pp. 33-39, 2000.

[90] Hui-Hui Li, ,Yi He, Pan-Pan Jin, Yang Cao, Mei-Hong Fan, Xiaoxin Zou, Guo-Dong Li, "Highly selective detection of trace hydrogen against CO and CH_4 by $Ag/Ag_2O–SnO_2$ composite microstructures," *Sens. Actuators B*, vol. 228, pp. 515-522, 2016.

[91] Y.-J. Jeong, C. Balamurugan, D.-W. Lee, "Enhanced CO_2 gas-sensing performance of ZnO nanopowder by La loaded during simple hydrothermal method," *Sens. Actuators B*, vol. 229, pp. 288-296, 2016.

[92] L. Giancaterini, C. Cantalini, M. Cittadini, M. Sturaro, M. Guglielmi, A. Martucci, A. Resmini, U. A. Tamburini, "Au and Pt nanoparticles effects on the optical and gas sensing properties of sol-gel based ZnO thin-film sensors," *IEEE Sensors Journal*, vol. 15, pp. 1068-1076, 2015.

[93] E. S. Babu, S. Ku Hong, "Effect of indium concentration on morphology of ZnO nanostructures grown by using CVD method and their application for H2 gas sensing," *Superlattices and Microstructures*, vol. 82, pp. 349–356, 2015.

[94] N.S. Ramgir, N. Datta, S. Kumar, S. Kailasaganapathi, U.V. Patil, N. Karmakar, M. Kaur, A.K. Debnath, D.C. Kothari, D.K. Aswal, S.K. Gupta, "Effect of Fe modification on H_2S sensing properties of rheotaxially grown and thermally oxidized SnO_2 thin films," *Mat. Chem. Physics*, vol. 156, pp. 227-237, 2015.

[95] W. Kim, M. Choi, K. Yong, "Generation of oxygen vacancies in ZnO nanorods/films and their effects on gas sensing properties," *Sens. Actuators B*, vol. 209, pp. 989-996, 2015.

[96] B. Wang, Z.O. Zheng, L.F. Zhu, Y.H. Yang, H.Y. Wu, "Self-assembled and Pd decorated Zn_2SnO_4/ZnO wire-sheet shape nano-heterostructures networks hydrogen gas sensor," *Sens. Actuators B*, vol. 195, pp. 549-561, 2014.

[97] J. Chen, J. Zhang, M. Wang, Y. Li, "High-temperature hydrogen sensor based on platinum nanoparticle-decorated SiC nanowire device," *Sens. Actuators B*, vol. 201, pp. 402-406, 2014.

[98] M. Dwivedi, J. Bhargava, A. Sharma, V. Vyas, G. Eranna, "CO sensor using ZnO thin film derived by RF magnetron sputtering techniques," *IEEE Sensors Journal*, vol. 14, pp. 1577-1582, 2014.

[99] P. S. Shewale, B. N. Kamble, A. V. Moholkar, J. H. Kim, M. D. Uplane "Influence of substrate temperature on H_2S gas sensing properties of nanocrystalline zinc oxide thin films prepared by advanced spray pyrolysis," *IEEE Sensors Journal*, vol. 13, pp. 1992-1998, 2013.

[100] P.S. Shewale, G.L. Agawane, S.W. Shin, A.V. Moholkar, J.Y. Lee, J.H. Kim, M.D. Uplane, "Thickness dependent H_2S sensing properties of nanocrystalline ZnO thin films derived by advanced spray pyrolysis," *Sens. Actuators B*, vol. 177, pp. 695-702, 2013.

[101] S. Benkara, S. Zerkout, H. Ghamri, "Synthesis of Sn doped ZnO/TiO_2 nanocomposite film and their application to H_2 gas sensing properties," *Mater. Sci. Semicond. Process.* vol.16, pp. 1271-1279, 2013.

[102] L. Chow, O. Lupan, G. Chai, H. Khallaf, L.K. Ono, B. R. Cuenya, I.M. Tiginyanu, V.V. Ursaki, V. Sontea, A. Schulte, "Synthesis and characterization of

Cu-doped ZnO one dimensional structures for miniaturized sensor applications with faster response," *Sens. Actuators A*, vol. 189, pp. 399-408, 2013.

[103] P.S. Shewale, V.B. Patil, S.W. Shin, J.H. Kim, M.D. Uplane, "H_2S gas sensing properties of nanocrystalline Cu-doped ZnO thin films prepared by advanced spray pyrolysis," *Sens. Actuators A*, vol. 186, pp. 226-234, 2013.

[104] L. N. Balakrishnan, S. Gowrishankar, N. Gopalakrishnan, "NH_3 sensing by p-ZnO thin films," *IEEE Sensors Journal*, vol.13, pp. 2055- 2060, 2013.

[105] T. Y. Chen, H. I. Chen, C. S. Hsu, C. C. Huang, J. S. Wu, P. C. Chou, W. C. Liu, "ZnO-based ammonia gas sensors with underlying Pt/Cr interdigitated electrodes," *IEEE Electron Device Letters*, vol. 33, pp. 1486-1488, 2012.

[106] P. Singh, V.N. Singh, K. Jain, T.D. Senguttuyan, "Pulse-like highly selective gas sensors based on ZnO nanostructures synthesized by a chemical route: Effect of tin doping and Pd loading," *Sens. Actuators B*, vol. 167, pp. 678-684, 2012.

[107] E. Bruneta, T. Maiera, G.C. Mutinati, S. Steinhauera, A. Köcka, C. Gspanb, W. Grogger, "Comparison of the gas sensing performance of SnO_2 thin ?lm and SnO_2 nanowire," *Sens. Actuators B*, vol. 165 pp. 110-118, 2012.

[108] P. Rai, Y. Yu, "Synthesis of floral assembly with single crystalline ZnO nanorods and its CO sensing property," *Sens. Actuators B*, vol. 161 pp. 748-754, 2012.

[109] L. Wang, Y. Kang, X. Liu, S. Zhang, W. Huang, S. Wang, "ZnO nanorod gas sensor for ethanol detection," *Sens. Actuators B*, vol. 162 pp. 237-243, 2012.

[110] G. Korotcenkov, B.K. Cho, "Ozone measuring: What can limit application of SnO_2-based conductometric gas sensors?" *Sens. Actuators B*, vol. 161 pp. 748-754, 2012.

[111] Y. Zeng, L. Qiao, Y. Bing, M. Wen, B. Zou, W. Zheng, T. Zhang, G. Zou, "Development of microstructure CO sensor based on hierarchically porous ZnO nanosheet thin films," *Sens. Actuators B*, vol. 173, pp. 897-902, 2012.

[112] M. Tonezzer, R.G. Lacerda, "Zinc oxide nanowires on carbon microfiber as flexible gas sensor," *Physica E*, vol. 44, pp. 1098-1105, 2012.

[113] C.H. Lin, W. C Chang, X. Qi, "Growth and characterization of pure and doped SnO_2 films for H_2 gas detection," *Procedia Engineering*, vol. 36, pp. 476–481, 2012.

[114] D. T. Phan, G. S. Chung, "Surface acoustic wave hydrogen sensors based on ZnO nanoparticles incorporated with a Pt catalyst," *Sens. Actuators B*, vol. 161, pp. 341-348, 2012.

[115] L.I. Trakhtenberg, G.N. Gerasimov, V.F. Gromov, T.V. Belysheva, O.J. Ilegbusi, "Effect of composition on sensing properties of SnO_2 + In_2O_3 mixed nanostructured films," *Sens. Actuators B*, vol. 169, pp. 32-38, 2012.

[116] E. D. Gaspera, M. Guglielmi, A. Martucci, L. Giancaterini, C. Cantalini, "Enhanced optical and electrical gas sensing response of sol–gel based NiO–Au and ZnO–Au nanostructured thin films," *Sens. Actuators B*, vol. 164, pp. 54-63, 2012.

[117] T.C. Lin, B.R. Huang, "Palladium nanoparticles modified carbon nanotube/nickel composite rods (Pd/CNT/Ni) for hydrogen sensing," *Sens. Actuators B*, vol. 162, pp. 108-113, 2012.

[118] M. Tonezzer, N.V. Hieu, "Size-dependent response of single-nanowire gas sensors," *Sens. Actuators B*, vol. 162, pp. 146-152, 2012.

[119] C. Liewhiran, N. Tamaekong, A. Wisitsoraat, S. Phanichphant, "Highly selective environmental sensors based on flame-spray-made SnO_2 nanoparticles," *Sens. Actuators B*, vol. 163, pp. 51-60, 2012.

[120] C. Zhang, A. Boudiba, M.G. Olivier, R. Snyders, M. Debliquy, "Magnetron sputtered tungsten oxide films activated by dip-coated platinum for ppm-level hydrogen detection," *Thin Solid Films*, vol. 520, pp. 3679-3683, 2012.

[121] Q. Yu, K. Wang, C. Luan, Y. Geng, G. Lian, D. Cui, " A dual-functional highly responsive gas sensor fabricated from SnO2 porous nanosolid," *Sens. Actuators B*, vol. 159, pp. 271-276, 2011.

[122] Y. Liu, T. Hang, Y. Xie, Z. Bao, J. Song, H. Zhang, E. Xie, "Effect of Mg doping on the hydrogen- sensing characteristics of ZnO thin films," *Sens. Actuators B*, vol. 160, pp. 266– 270, 2011.

[123] D. Shaposhnika, R. Pavelkob, E. Llobeta, F. G. Guiradoa, X. Vilanova, **"**Hydrogen sensors on the basis of SnO_2-TiO_2 systems," *Procedia Engineering*, vol. 25, pp. 1133-1136, 2011.

[124] X. Liu, J. Zhang, X. Guo, S. Wu, S. Wang, "Enhanced sensor response of Ni-doped SnO_2 hollow spheres," *Sens. Actuators B*, vol. 152, pp. 162– 167, 2011.

[125] A. Qurashi, M. Faiz, N. Tabet, M. W. Alam, "Low temperature synthesis of hexagonal ZnO nanorods and their hydrogen sensing properties," *Superlattices and Microstructures*, vol. 50, pp. 173-180, 2011.

[126] S. F. Bamsaoud, S.B. Rane, R.N. Karekar, R.C. Aiyer, "Nano particulate SnO_2 based resistive films as a hydrogen and acetone vapour sensor," *Sens. Actuators B*, vol. 153, pp. 382-391, 2011.

[127] M. Chen, Z. Wang, D. Han, F. Gu, G. Guo, "High-sensitivity NO_2 gas sensors based on flower-like and tube-like ZnO nanomaterials," *Sens. Actuators B*, vol. 157, pp. 565-574, 2011.

[128] J. Zhao, W. Wang, Y. Liu, J. Ma, X. Li, Y. Du, G. Lu, "Ordered mesoporous Pd/SnO_2 synthesized by a nanocasting route for high hydrogen sensing performance," *Sens. Actuators B*, vol. 160, pp. 604-608, 2011.

[129] S.W. Tsai, J.C. Chiou, "Improved crystalline structure and H_2S sensing performance of $CuO–Au–SnO_2$ thin film using SiO_2 additive concentration," *Sens. Actuators B*, vol. 152, pp. 176-182, 2011.

[130] N.S. Ramgir, M. Ghosh, P. Veerender, N. Datta, M. Kaur, D.K. Aswal, S.K. Gupta, "Growth and gas sensing characteristics of p-and n-type ZnO nanostructures," *Sens. Actuators B*, vol. 156, pp. 875-880, 2011.

[131] A.D. Garje, A. Inamdar, R.C. Aiyer, "CO and LPG Sensing Properties of Cu-Doped SnO_2 Pellets Using Pulsed Laser Ablation with the Effect of Ablation Time and Sintering Temperature," *Appl. Ceramic. Tech.*, vol. 8, pp. 691-699, 2010.

[132] H. Zhang, Z. Li, L. Liu, X. Xu, Z. Wang, W. Wang, W. Zheng, B. Dong, C. Wang, "Enhancement of hydrogen monitoring properties based on $Pd–SnO_2$ composite nanofibers," *Sens. Actuators B*, vol. 147, pp. 111-115, 2010.

[133] N.H. Al-Hardan, M.J. Abdullah, A.A. Aziz, "Sensing mechanism of hydrogen gas sensor based on RF-sputtered ZnO thin films," *Int. J. Hydrogen Energy*, vol. 35, pp. 4428-4434, 2010.

[134] J. G. Partridge, M. R. Field, A. Z. Sadek, K. Kalantar-zadeh, J. Du Plessis, M. B. Taylor, A. Atanacio, K. E. Prince, D. G. McCulloch, "Fabrication, structural characterization and testing of a nanostructured tin oxide gas sensor," *IEEE Sensors Journal*, vol. 9, pp. 563-568, 2009.

[135] K.J. Jeon, J.M. Lee, E. Lee, W. Lee, "Individual Pd nanowire hydrogen sensors fabricated by electron-beam lithography," *Nanotechnology*, vol. 20, pp.135502-135507, 2009.

[136] I. Fasaki, M. Suchea, G. Mousdis, G. Kiriakidis, M. Kompitsas, "The effect of Au and Pt nanoclusters on the structural and hydrogen sensing properties of SnO_2 thin films," ," *Thin Solid Films*, vol. 518, pp. 1109-1113, 2009.

[137] H. Liu, S.P. Gong, Y.X. Hu, J.Q. Liu, D.X. Zhou, "Properties and mechanism study of SnO_2 nanocrystals for H_2S thick-film sensors," *Sens. Actuators B*, vol. 140, pp. 190-195, 2009.

[138] M. Vilaseca, J. Coronas, A. Cirera, A. Cornet, J.R. Morante, J. Santamaria, "Development and application of micromachined Pd/SnO_2 gas sensors with zeolite coatings," *Sens. Actuators B*, vol. 133, pp. 435-441, 2008.

[139] A.B. Bodade, A.M. Bende, G.N. Chaudhari, "Synthesis and characterization of CdO-doped nanocrystalline ZnO: TiO_2-based H_2S gas sensor," *Vacuum*, vol. 82, pp. 588-593, 2008.

[140] J. Gong, J. Sun, Q. Chen, "Micromachined sol-gel carbon nanotube/SnO_2 nanocomposite hydrogen sensor," *Sens. Actuators B*, vol. 130, pp. 829-835, 2008.

[141] J. Tamaki, Y. Nakataya, S. Konishi, "Micro gap effect on dilute H_2S sensing properties of SnO_2 thin film microsensors," *Sens. Actuators B*, vol. 130, pp. 400-404, 2008.

[142] Y.S. Sonawane, K.G. Kanade, B.B. Kale, R.C. Aiyer, "Electrical and gas sensing properties of self-aligned copper-doped zinc oxide nanoparticles," *Mater. Res. Bull.*, vol. 43, pp. 2719-2726, 2008.

[143] A. Z. Sadek, S. Choopun, W. Wlodarski, S. J. Ippolito, K. Kalantar-zadeh, "Characterization of ZnO nanobelt-based gas sensor for H_2, NO_2, and hydrocarbon sensing," *IEEE Sensors Journal*, vol. 7, pp. 919-924, 2007.

[144] Ch. Pandis, N. Brilis, E. Bourithis, D. Tsamakis, H. Ali, S. Krishnamoorthy, A. A. Iliadis, M. Kompitsas, "Low-temperature hydrogen sensors based on Au naoclusters and Schottky contacts on ZnO films deposited by pulsed laser deposition on Si and SiO_2 substrates," *IEEE Sensors Journal*, vol. 7, pp. 448-454, 2007.

[145] T.J. Hsueh, C.L. Hsu, S. J. Chang, I. C. Chen, "Laterally grown ZnO nanowire ethanol gas sensors," *Sens. Actuators B*, vol. 126, pp. 473-477, 2007.

[146] P. Bhattacharyya, P.K. Basu, H. Saha, S. Basu, "Fast response methane sensor using nanocrystalline zinc oxide thin films derived by sol–gel method," *Sens. Actuators B*, vol. 124, pp. 62-67, 2007.

[147] V.R. Shinde, T.P. Gujar, C.D. Lokhande, "LPG sensing properties of ZnO films prepared by spray pyrolysis method: Effect of molarity of precursor solution," *Sens. Actuators B*, vol. 120, pp. 551-559, 2007.

[148] H. Gong, J.Q. Hu, J.H. Wang, C.H. Ong, F.R. Zhu, "Nano-crystalline Cu-doped ZnO thin film gas sensor for CO," *Sens. Actuators B*, vol. 115, pp. 247-251, 2006.

[149] S. M. Chou, L. G. Teoh, W. H. Lai, Y. H. Su, M. H. Hon, "ZnO: Al thin film gas sensor for detection of ethanol vapor," *Sensors*, vol. 6, pp. 1420-1427, 2006.

[150] S. Chakraborty, A. Sen, H.S. Maiti, "Complex plane impedance plot as a figure of merit for tin dioxide-based methane sensors," *Sens. Actuators B*, vol. 119, pp. 431-434, 2006.

[151] S. Aygun, D. Cann, "Hydrogen sensitivity of doped CuO/ZnO Heterocontact sensors," *Sens. Actuators B*, vol. 106, pp. 837–842, 2005.

[152] D. D. Vuong, G. Sakai, K. Shimanoe, N. Yamazoe, "Hydrogen sulfide gas sensing properties of thin films derived from SnO_2 sols different in grain size," *Sens. Actuators B*, vol. 105, pp. 437-442, 2005.

[153] S. Choi, G. Sakai, K. Shimanoe, N. Yamazoe, Sensing properties of Au-loaded SnO_2-Co_3O_4 composites to CO and H_2," *Sens. Actuators B*, vol. 107, pp. 397-401, 2005.

[154] J.M. Lee, B.U. Moon, C.H. Shim, B.C. Kim, M. B. Lee, D.D. Lee, J.H. Lee, "H_2S microgas sensor fabricated by thermal oxidation of Cu/Sn double layer," *Sens. Actuators B*, vol. 108, pp. 84-88, 2005.

[155] S.T. Shishiyanu, T. S. Shishiyanu, O. I. Lupan, "Sensing characteristics of tin-doped ZnO thin films as NO_2 gas sensor," *Sens. Actuators B*, vol. 107, pp. 379-386, 2005.

[156] A. F. Aktaruzzaman, G. L. Sharma, L. K. Malhotra, "Electrical, optical and annealing characteristics of ZnO: Al films prepared by spray pyrolysis," *Thin Solid Films*, vol. 198, pp. 67-74, 1991.

[157] S.C. Roy, M.C. Bhatnagar, G.L. Sharma, S. B. Samanta, "Novel ammonia-sensing phenomena in sol-gel derived Ba0.5Sr0.5TiO3 tin films," *Sens. Actuators B*, vol. 110, pp. 299-303, 2005.

[158] M. K. Singh, G. L. Sharma, S. Dussan, R. S. Katiyar, "Structural properties of multiferroic $CuFeO_2$ thin films prepared by RF sputtering," *17th IEEE international symposium on the application of ferroelectrics*," vol. 2, pp. 1-2, 2008.

[159] M. Echizen, S. Motoyama, T. Tatsuta, O. Tsuji, R. S. Katiyar, A. Kumar, J. F. Scott, "Comparison of the electrical properties of ZnO thin films on different substrates by pulsed laser deposition," *INTEGR FERROELECTRICS*, vol. 133, pp. 9-14, 2012.

[160] L. Boon-Brett, J. Bousek, G. Black, P. Moretto, P. Castello, T. Hubert et al., "Identifying performance gaps in hydrogen safety sensor technology for automotive and stationary applications," *Int. J. Hydrogen Energy*, vol. 35, pp. 373-384, 2010.

[161] L. Barreto, A. Makihira, K. Riahi, "The hydrogen economy in the 21st century: a sustainable development scenario," *Int. J. Hydrogen Energy*, vol. 28, pp. 267–284, 2003.

[162] T. Hübert, L. Boon-Brett, G. Black, U. Banach, "Hydrogen sensors- A review," *Sens. Actuators B*, vol. 157, pp. 329-352, 2011.

[163] W.J. Buttner, M.B. Post, R. Burgess, C. Rivkin, "An overview of hydrogen safety sensors and requirements," *Int. J. Hydrogen. Energy*, vol. 36, pp. 2462-2470, 2011.

[164] V. Aroutiounian, "Hydrogen detectors," *Int. Sci. J. Altern. Energy Ecol*, vol. 3, pp. 21-31, 2005.

[165] H. Gu, Z. Wang, Y. Hu, "Hydrogen gas sensors based on semiconductor oxide nanostructures," *Sensors*, vol. 12, pp. 5517-5550, 2012.

[166] F. Paraguay, M. Miki-Yoshida, J. Morales, J. Solis, W. Estrada, "Influence of Al, In, Cu, Fe, and Sn dopants on the response of thin film ZnO gas sensor to ethanol," *Thin Solid Films*, vol. 373, pp. 137-140, 2000.

[167] S. Rani, S. C. Roy, M. C. Bhatnagar, "Effect of Fe doping on the gas sensing properties of nano-crystalline SnO_2 thin films," *Sens. Actuators B*, vol. 122, pp. 204-210, 2007.

[168] Z. Zhoua, K. Katoa, T. Komakia, M. Yoshinoa, H. Yukawaa, M. Morinagaa, K. Moritab, "Effects of dopants and hydrogen on the electrical conductivity of ZnO," *J. Eur. Ceram. Soc.*, vol. 24, pp. 139–146, 2004.

[169] Z. B. Bahsi, A. Y. Oral, "Effects of Mn and Cu doping on the microstructures and optical properties of sol–gel derived ZnO thin films," *Opt. Mater.*, vol. 29, pp. 672–678, 2007 .

[170] S. A. Ansari, A. Nisar, B. Fatma, W. Khan, A.H. Naqvi, "Investigation on structural, optical and dielectric properties of Co doped ZnO nanoparticles synthesized by gel-combustion route," *Mater. Sci. Eng.*, vol. 177, pp. 428-435, 2012.

[171] C.S. Prajapati, P.P. Sahay, "Influence of In doping on the structural, optical and acetone sensing properties of ZnO nanoparticulate thin films," *Mater. Sci. Semicond. Process*, vol. 16, pp. 200–210, 2013.

[172] J. Mizsei, "How can sensitive and selective semiconductor gas sensors be made?" *Sens. Actuators B*, vol. 23, pp. 173–176, 1995.

[173] S. Agarwal, G.L. Sharma, "Humidity sensing properties of (Ba, Sr) TiO3 thin films grown by hydrothermal-electrochemical method," *Sens. Actuators B*, vol. 85, pp. 205-211, 2002.

[174] A. Kumar, N. Ortega, S. Dussan, S. Kumari, D. Sanchez, J. Scott, R.S. Katiyar, "Multiferroic memory: A disruptive technology or future technology?," *Solid State Phen.*, vol. 189, pp. 1-14, 2012.

[175] N.L. Hung, E. Ahn, S. Park, H. Jung, H. Kim, S.K. Hong, D. Kim, C. Hwang, "Synthesis and hydrogen gas sensing properties of ZnO wirelike thin films," *J. Vaccum Sci. Technol. A*, vol. 27, pp. 13471-13475, 2009.

[176] R. Thomas, J.J. Saavedra-Arias, N.K. Karan, N.M. Murari, R.S. Katiyar, P. Ehrhatt, R. Waser, "Thin films of high-k dysprosium, scandate prepared by metal organic chemical vapor deposition or metal-insulator-metal capacitor applications," *Solid State Comm.*, vol. 147, pp. 332-335, 2008.

[177] D.A. Sanchez, A. Kumar, N. Ortega, R.S. Katiyar, J.F. Scott, "Near–room temperature relaxor multiferroic," *App. Phy. Lett*. vol. 97, pp. 202910-202913, 2010.

[178] C.J. Brinker, S.W. Scherer, Sol-Gel science: the physics and chemistry of sol–gel processing. Academic Press, New York, 1990.

[179] S. Hatamie, V. Dhas, B.B. Kole, I.S. Mutta, S.N. Kole, "Polymer embedded stannic oxide nanoparticles as humidity sensors," *Mat. Sci. Engg. C,* vol. 29, pp. 847-850, 2009.

[180] C. Hu, X. Wu, X. Mo, L.Sui, Y. Chi, H. Wei, L. Lu, "PVA-associated solovothermal fabrication of tin oxide sub-microrods," *J. Cryst. Growth,* vol. 265, pp. 235-240, 2004.

[181] L.R.B. Santos, C.V. Santilli, S.H. Pulcinells, "Sol-Gel transition in SnO_2 colloidal suspension visco elastic properties," *J. Non cryst. Solids,* vol. 247, pp. 153-157, 1999.

[182] H.A. Khorami, M. Keyanpour-Rod, M.R. Vaezi, "Synthesis of SnO_2/ZnO composite nanofibers by electrospining method and study of its ethanol sensing properties," *App. Surf. Sci.,* vol. 257, pp. 7988-7992, 2011.

[183] G. Korotcenkov, B.K. Cho, Gulina, V Tolstoy, "Ozone sensors based on Sno_2 films modified by Sno_2-Au nanocomposition," *Sens. Actuators B,* vol. 138, pp. 512-517, 2009.

[184] S.wang, Y.Zhao, J.Huanos, Y.Way, H.Ren.S.Wu, S.Zhang, W.Huang, "Low temperature Co gas sensors based on Au/Sno_2 thick film," *Appl. Surf. Science,* vol. 253 pp. 3057-3061, 2007.

[185] J.Gong, Q.Chen, M.R. Lian, N.C. Lin, R.G. Stevensor, F.adami, "Micro machined nanocrystalline silver doped Sno_2 H_2S sensor," *Sens.Actuators B,* vol. 114, pp. 32-39, 2006.

[186] R. Eason, Pulsed Laser Deposition of Thin films, Applications-LED Growth of Functional Materials, John Wiley & Sons, Inc., Hoboken, New Jersey Publication, 2007.

[187] H.P. Klug, L.E. Alexander, X-ray diffraction procedures, John Wiley and Sons Inc., New York, 1954.

[188] B.E. Warren, X-ray Diffraction, Dover publications, Inc., New York 1990.

[189] J.I. Goldstein, Scanning Electron Microscopy and X-Ray Microanalysis, 2nd ed. Plenum, New York, 1992.

[190] G. Binning, C.F. Quate, "Atomic force microscope," *Phys. Rev. Lett.,* vol. 56, pp. 930-934, 1986.

[191] P. Gorostiza, M.S., Universitat de Barcelona, 1994.

[192] R.K. Joshi, F.E.Krus, O.Dmitrieva, "Gas sensing behavior of $SnO_{1.8}$: A_8 films composed of size selected nanoparticles," *J.Nanoparticle Research*, vol. 8, pp. 797-808, 2006.

[193] A.Diesuez, A.R. Rodrisuez, J.R.Morarte, J.Kappler, N.Barsan, W.Gopel, "Nanoparticles on sintering for gas sensor optimization: imposed sol-gel fabrication nanocrystalline SnO_2 thick film gas sensor for NO_2 detection B_T calcination catalytic metal insulation and sensing treatments," *Sens.Actuators B*, vol. 60, pp. 125-137, 1999.

[194] P. Ayyub, V.R. Palkar, S. Chattopadhyay, M. Multani, "Effect of crystal size reduction on lattice symmetry and cooperative properties," *Phys. Rev. B*, vol. 51, pp. 6135-6139, 1995.

[195] Q. A. Drmosh, S. G. Rao, Z. H. Yamani, M.A. Gondal, "Crystalline nanostructured Cu doped ZnO thin films grown at room temperature by pulsed lased deposition technique and their characterization," *Appl. Surf. Sci*., vol. 270, pp. 104-108, 2013.

[196] X.B. Wang, C. Song, K.W. Geng, F. Zeng, F. Pan, "Photoluminescence and Raman scattering of Cu-doped ZnO films prepared by magnetron sputtering," *Appl. Surf. Sci*., vol. 253, pp. 6905-6905, 2007..

[197] Z.Jin, H.J. Zhou, Z.L. Jin, R.F. Sarinell and C.C. Liu, "Applications of nano-crystalline porous tin oxide thin film for co sensing," *Sens.Actuators B*, vol. 52, pp. 188-194, 1998.

[198] S.H. Jeong, B.N. Park, S.B. Lee, J.H. Boo, "Study on the doping effect of Li-doped ZnO film," Thin Solid Films, vol. 516, pp. 5586-5589, 2008.

[199] J.Q. Xu, Q.Y. Pan, Y.A. Shun, Z.Z. Tian, "Grain size control and gas sensing properties of ZnO gas sensor," Sens. Actuators B, vol. 66, pp. 277–279, 2000.

[200] T.R.N. Kutty, N. Raghu, "Varistors based on polycrystalline ZnO: Cu," *Appl. Phys. Lett.*, vol. 54, pp. 1796-1798, 1989.

[201] N.H. Al-Hardan, M.J. Abdullah, A.A. Aziz, "The gas response enhancement from ZnO film for H_2 gas detection," *Appl. Surf. Sci.*, vol. 255, pp. 7794-7797, 2009.

[202] M.K. Puchert, A. Hartmann, R.N. Lamb, J.W. Martin, "Highly resistive sputtered ZnO films implanted with copper," *J. Mater. Res.*, vol. 11, pp. 2463-2469, 1996.

[203] S.R. Morrison, "Mechanism of semiconductor gas sensor operation," *Sens. Actuators*, vol. 11, pp. 283-287, 1987.

[204] J.F. Chang, H.H. Kuo, I.C. Leu, M.H. Hon, "The effects of thickness and operation temperature on ZnO: Al thin film CO gas sensor," *Sens. Actuators B*, vol. 84, pp. 258-264, 2002.

[205] N.D. Hoa, S.Y. An, N.Q. Dung, N.V. Quy, D. Kim, "Synthesis of p-type semiconducting cupric oxide thin films and their application to hydrogen detection," *Sens. Actuators B*, vol. 146, pp. 239-244, 2010.

[206] A. Chapelle, M.H. Yaacob, I. Pasquet, L. Presmanes, A. Barnabe, P. Tailhades et al., "Structural and gas-sensing properties of CuO-$Cu_xFe_{3-x}O_4$ nanostructured thin films," *Sens. Actuators B*, vol. 153, pp. 117-124, 2011.

[207] K. Mukherjee, S.B. Majumder, Hydrogen sensing characteristics of nano-crystalline $Mg_{0.5}Zn_{0.5}Fe_2O_4$ thin film: Effect of film thickness and operating temperature," *Int. J. Hydrogen Energy*, vol. 39, pp. 1185-1191, 2014.

[208] M. Ahsan, M.Z. Ahmad, T. Tesfamichael, J. Bell, W. Wlodarski, N. Motta, "Low temperature response of nanostructured tungsten oxide thin films toward hydrogen and ethanol," *Sens. Actuators B*, vol. 173, pp. 789-796, 2012.

[209] N. Yamazoe, N. Miura, "Some basic aspects of semiconductor gas sensors," in: *S. Yamauchi* (Ed.), vol.4, Chemical Sensor Technology, Elsevier, Kodanasha Ltd, Tokyo,Japan,1992,pp.19-42.

[210] G. A. Mohamed, A. B. Abd El-Moiz, M. Rashad, "Li-doping effects on the electrical properties of ZnO films prepared by the chemical-bath deposition method," *Physica B: Condensed Matter*, vol. 370, pp.158-167, 2005.

[211] D. C. Look, B. Claflin, "P-type doping and devices based on ZnO," *Phys. Stat. Sol. B.*, vol. 241, pp. 624-630, 2004.

[212] S. B. Zhang, S. H. Wei, A. F. Zunger, "Intrinsic n-type versus p-type doping asymmetry and the defect physics of ZnO", *Phys. Rev. B*, vol. 63, pp. 075205-075212, 2001.

[213] H.J. Koa, Y. Chenb, S.K. Hong, T. Yao, "Doping effects in ZnO layers Li_3N as a doping source," *J. Cryst. Growth*, vol. 251, pp. 628-632, 2003.

[214] J. Hu, H. Y. He, B. C.Pana, "Hydrogen diffusion behavior in N doped ZnO: First-principles study," *J. Appl. Phys.*, vol. 103, pp. 113706-113711, 2008.

[215] S.H. Jeong, B.N. Park, S.B. Lee, J.H. Boo, "Study on the doping effect of Li-doped ZnO film," *Thin Solid Films,* vol. 516, pp. 5586-5589, 2008.

[216] J.R. Duclère, M. Novotny, A. Meaney, R. O'Haire, E. McGlynn, M.O. Henry, J.P.Mosnier, "Properties of Li-, P- and N-doped ZnO thin films prepared by pulsed laser deposition," *Superlattices and Microstructures,* vol. 38, pp. 397-405, 2005.